

Supplementary Materials for

Equilibrating Parent Aminomercaptocarbene and CO₂ with 2-Amino-2-Thioacetic Acid *via* Heavy-Atom Quantum Tunneling

Bastian Bernhardt,[†] Markus Schaueremann,[†] Ephrath Solel, André K. Eckhardt, and Peter R. Schreiner*

Institute of Organic Chemistry, Justus Liebig University, Heinrich-Buff-Ring 17, 35392 Giessen, Germany

*prs@uni-giessen.de

[†]These authors contributed equally.

This PDF file includes:

Materials and Methods, Supplementary Text, Figs. S1 to S50, Tables S1 to S26, and References (1-29).

Table of Contents

Methods	S2
Synthesis of the Starting Materials.....	S3
CO ₂ -Exchange Experiments in Solution	S4
NMR Spectra.....	S5
Matrix IR Spectra	S12
IR Spectroscopic Data.....	S24
Matrix UV/VIS Spectra.....	S28
Kinetic Analyses	S30
NBO and QTAIM Analysis.....	S38
Computed Potential Energy Surfaces.....	S40
Other Carbene-CO ₂ Complexes	S47
Tunneling Computations	S51
Cartesian Coordinates of Computed Structures	S62
References	S101
Full Citations for Electronic Structure Codes	S103

Methods

Matrix Isolation Studies

All matrix isolation experiments were performed with a Sumitomo cryostat system consisting of an F-70 compressor unit and an RDK 408D2 closed-cycle refrigerator cold head. For the infrared (IR) measurements polished KBr windows in the vacuum shroud and a CsI window on the sample holder were used. Silicon diodes attached to the sample holder measured the temperature (deposition at 15 K, measurements at 3 K if not stated otherwise). During the experiments, pure 2-amino-2-thioacetic acid (**2**) was kept in a storage bulb in the dark and at room temperature (r.t.). The matrix host gas (Ar, gas purity of 99.999%) was stored in a 2 L glass balloon that was refilled and flushed three times with Ar before every experiment. The typical deposition time of our experiments was 1 h in which a total amount of ca. 60 mbar of Ar together with **2** were deposited on both sides of the matrix window. For irradiation a high-pressure mercury lamp (SP200) in conjunction with an MSH 150 monochromator system from LOT-QuantumDesign GmbH was used. The IR spectra were recorded with a Bruker Vertex 70 FTIR spectrometer equipped with a standard KBr or wide-range beam-splitter in a range from 7000 cm^{-1} to 350 cm^{-1} (resolution: 0.7 cm^{-1}). For every measurement 50 scans were performed. For ultraviolet/visible (UV/Vis) measurements a Jasco V-760 spectrophotometer was used in the range from 190 nm to 800 nm (resolution: 1 nm). Prior to deposition a background spectrum of the cold matrix window was recorded. During deposition the matrix was kept in the dark to avoid unwanted photochemistry.

Computations

All computations at the B3LYP^{1,2}/6-311++G(3df,3pd)^{3,4} and the MP2^{5,6}/def2-QZVPP^{7,8} levels of theory using an ultrafine grid and very tight geometry convergence criteria were performed with Gaussian16 Revision B.01 (full citations of electronic structure codes are given at the end of this document). Anharmonic frequencies at the B3LYP/6-311++G(3df,3pd) level of theory were computed using the Freq=Anharmonic keyword. The computed minima on the PES feature no imaginary frequencies while all transition states possess one such frequency. UV/Vis spectra were computed at the TD-B3LYP/6-311++G(3df,3pd) level of theory. Bond and ring critical points were computed using the output=wfn keyword at the B3LYP/6-311++G(3df,3pd) level of theory and visualized with AIMAll studio.

CVT/SCT rate constants were computed with POLYRATE 2017 at B3LYP/6-311++G(d,p).

Natural bond orbitals (NBO), natural resonance theory (NRT), and Wiberg bond indices were computed with NBO7 at the B3LYP/6-311++G(3df,3pd) level of theory based on geometries at the same level.

For coupled-cluster computations (CCSD(T)^{9,10}/cc-pVTZ¹¹⁻¹⁴) CFOUR 1.0 was used with the following keywords: ABCDTYPE=AOBASIS, CC_PROG=ECC, SCF_CONV=8, and CC_CONV=10; CONVERGENCE=8 in addition for geometry optimizations; VIB=EXACT for analytical computations of harmonic frequencies; METHOD=TS for transition states.

Bond and ring critical points and the Laplacian have been visualized using the AIMAll software package¹⁵ with Bader's quantum theory of atoms in molecules (QTAIM)¹⁶.

Synthesis of the Starting Materials

2-Amino-2-Thioacetic Acid (**2**)

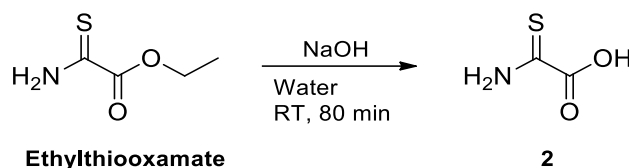


Fig. S1. Synthesis of 2-amino-2-thioacetic acid (**2**).

Ethylthiooxamate was obtained from TCI Europe N. V. in > 98% purity and was used without further purification. 0.30 g (2.25 mmol) ethylthiooxamate was dissolved in 20 mL aqueous NaOH (2.8 mol L⁻¹) and stirred for 80 min at r.t. The solution was cooled to 0 °C and concentrated aqueous HCl (12 mol L⁻¹) was added until pH = 3-4 was reached. The solution was extracted four times with 80 mL ethyl acetate in total. The solvent was removed and **2** was obtained as a yellow solid. If necessary, the product was purified by sublimation.

Yield: 74 mg (0.70 mmol, 31%).

¹H NMR (400 MHz, DMSO-*d*₆): δ = 10.2 (s, 1H (NH)), 9.84 (s, 1H (NH)), not visible (broad s, 1H (OH)) ppm.

¹³C{¹H} NMR (101 MHz, DMSO-*d*₆): δ = 192.4, 164.1 ppm.

IR (ATR): ν = 3406.5, 3289.6, 2722.7, 2410.6, 1720.4, 1593.4, 1444.4, 1406.6, 1240.5, 1183.9, 919.6, 846.5, 752.0, 692.4, 636.6, 589.3, 469.6 cm⁻¹.

HRMS (ESI): *m/z* = 103.9811 [M-H]⁺ (calcd. *m/z* = 103.9812).

All-Deutero-2-Amino-2-Thioacetic Acid (**2-d**₃)

176 mg **2** was dissolved in 20 mL D₂O (99.9%) purchased from Deutero GmbH. After 14 days the solvent was removed and the product was obtained as a yellow solid. If necessary, the product was purified by sublimation.

Yield: 181 mg (0.68 mmol, quant.).

¹H NMR (400 MHz, DMSO-*d*₆): δ = 10.2 (s, 1H (NH)), 9.87 (s, 1H (NH)) (visible through exchange with water in the solvent), not visible (broad s, 1H (OH)) ppm.

¹³C{¹H} NMR (101 MHz, DMSO-*d*₆): δ = 192.1, 163.9 ppm.

IR (ATR): ν = 2902.9, 2559.8, 2408.5, 2091.6, 1971.5, 1705.4, 1478.2, 1322.4, 1226.4, 1158.7, 1013.1, 774.2, 692.9, 616.1, 537.7, 467.6 cm⁻¹.

HRMS (ESI): *m/z* = 105.9934 [M-D]⁺ (calcd. *m/z* = 105.9937).

High resolution mass spectrometry was performed with a Bruker MicroTOF (negative mode ESI-MS).

CO₂-Exchange Experiments in Solution

Inert Conditions

In a glove box 50 mg **K-2** were dispersed in 8 ml of dry DMF in a Fischer-Porter tube. The tube was degassed three times and filled with 1 atm of ¹³CO₂. The solution was stirred for 20 h at 70 °C. The solvent was removed *via* distillation (50 °C at 30 mbars).

Standard Conditions

50 mg **K-2** were dispersed in 8 ml of DMF in a Fischer-Porter tube. The tube was degassed three times and filled with 1 atm of ¹³CO₂. The solution was stirred for 20 h at 70 °C. The solvent was removed *via* distillation (50 °C at 30 mbars).

NMR Spectra

All NMR spectra were recorded with a Bruker AV400 spectrometer at 298 K. The chemical shifts (δ) are given in ppm relative to the respective solvent residual peak of DMSO- d_6 ($\delta = 2.50$ and 39.5 ppm). ATR-IR spectra were recorded on a Bruker Alpha spectrometer ($4000 - 400 \text{ cm}^{-1}$).

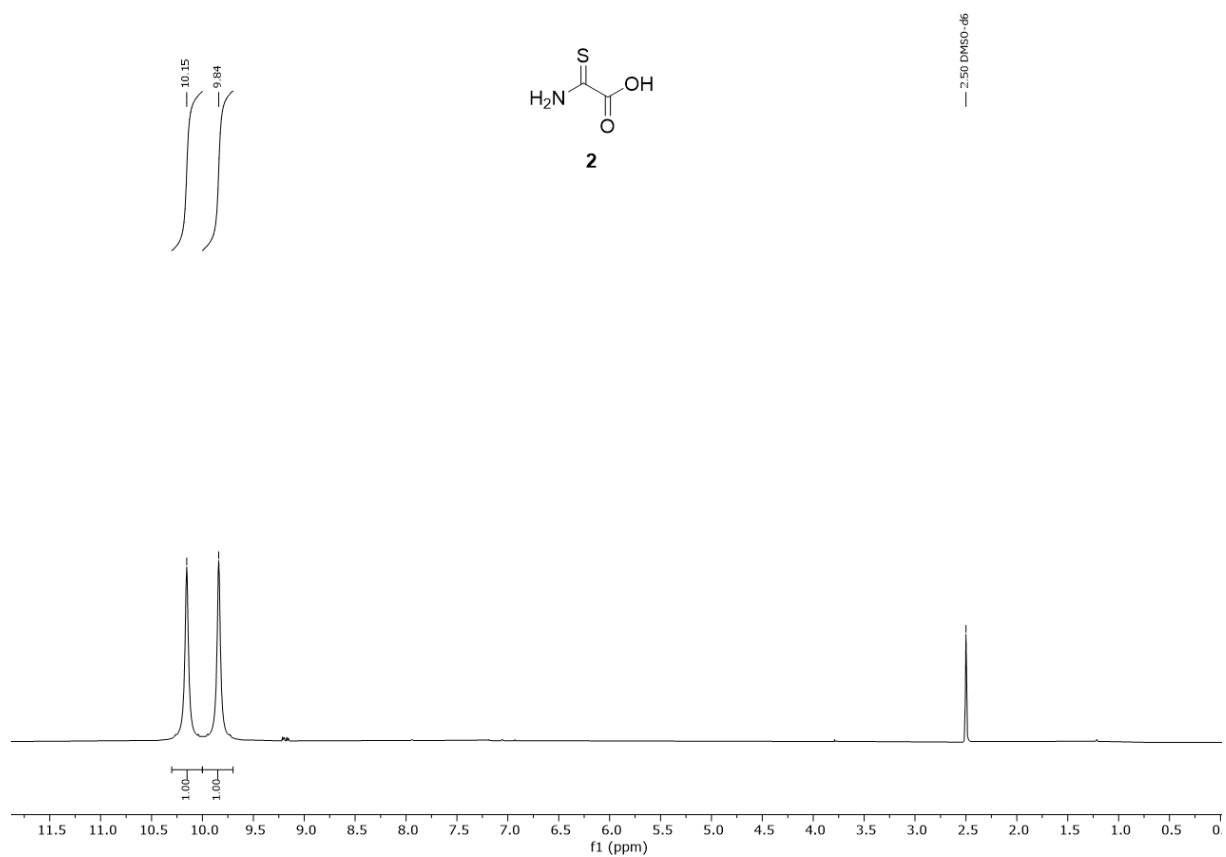


Fig. S2. ^1H NMR (400 MHz, DMSO- d_6) of 2-amino-2-thioxoacetic acid (**2**).

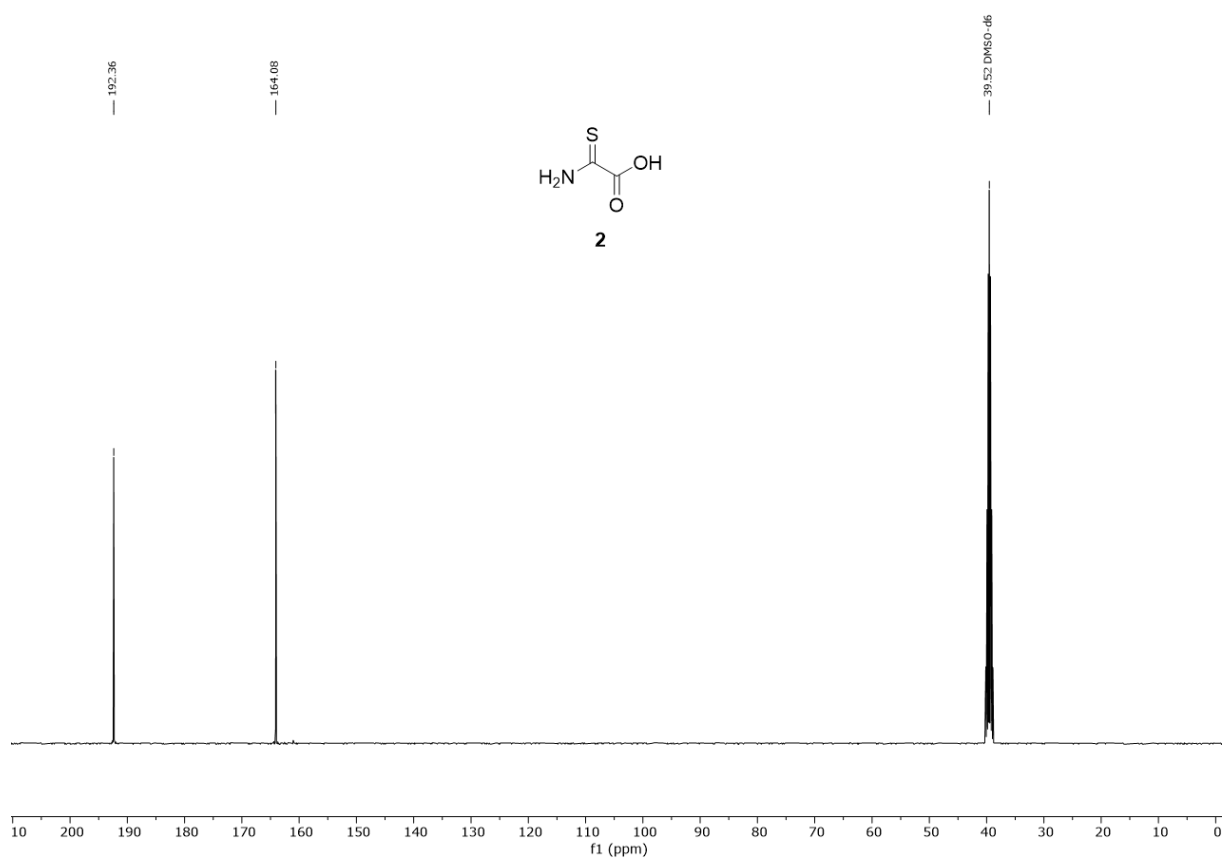


Fig. S3. $^{13}\text{C}\{^1\text{H}\}$ NMR (101 MHz, $\text{DMSO-}d_6$) of 2-amino-2-thioxoacetic acid (**2**).

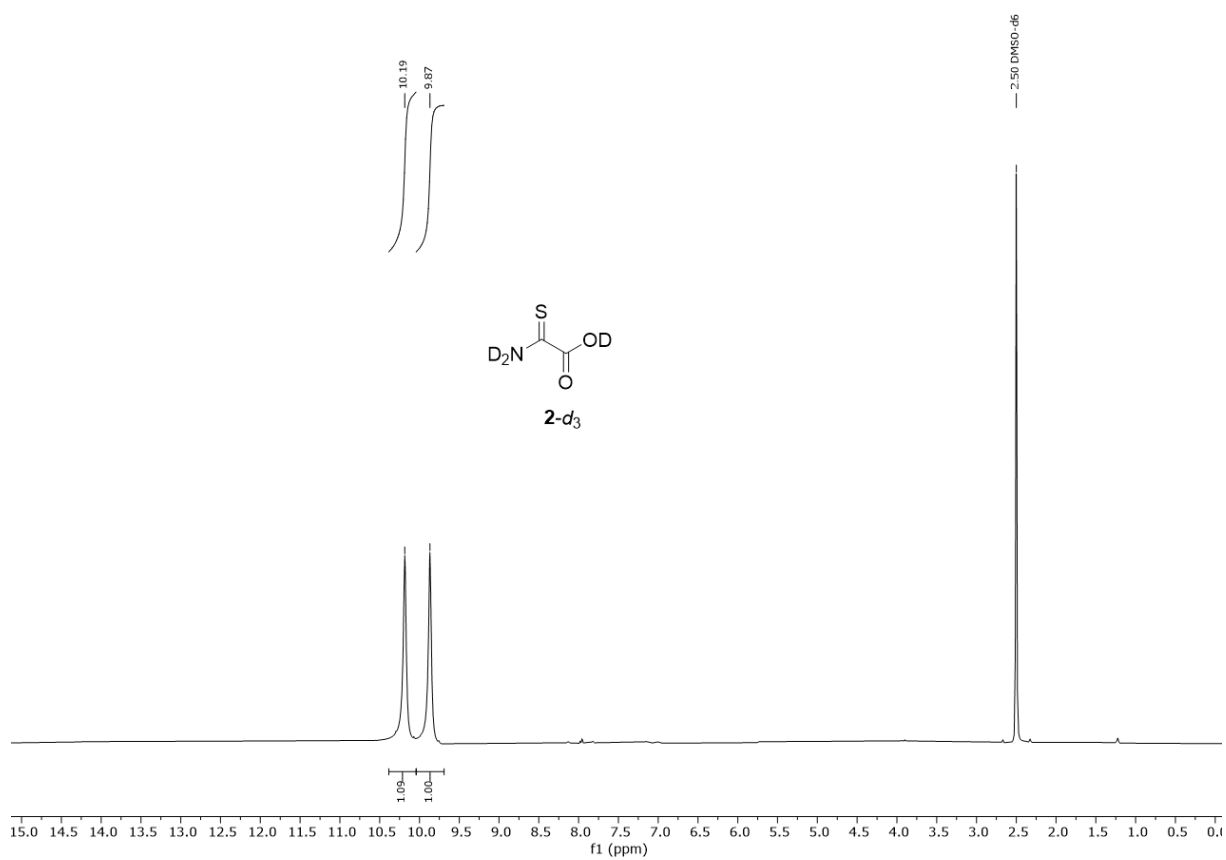


Fig. S4. ^1H NMR (400 MHz, $\text{DMSO-}d_6$) of 2-amino-2-thioxoacetic acid- d_3 (**2- d_3**) (visible through exchange with water in the solvent).

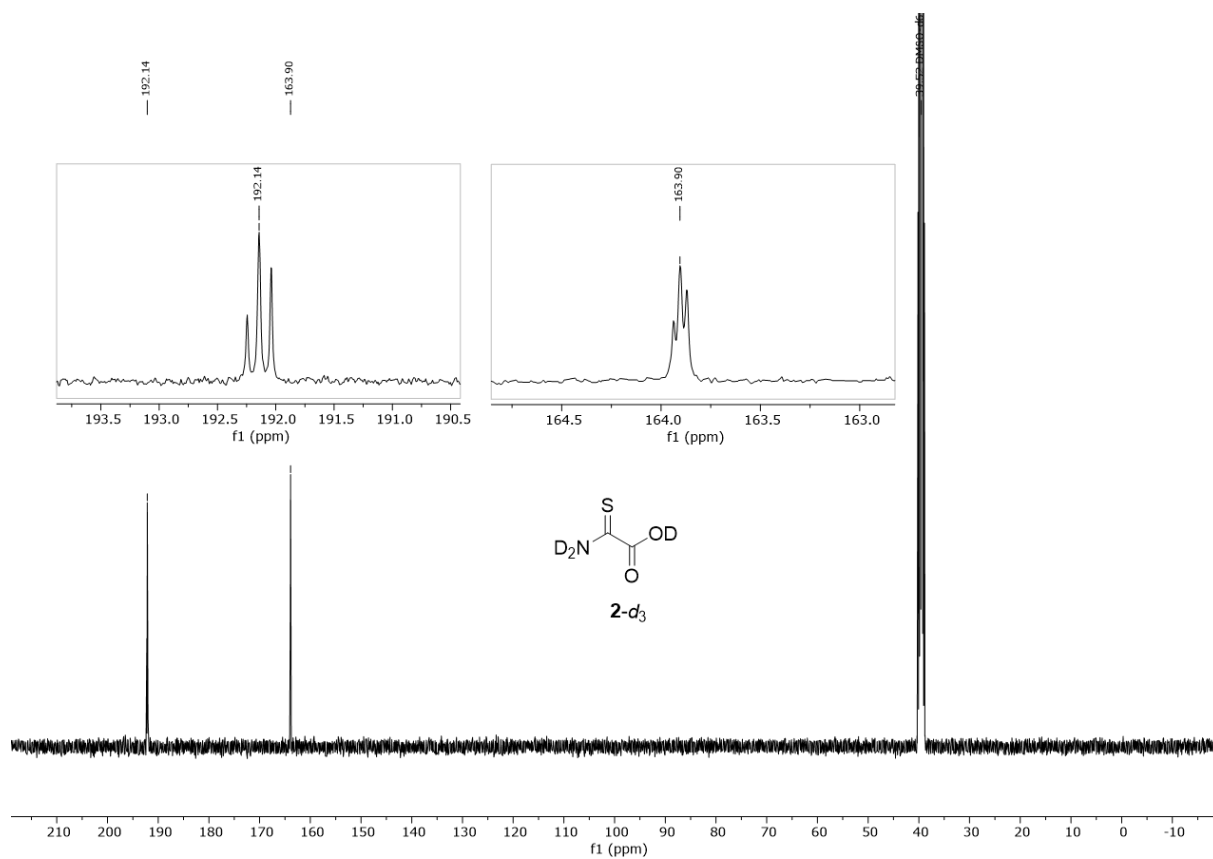


Fig. S5. $^{13}\text{C}\{^1\text{H}\}$ NMR (101 MHz, $\text{DMSO-}d_6$) of 2-amino-2-thioxoacetic acid- d_3 (**2- d_3**) (splitting visualizes complete deuteration).

$^{13}\text{C}_2$ -exchange experiment

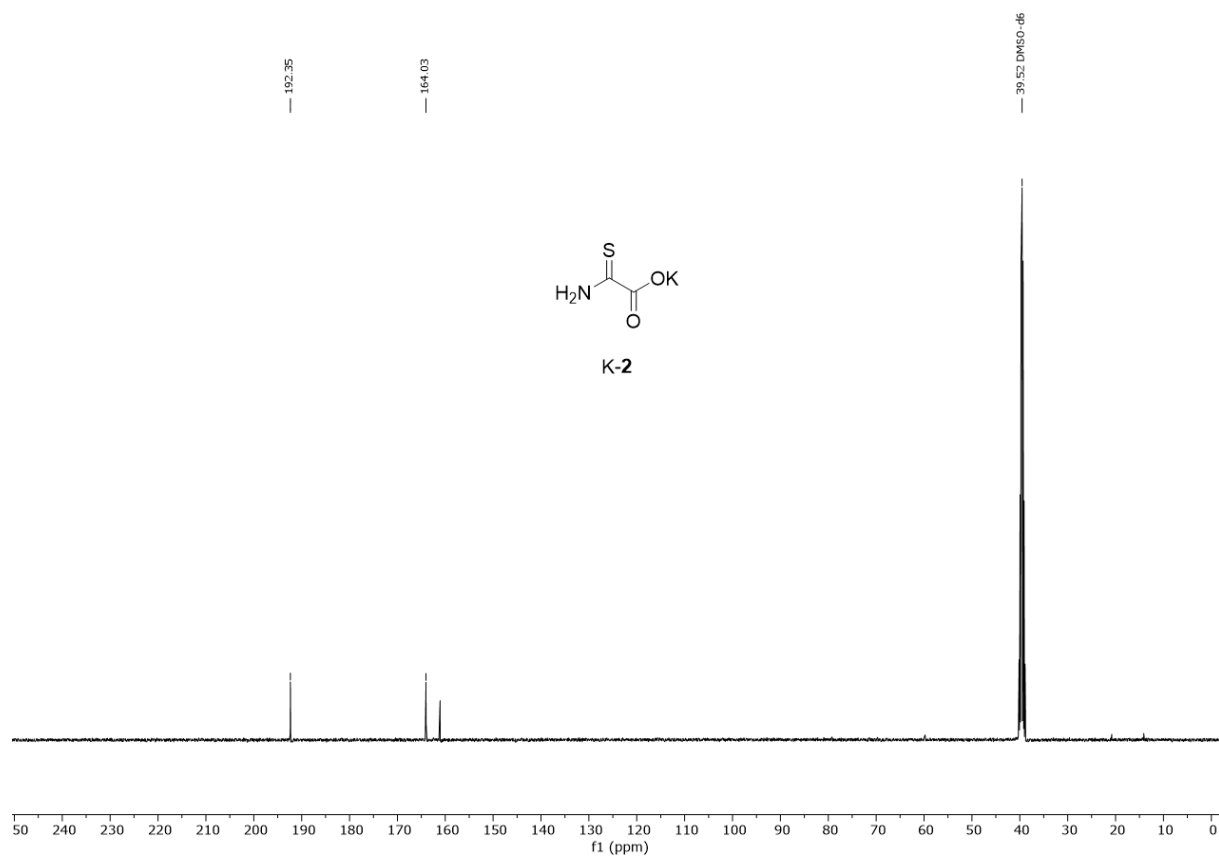


Fig. S6. $^{13}\text{C}\{^1\text{H}\}$ NMR (101 MHz, $\text{DMSO-}d_6$) of 2-amino-2-thioxoacetic acid potassium salt (K-2).

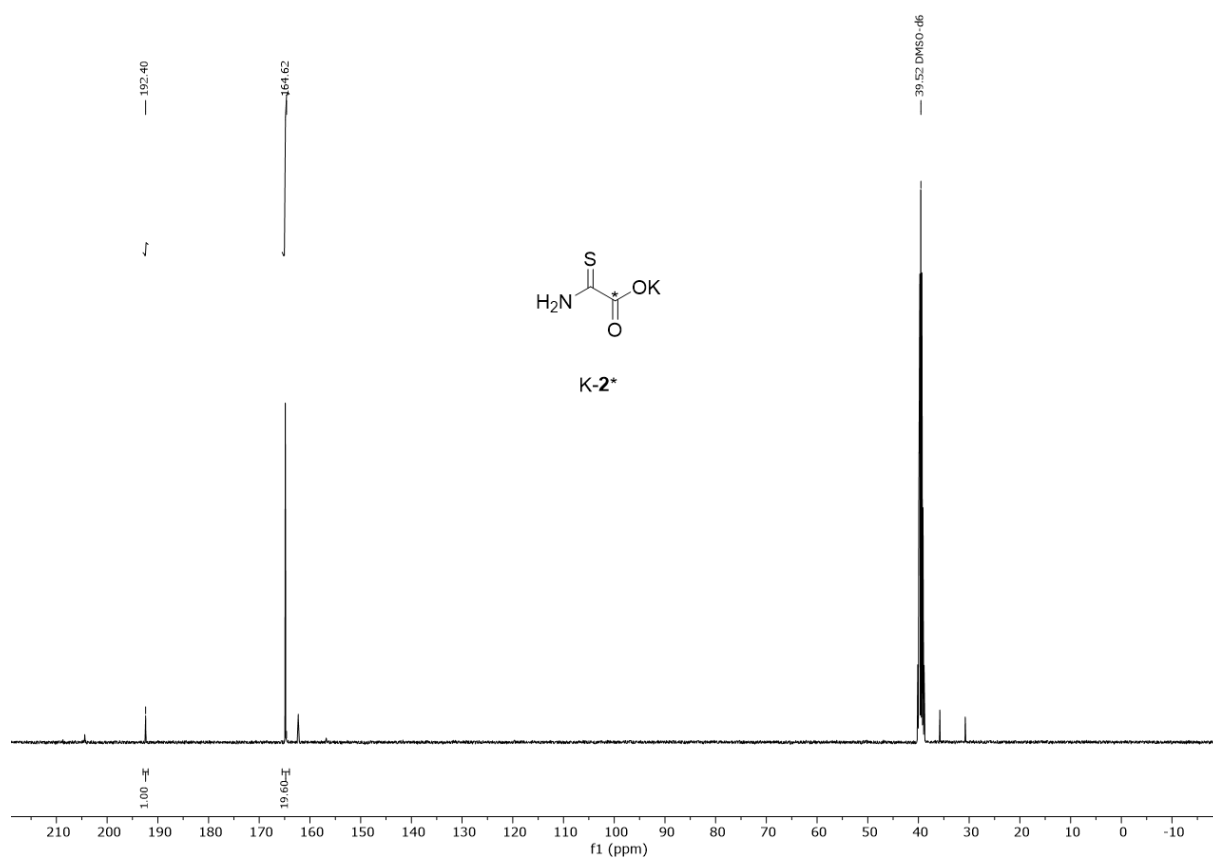


Fig. S7. $^{13}\text{C}\{^1\text{H}\}$ NMR (101 MHz, DMSO- d_6) of ^{13}C -labelled 2-amino-2-thioxoacetic acid potassium salt (K-2*).

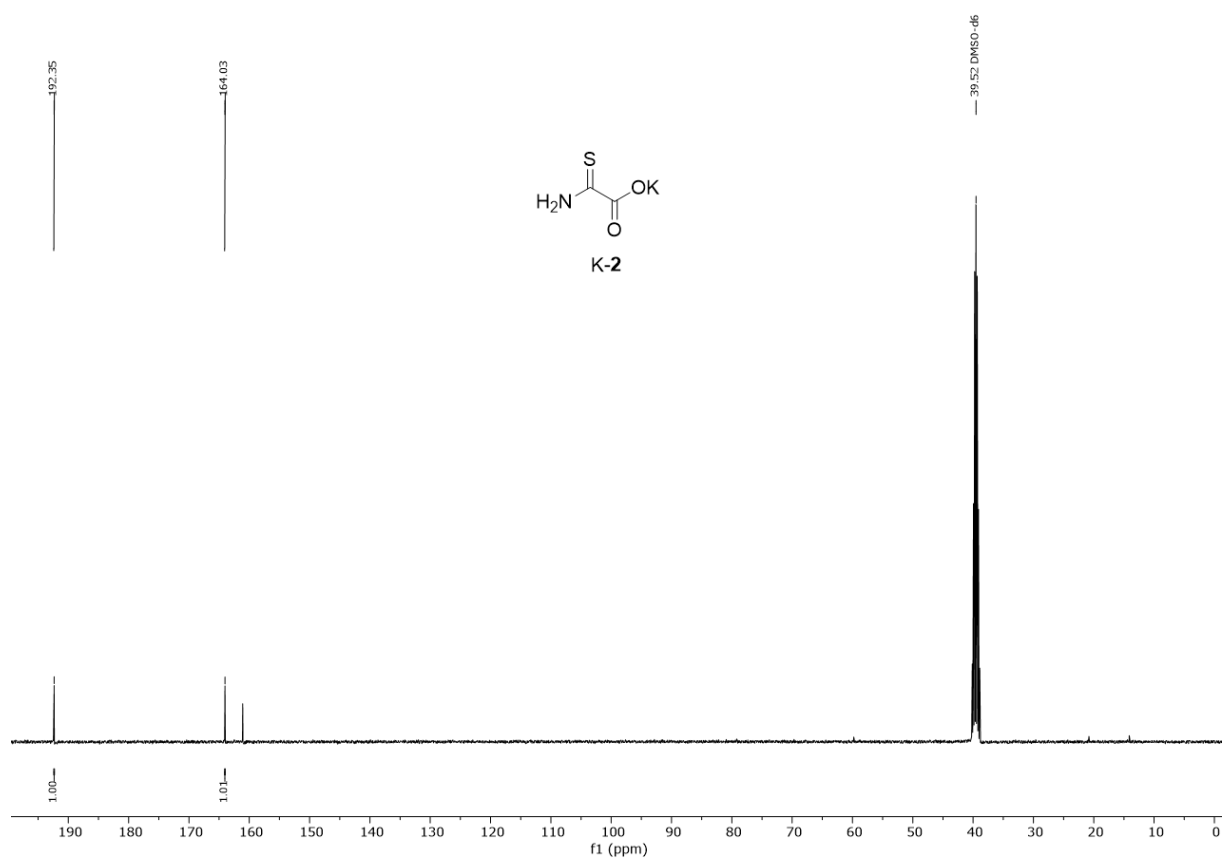


Fig. S8: ^{13}C NMR (101 MHz, $\text{DMSO-}d_6$) of potassium-2-amino-2-thioacetic acetate (K-2) with DMF.

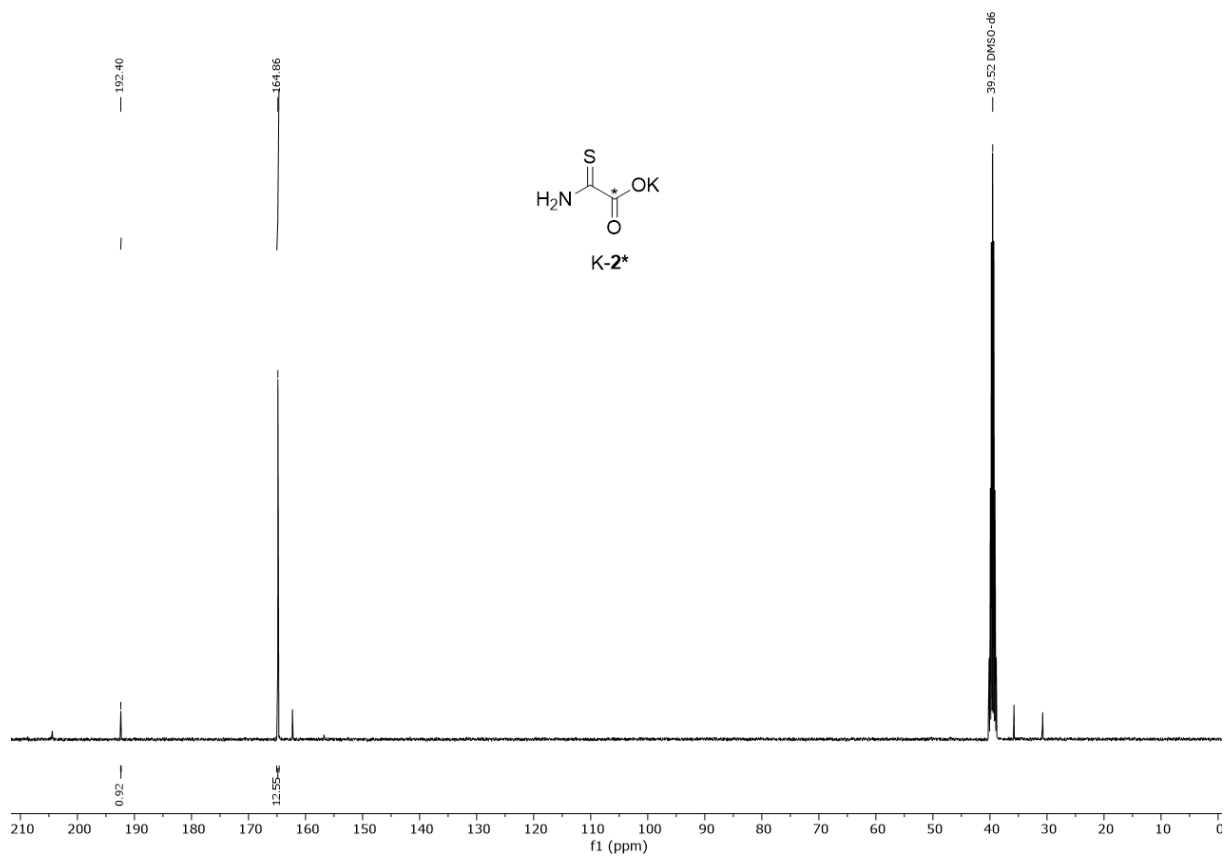


Fig. S9: ^{13}C NMR (101 MHz, DMSO- d_6) of C-labelled potassium-2-amino-2-thioacetic acetate (K-2*) with DMF (12,7% enrichment of ^{13}C).

Matrix IR Spectra

2-Amino-2-Thioxoacetic Acid

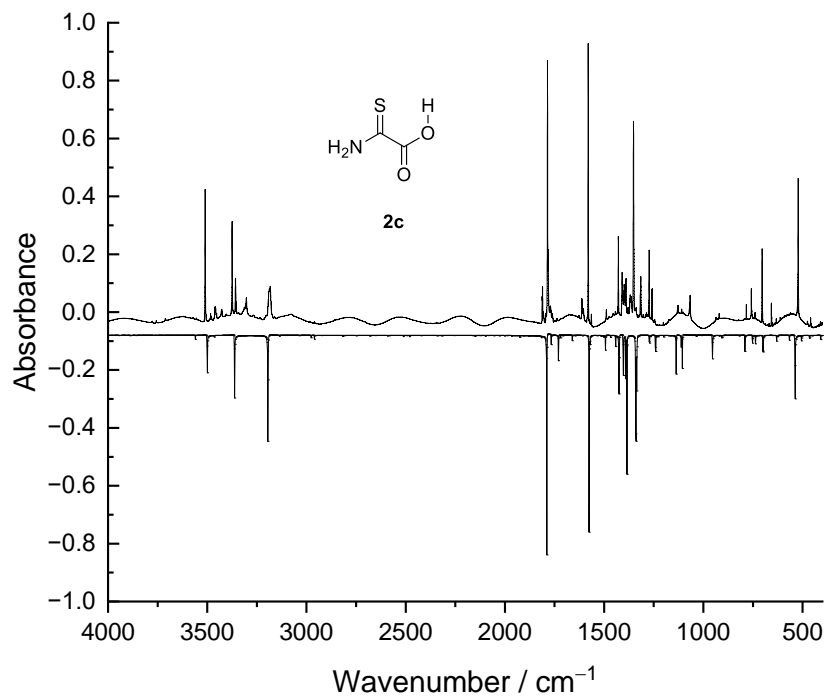


Fig. S10. Experimental spectrum of 2-amino-2-thioxoacetic acid recorded at 3 K in an Ar matrix (upper trace) compared to the computed anharmonic spectrum at the B3LYP/6-311++G(3df,3pd) level of theory (most stable conformer **2c**, lower trace).

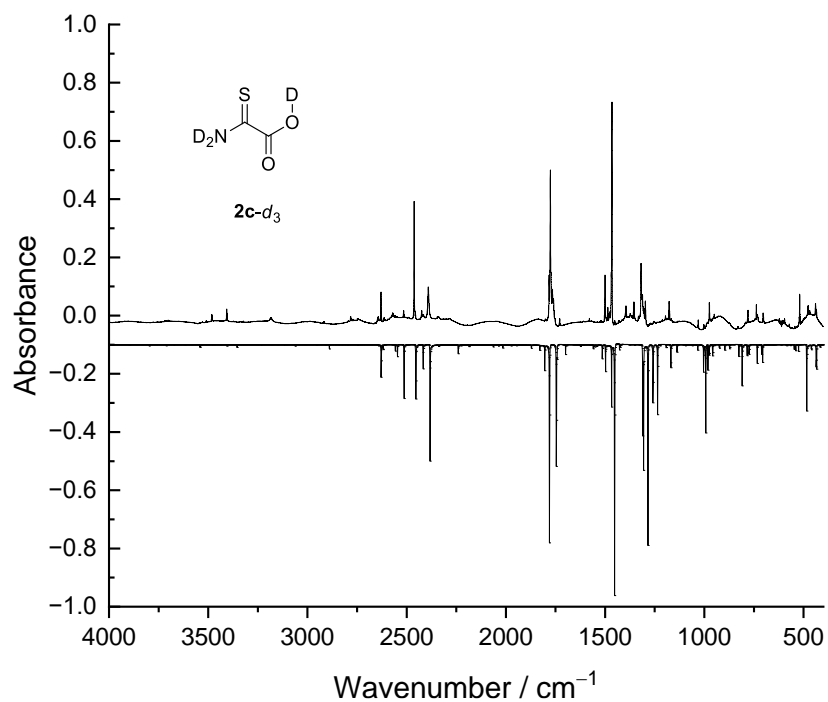


Fig S11. Experimental spectrum of trideuterated 2-amino-2-thioacetic acid recorded at 3 K in an Ar matrix (upper trace) compared to the computed anharmonic spectrum at the B3LYP/6-311++G(3df,3pd) level of theory (most stable conformer **2c-d₃**, lower trace).

Pyrolysis of 2-Amino-2-Thioacetic Acid (2)

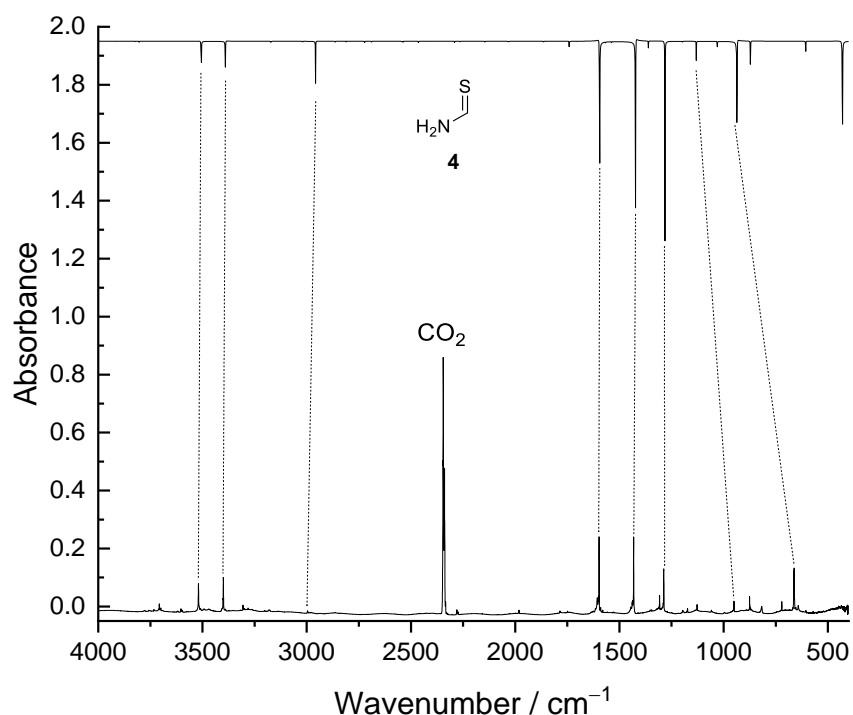


Fig. S12. Under HVFP conditions **2** decomposes to CO₂ and thioformamide¹⁷ (**4**; computed anharmonic spectrum at the B3LYP/6-311++G(3df,3pd) level of theory). Changing the pyrolysis temperature from 300 °C to 1150 °C increases the degree of decomposition. Aminomercaptomethylene (**1**) could not be detected in any HVFP experiment.

Photolysis of 2-Amino-2-Thioacetic Acid (**2**)

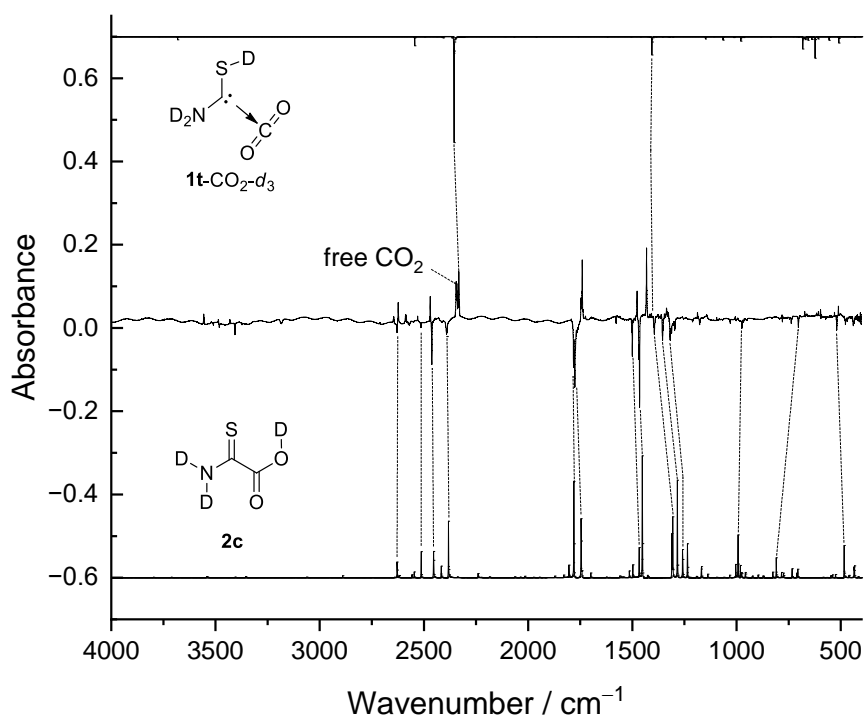


Fig. S13. Irradiation of perdeuterated **2c-d₃** at 254 nm for 4 min generates **1t-CO₂-d₃**. The corresponding difference spectrum between 1 min and 4 min of irradiation is compared to the computed spectra of **1t-CO₂-d₃** computed at the B3LYP/6-311++G(3df,3pd) level of theory. The corresponding spectra for the undeuterated isotopologue are depicted in the main text.

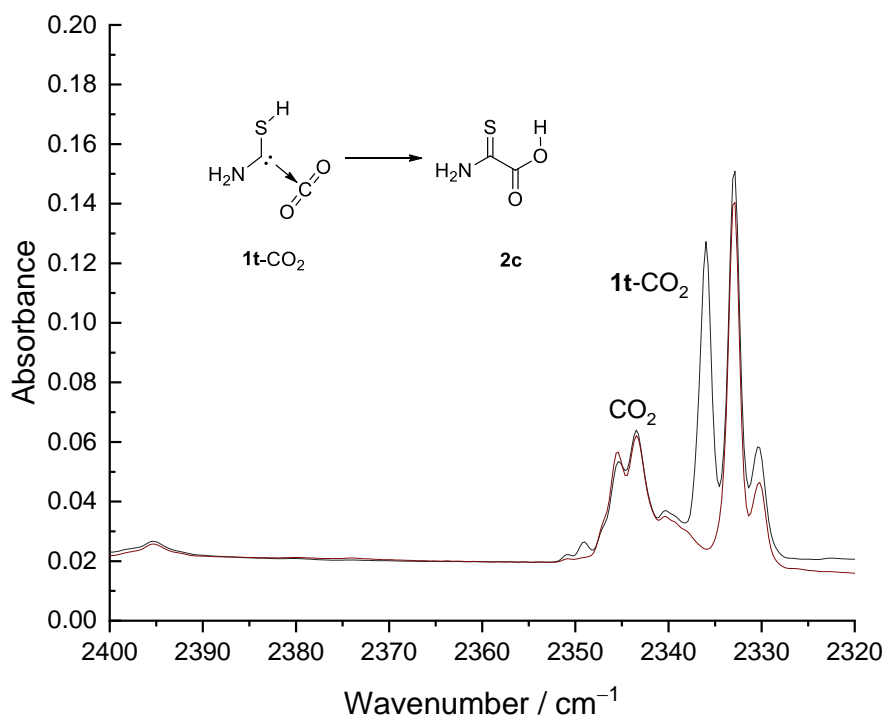


Fig. S14. To exclude activation induced by the IR spectrometer the matrix was kept for 70 h in the dark and **1t-CO₂** still vanishes.

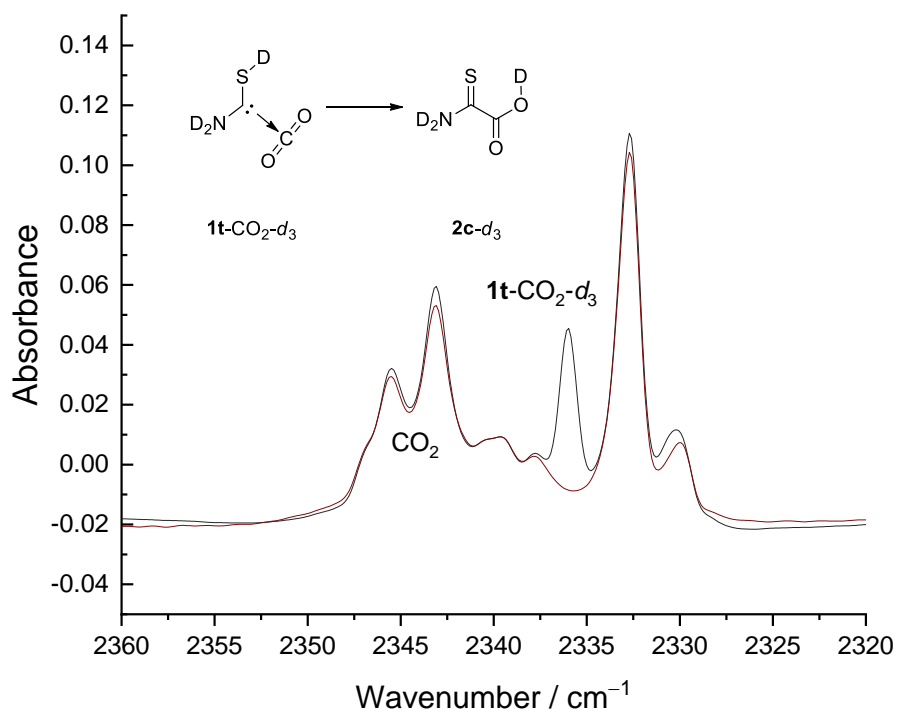


Fig. S15. To exclude activation induced by the IR spectrometer the matrix was kept in the dark for 67 h and $1t\text{-CO}_2\text{-}d_3$ still vanishes.

Further irradiation decomposes both complexes but to a different extent (Fig. S13). The black trace shows the spectrum of the starting material. After 1 min of irradiation (254 nm) **1t**-CO₂ starts to form and nearly no free CO₂ has evolved. The spectrum measured after irradiation for additional 3 min (red trace) shows strong absorptions of CO₂ and the complex bands further ensue. After another 10 min of irradiation the CO₂ bands ensue but the complex's bands start to decrease.

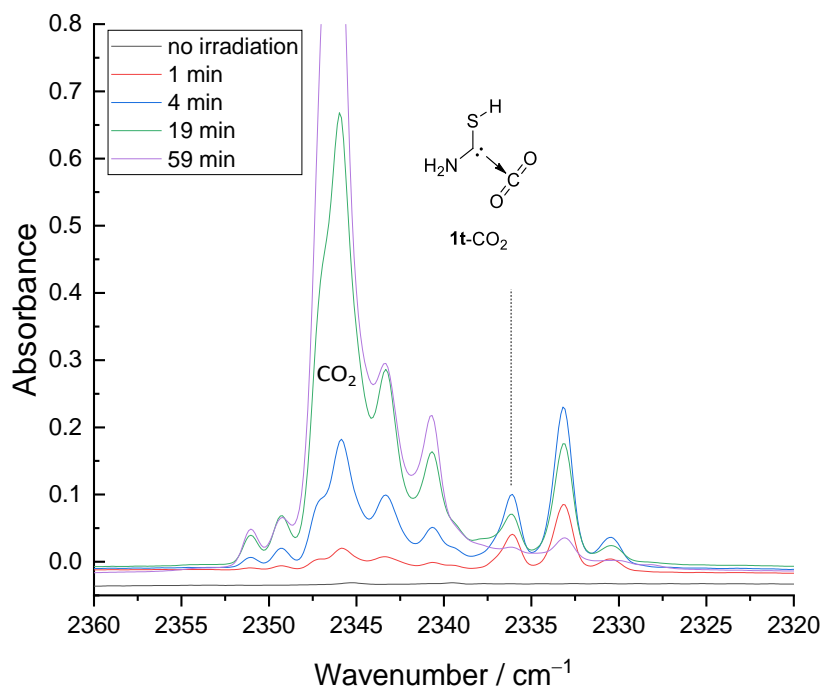


Fig. S16. Optimal irradiation time. The black spectrum was measured after deposition of precursor **2**. When the matrix is irradiated at 254 nm for 1 min (red spectrum) **1t**-CO₂ starts to form. Upon further irradiation for 3 min the bands of the complex ensue and free CO₂ starts to form (blue spectrum). Further irradiation for 15 min leads to decomposition of **1t**-CO₂.

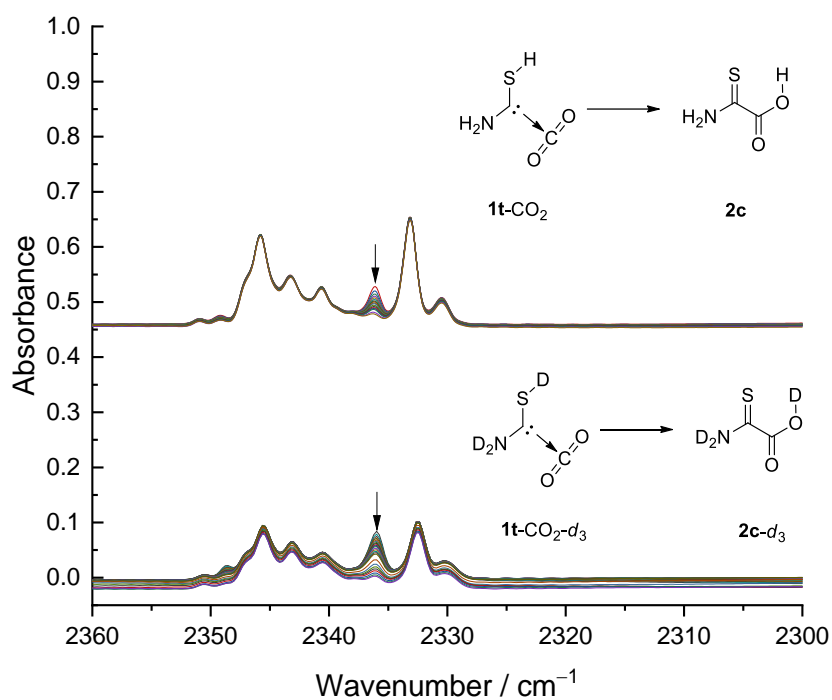


Fig. S17. Both **1t**-CO₂ and its perdeuterated isotopologue **1t**-CO₂-d₃ react back to the starting material **2** with half-lives of 31 min and 90 min, respectively.

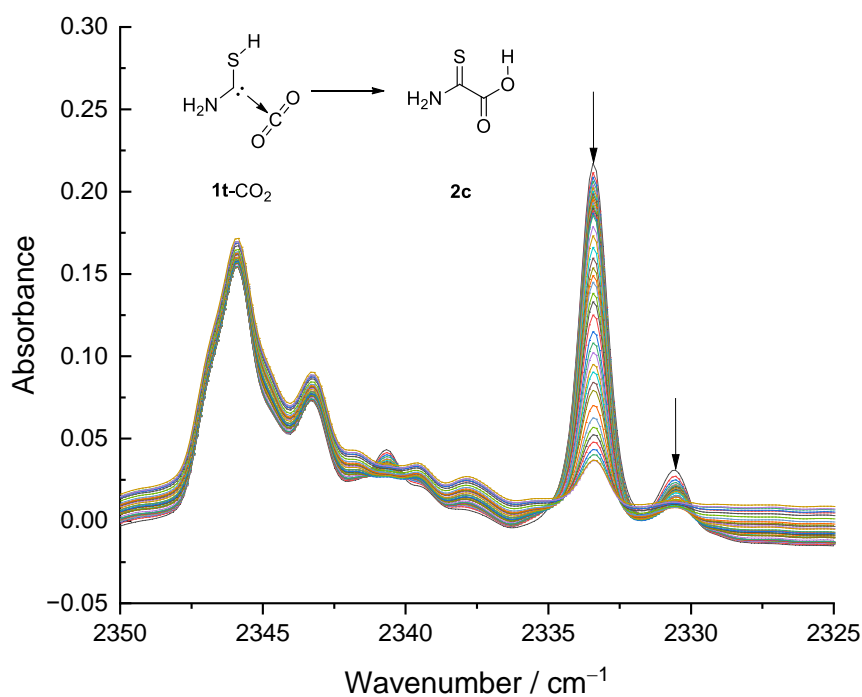


Fig. S18. Two other matrix sites of **1t**-CO₂ lead to slower kinetics at 20 K (left arrow: 95 h, right arrow 16 h).

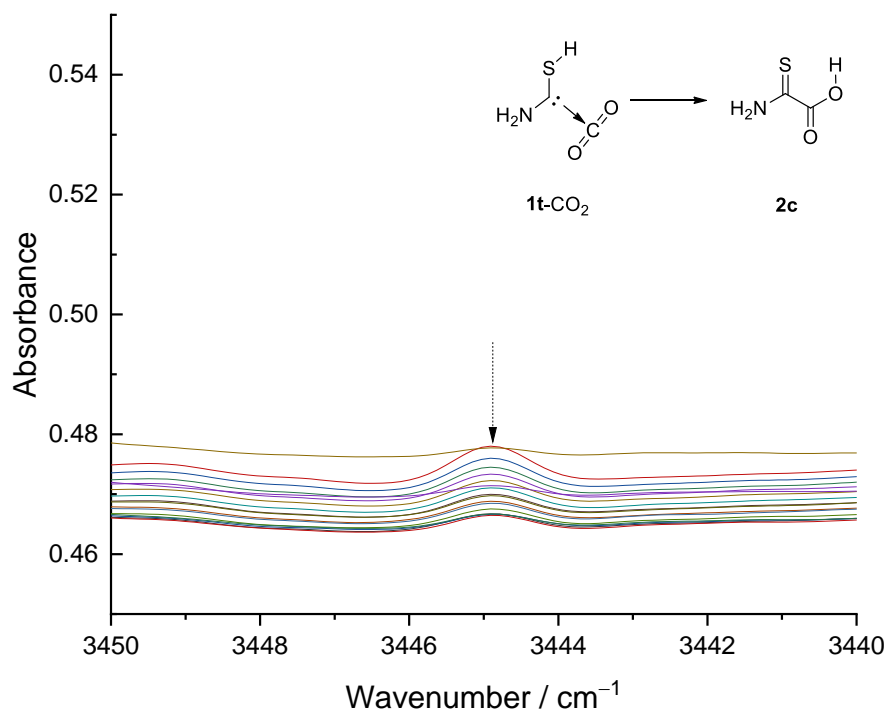


Fig. S19. Decrease of the $\nu(\text{NH})$ vibration of **1t-CO₂** over time. Note that the band intensity is small compared to the baseline shift.

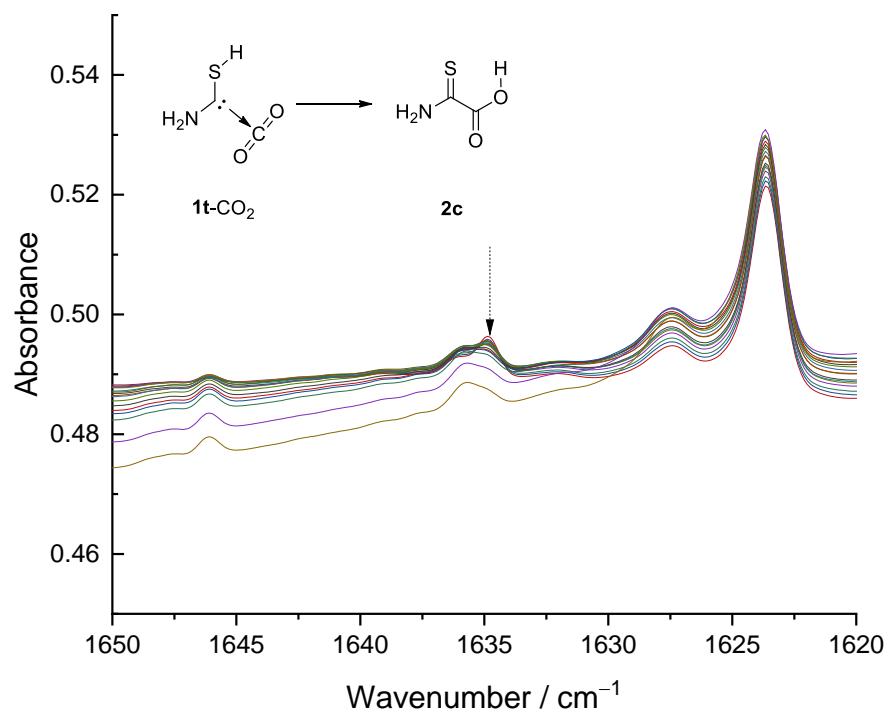


Fig. S20. Decrease of the $\nu(\text{NH}_2)$ vibration of **1t-CO₂** over time.

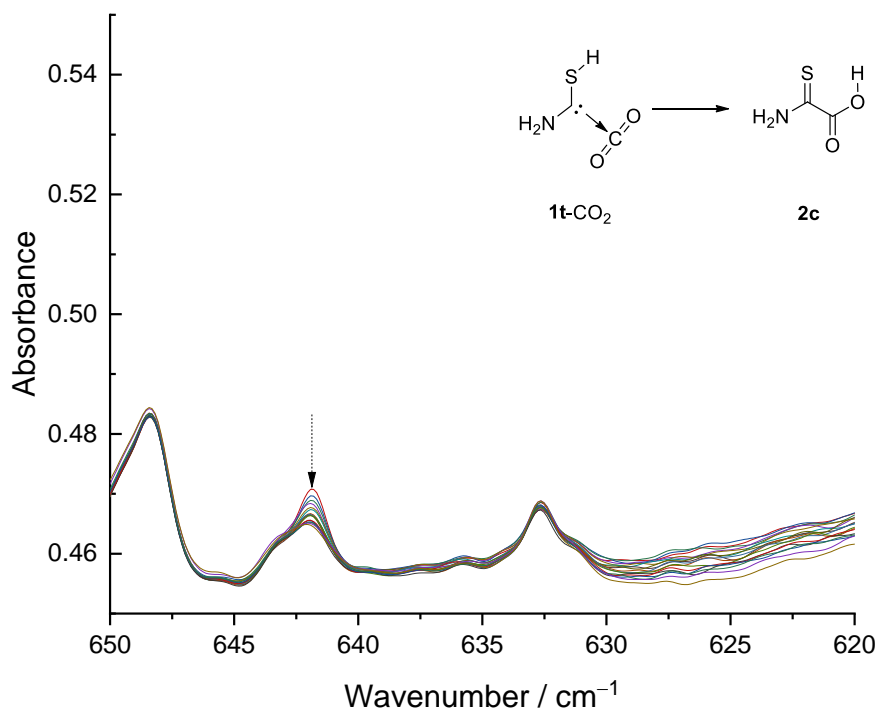


Fig. S21. Decrease of the $\delta(\text{CO}_2)$ vibration of **1t-CO₂** over time.

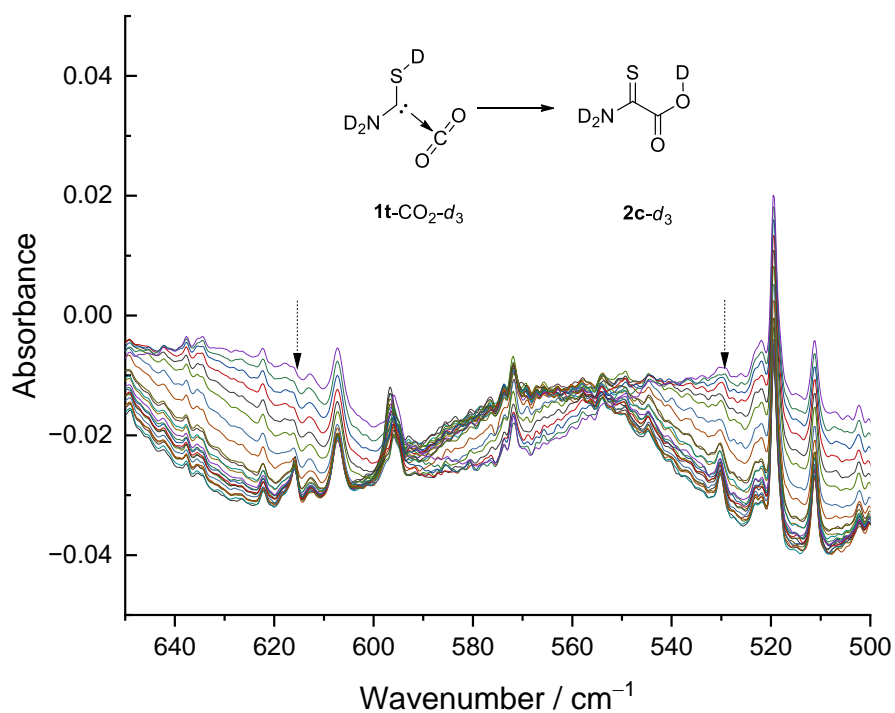


Fig. S22. Decrease of the $\omega(\text{ND}_2)$ and $\delta(\text{CO}_2)$ vibrations of **1t-CO₂-d₃** over time. Note that the band intensity is small compared to the baseline shift.

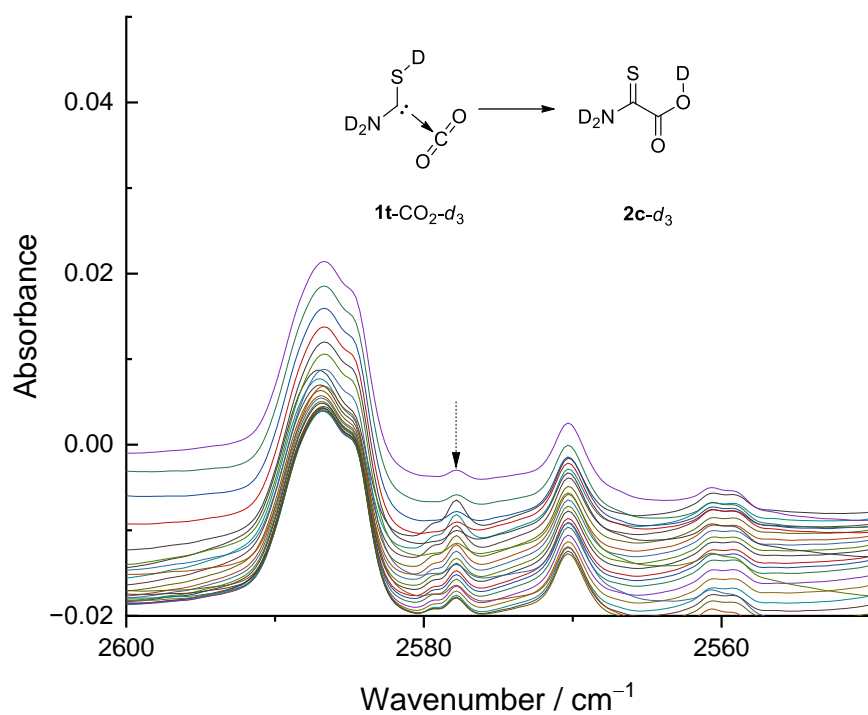


Fig. S23. Decrease of the $\nu_{\text{as}}(\text{ND}_2)$ vibration of **1t-CO₂-d₃** over time. Note that the band intensity is small compared to the baseline shift.

Rotamerization of 2-Amino-2-Thioacetic Acid (**2**)

Upon irradiation of an Ar matrix containing **2c** at 254 nm for 1 min **2c** rotamerizes to **2t**. When keeping the resulting matrix in the dark **2t** vanishes with a half-life of 1.5 h (CVT/SCT//B3LYP/6-311+G(d,p): 1.3 h at 10 K). Repeating the same experiment with perdeuterated **2**, we do not observe this spontaneous reverse reaction. This clearly hints towards a QMT reaction from **2t** to **2c**, which is associated with an activation barrier of 9.9 kcal mol⁻¹ at the CCSD(T)/cc-pVTZ level of theory.

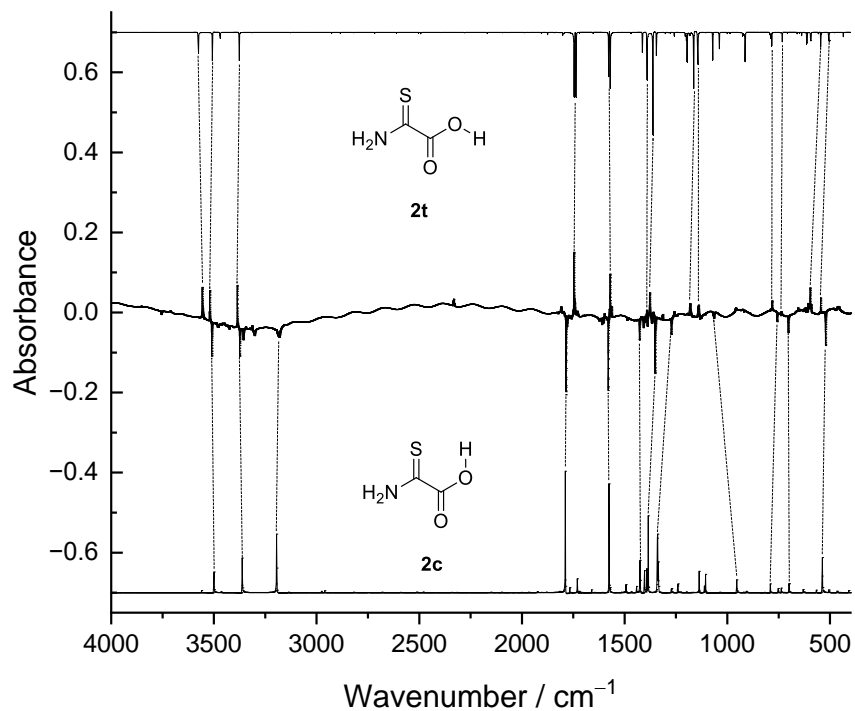


Fig. S24. Experimental difference spectrum compared to the computed anharmonic spectra of **2c** and **2t** at the B3LYP/6-311++G(3df,3pd) level of theory. Upon irradiation at 254 nm for 1 min **2c** rotamerizes to **2t**.

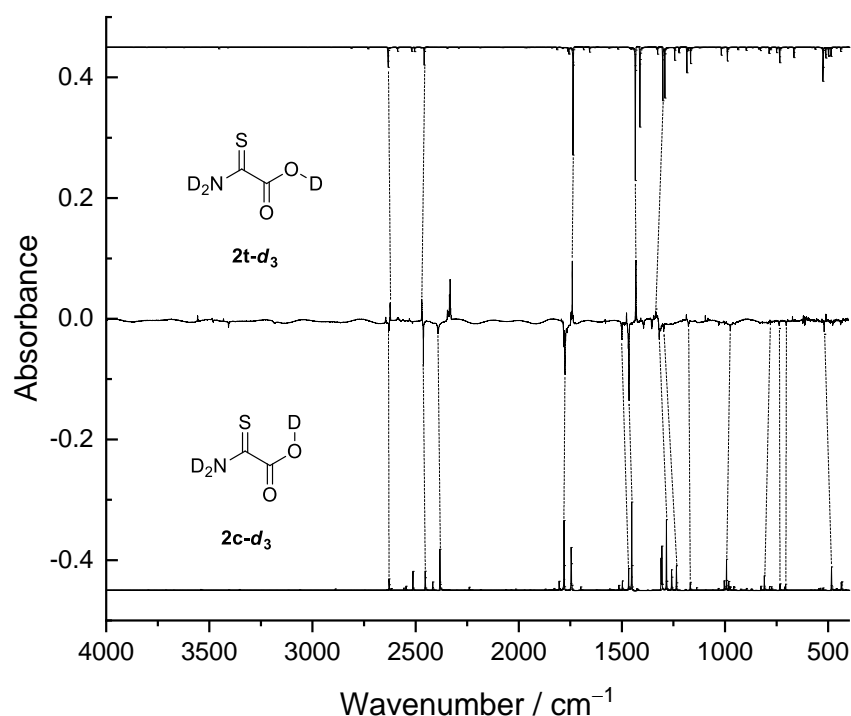


Fig. S25. Experimental difference spectrum compared to the computed anharmonic spectra of **2c-d₃** and **2t-d₃** at the B3LYP/6-311++G(3df,3pd) level of theory. Upon irradiation at 254 nm for 1 min **2t-d₃** rotamerizes to **2c-d₃**.

Isomerization of 2-Amino-2-Thioxoacetic Acid (**2**)

Thiolimine tautomers form under UV-irradiation from the corresponding thioamides^{18,19}. Both **2c** and **2t** can undergo isomerization to 16 conceivable conformers of the corresponding thiolimine (**3**) via 1,3[*H*]-shifts and consecutive rotamerizations. After 4 min of irradiation, we observed two new bands in the CO-stretching region, which we assign to two thiolimine conformers that are formed in one elementary step from **2c** and **2t**, respectively. These two species (**3a** and **3b**) vanish with half-lives of 1.8 h and 2.3 h. When investigating the perdeuterated starting material, the corresponding bands do not vanish implicating that these 1,3[*H*]-shifts are also QMT reactions. Only two such cases of 1,3[*H*]-shifts via QMT are reported for thioamides^{18,20,21}. Interconversions of thiolimine conformers via SH rotational QMT have been reported recently^{17,19} and might contribute to the overall decrease of the thiolimine concentration over time.

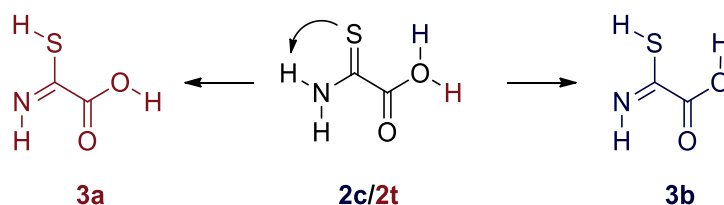


Fig. S26. Thiolimines **3a** and **3b** are the only of 16 conceivable conformers of **3** that can form in one elemental step from **2c** and **2t** without further rotamerizations.

Fig. 27 shows the carbonyl region of the IR spectrum, in which **3a** and **3b** show the highest band intensities. **3a** and **3b** react back to the starting material when keeping the matrix in the dark.

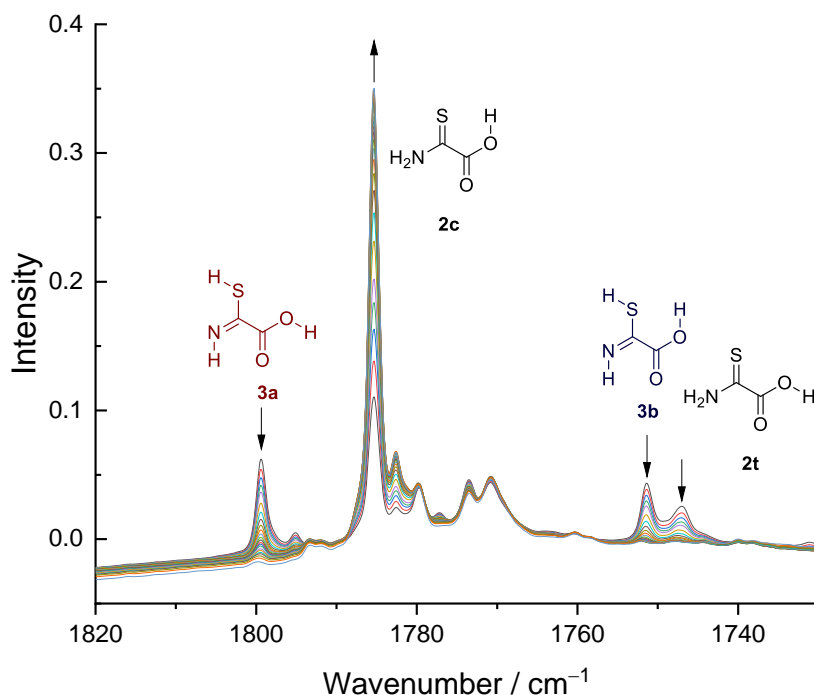


Fig. S27. A 1,3[*H*] shift leads to various thiolimine conformers of the precursor. We assign those bands tentatively to **3a** and **3b**. They vanish over time and reform the precursor **2c**. In the perdeuterated case, the corresponding bands remain unchanged.

Thiazolylidene-CO₂ Complex (**13**)

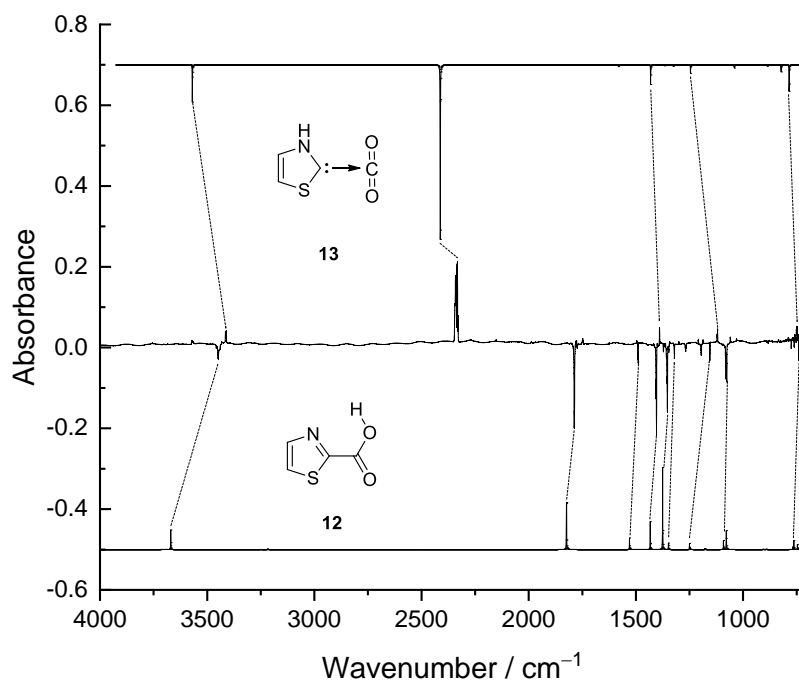


Fig. S28. Top: Computed spectrum of **13** at the B3LYP/6-311++G(3df,3pd) level of theory. Bottom: Computed spectrum of **12** at the B3LYP/6-311++G(3df,3pd) level of theory. Middle: Difference spectrum before and after irradiation of the matrix with 254 nm for 10 min. All observed bands agree with reported reference data.²²

IR Spectroscopic Data

Table S1. Comparison of experimental vibrational frequencies **1t**-CO₂ isolated in an argon matrix at 3 K and computed vibrational frequencies at the B3LYP/6-311++G(3df,3pd) level of theory (unscaled).

Assignment ^a	Sym.	$\tilde{\nu}_{\text{anharm.}} / \text{cm}^{-1}$	$I_{\text{rel.}} / \text{km mol}^{-1}$	$\tilde{\nu}_{\text{harm.}} / \text{cm}^{-1}$	$I_{\text{rel.}} / \text{km mol}^{-1}$	$\tilde{\nu}_{\text{exp.}} / \text{cm}^{-1}$	$I_{\text{rel.}}^{\text{b}}$
$\delta(\text{CCO})$	a'	52.2	2.6	47.0	3.5	o.o.r.	o.o.r.
$\tau(\text{CC})$	a''	57.9	2.7	51.4	1.7	o.o.r.	o.o.r.
$\omega(\text{CC})$	a''	86.3	1.5	101.6	8.6	o.o.r.	o.o.r.
$\delta(\text{CCN})$	a'	116.7	7.8	102.1	0.5	o.o.r.	o.o.r.
$\delta(\text{CCO})$	a'	139.5	0.5	147.3	0.4	o.o.r.	o.o.r.
$\delta(\text{NCS})$	a'	398.4	12.3	399.9	12.5	n.o.	n.o.
$\tau(\text{CS})$	a''	451.7	22.4	431.6	26.7	n.o.	n.o.
$\delta(\text{CO}_2)$	a'	625.3	114.9	628.5	122.0	641.8	w
$\omega(\text{CO}_2)$	a''	650.4	94.4	674.9	1.5	n.o.	n.o.
$\omega(\text{NH}_2)$	a''	670.8	15.1	683.6	148.7	n.o.	n.o.
$\nu(\text{CS})$	a'	684.2	34.9	705.5	32.9	n.o.	n.o.
$\tau(\text{CN})$	a''	728.3	24.4	733.6	2.6	n.o.	n.o.
$\delta(\text{CSH})$	a'	955.7	13.2	970.8	14.1	n.o.	n.o.
$\delta(\text{CNH})$	a'	1176.2	18.0	1204.5	16.4	n.o.	n.o.
$\nu_{\text{s}}(\text{CO}_2)$	a'	1380.7	1.2	1366.1	1.6	n.o.	n.o.
$\nu(\text{CN})$	a'	1395.7	10.9	1405.9	98.0	n.o.	n.o.
$\delta(\text{NH}_2)$	a'	1633.0	58.2	1664.5	77.7	1634.8	w
						2336.1,	
$\nu_{\text{as}}(\text{CO}_2)$	a'	2356.7	516.4	2404.6	562.2	2333.2,	s
						2330.4	
$\nu(\text{SH})$	a'	2570.8	0.5	2685.1	0.8	n.o.	n.o.
$\nu_{\text{s}}(\text{NH}_2)$	a'	3175.1	11.4	3404.2	8.8	n.o.	n.o.
$\nu_{\text{as}}(\text{NH}_2)$	a'	3404.6	67.4	3586.6	86.1	3444.9	w

a: assignments (ν = stretching, δ = bending, ω = wagging, τ = twisting, ρ = rocking; s = symmetric, as = antisymmetric).

b: rel. experimental intensities (vw = very weak, w = weak, m = middle, s = strong, vs = very strong); n.o. = not observed; o.o.r. = out of range.

Table S2. Comparison of experimental vibrational frequencies of **1t**-CO₂-d₃ isolated in an argon matrix at 3 K and computed vibrational frequencies at the B3LYP/6-311++G(3df,3pd) level of theory (unscaled).

Assignment ^a	Sym.	$\tilde{\nu}_{\text{anharm.}} / \text{cm}^{-1}$	$I_{\text{rel.}} / \text{km mol}^{-1}$	$\tilde{\nu}_{\text{harm.}} / \text{cm}^{-1}$	$I_{\text{rel.}} / \text{km mol}^{-1}$	$\tilde{\nu}_{\text{exp.}} / \text{cm}^{-1}$	$I_{\text{rel.}}^{\text{b}}$
$\delta(\text{CCO})$	a'	51.4	2.7	45.9	3.3	o.o.r.	o.o.r.
$\tau(\text{CC})$	a''	54.4	2.7	49.1	1.4	o.o.r.	o.o.r.
$\omega(\text{CC})$	a''	84.0	1.0	93.2	5.8	o.o.r.	o.o.r.
$\delta(\text{CCN})$	a'	104.2	4.4	97.7	0.4	o.o.r.	o.o.r.
$\delta(\text{CCO})$	a'	137.4	0.4	145.8	0.3	o.o.r.	o.o.r.
$\tau(\text{CS})$	a''	326.1	18.0	317.7	20.4	o.o.r.	o.o.r.
$\delta(\text{NCS})$	a'	356.7	10.2	358.2	10.1	n.o.	n.o.
$\omega(\text{ND}_2)$	a''	510.2	39.0	522.0	45.7	530.2	w
$\omega(\text{NCS})$	a''	557.6	17.4	569.7	12.6	n.o.	n.o.
$\delta(\text{CO}_2)$	a'	624.3	102.2	628.2	119.1	615.9	w
$\nu(\text{CS})$	a''	670.6	11.2	671.2	33.1	n.o.	n.o.
$\omega(\text{CO}_2)$	a'	671.8	15.1	676.0	27.3	n.o.	n.o.
$\delta(\text{CSD})$	a'	702.9	3.8	713.6	2.5	n.o.	n.o.
$\delta(\text{CND})$	a'	967.6	8.4	987.2	14.4	n.o.	n.o.
$\delta(\text{ND}_2)$	a'	1150.8	15.7	1168.5	17.9	n.o.	n.o.
$\nu_{\text{s}}(\text{CO}_2)$	a'	1386.8	2.7	1366.4	3.4	n.o.	n.o.
$\nu(\text{CN})$	a'	1406.9	112.9	1438.7	130.5	1408.3	w
$\nu(\text{SD})$	a'	1869.7	0.2	1929.0	0.2	n.o.	n.o.
						2336.0,	
$\nu_{\text{as}}(\text{CO}_2)$	a'	2356.3	529.6	2404.2	564.2	2332.6,	s
						2330.2	
$\nu_{\text{s}}(\text{ND}_2)$	a'	2365.3	8.2	2464.6	10.0	n.o.	n.o.
$\nu_{\text{as}}(\text{ND}_2)$	a'	2544.9	42.1	2645.3	50.0	2577.9	w

a: assignments (ν = stretching, δ = bending, ω = wagging, τ = twisting, ρ = rocking; s = symmetric, as = antisymmetric).

b: rel. experimental intensities (vw = very weak, w = weak, m = middle, s = strong, vs = very strong); n.o. = not observed; o.o.r. = out of range.

Table S3. Computed vibrational frequencies of **1c-CO₂** at the B3LYP/6-311++G(3df,3pd) level of theory (unscaled). We did not observe **1c-CO₂** experimentally.

Assignment ^a	Sym.	$\tilde{\nu}_{\text{anharm.}} / \text{cm}^{-1}$	$I_{\text{rel.}} / \text{km mol}^{-1}$	$\tilde{\nu}_{\text{harm.}} / \text{cm}^{-1}$	$I_{\text{rel.}} / \text{km mol}^{-1}$	$\tilde{\nu}_{\text{exp.}} / \text{cm}^{-1}$	$I_{\text{rel.}}^{\text{b}}$
$\delta(\text{CCO})$	a'	38.4	7.4	46.2	4.9	o.o.r.	o.o.r.
$\tau(\text{CC})$	a''	45.8	4.9	49.0	4.5	o.o.r.	o.o.r.
$\omega(\text{CC})$	a''	47.2	24.4	103.1	29.9	o.o.r.	o.o.r.
$\delta(\text{CCN})$	a'	85.6	1.4	103.6	2.2	o.o.r.	o.o.r.
$\delta(\text{CCO})$	a'	124.5	0.4	135.2	0.2	o.o.r.	o.o.r.
$\delta(\text{NCS})$	a'	391.1	6.9	396.6	6.1	n.o.	n.o.
$\tau(\text{CS})$	a''	481.5	0.0	524.6	0.0	n.o.	n.o.
$\delta(\text{CO}_2)$	a'	625.6	102.2	637.8	110.0	n.o.	n.o.
$\omega(\text{NH}_2)$	a''	636.0	101.5	669.1	76.2	n.o.	n.o.
$\omega(\text{CO}_2)$	a''	675.9	36.2	677.8	76.7	n.o.	n.o.
$\nu(\text{CS})$	a'	689.4	21.5	709.2	21.1	n.o.	n.o.
$\tau(\text{CN})$	a''	724.4	10.5	729.2	2.8	n.o.	n.o.
$\delta(\text{CSH})$	a'	906.9	38.9	941.6	40.3	n.o.	n.o.
$\delta(\text{CNH})$	a'	1158.9	8.7	1189.0	8.7	n.o.	n.o.
$\nu_{\text{s}}(\text{CO}_2)$	a'	1389.6	1.8	1368.7	1.3	n.o.	n.o.
$\nu(\text{CN})$	a'	1418.8	42.5	1427.9	94.0	n.o.	n.o.
$\delta(\text{NH}_2)$	a'	1625.7	64.7	1656.1	83.9	n.o.	n.o.
$\nu_{\text{as}}(\text{CO}_2)$	a'	2271.7	549.7	2408.3	567.8	n.o.	n.o.
$\nu(\text{SH})$	a'	2361.2	115.5	2413.2	122.2	n.o.	n.o.
$\nu_{\text{s}}(\text{NH}_2)$	a'	3156.9	19.3	3383.9	19.6	n.o.	n.o.
$\nu_{\text{as}}(\text{NH}_2)$	a'	3409.5	58.5	3582.2	77.2	n.o.	n.o.

a: assignments (ν = stretching, δ = bending, ω = wagging, τ = twisting, ρ = rocking; s = symmetric, as = antisymmetric).

b: rel. experimental intensities (vw = very weak, w = weak, m = middle, s = strong, vs = very strong); n.o. = not observed; o.o.r. = out of range.

Table S4. Computed vibrational frequencies of **1c-CO₂-d₃** at the B3LYP/6-311++G(3df,3pd) level of theory (unscaled). We did not observe **1c-CO₂-d₃** experimentally.

Assignment ^a	Sym.	$\tilde{\nu}_{\text{anharm.}} / \text{cm}^{-1}$	$I_{\text{rel.}} / \text{km mol}^{-1}$	$\tilde{\nu}_{\text{harm.}} / \text{cm}^{-1}$	$I_{\text{rel.}} / \text{km mol}^{-1}$	$\tilde{\nu}_{\text{exp.}} / \text{cm}^{-1}$	$I_{\text{rel.}}^{\text{b}}$
$\delta(\text{CCO})$	a'	7.7	3.5	45.7	4.7	o.o.r.	o.o.r.
$\tau(\text{CC})$	a''	47.0	4.8	47.4	4.2	o.o.r.	o.o.r.
$\omega(\text{CC})$	a''	83.7	1.2	89.7	19.7	o.o.r.	o.o.r.
$\delta(\text{CCN})$	a'	87.8	3.2	98.5	1.7	o.o.r.	o.o.r.
$\delta(\text{CCO})$	a'	127.0	0.2	134.7	0.2	o.o.r.	o.o.r.
$\delta(\text{NCS})$	a'	334.7	4.9	339.7	4.5	o.o.r.	o.o.r.
$\tau(\text{CS})$	a''	374.2	2.1	395.7	2.4	n.o.	n.o.
$\omega(\text{ND}_2)$	a''	499.9	44.7	516.5	46.9	n.o.	n.o.
$\omega(\text{NCS})$	a''	552.3	12.1	565.3	11.5	n.o.	n.o.
$\delta(\text{CO}_2)$	a'	634.7	100.6	636.9	108.7	n.o.	n.o.
$\omega(\text{CO}_2)$	a''	673.7	27.3	676.8	27.9	n.o.	n.o.
$\nu(\text{CS})$	a'	663.8	3.4	685.7	5.6	n.o.	n.o.
$\delta(\text{CSD})$	a'	689.7	33.1	707.1	32.5	n.o.	n.o.
$\delta(\text{CND})$	a'	952.2	18.6	970.8	15.8	n.o.	n.o.
$\delta(\text{ND}_2)$	a'	1154.2	19.5	1171.0	21.6	n.o.	n.o.
$\nu_{\text{s}}(\text{CO}_2)$	a'	1390.8	3.5	1368.8	2.1	n.o.	n.o.
$\nu(\text{CN})$	a'	1428.4	102.2	1458.3	118.2	n.o.	n.o.
$\nu(\text{SD})$	a'	1662.6	57.8	1733.5	57.8	n.o.	n.o.
$\nu_{\text{as}}(\text{CO}_2)$	a'	2360.6	546.6	2408.0	576.5	n.o.	n.o.
$\nu_{\text{s}}(\text{ND}_2)$	a'	2339.9	10.0	2450.1	18.9	n.o.	n.o.
$\nu_{\text{as}}(\text{ND}_2)$	a'	2542.4	34.9	2641.1	43.0	n.o.	n.o.

a: assignments (ν = stretching, δ = bending, ω = wagging, τ = twisting, ρ = rocking; s = symmetric, as = antisymmetric).

b: rel. experimental intensities (vw = very weak, w = weak, m = middle, s = strong, vs = very strong); n.o. = not observed; o.o.r. = out of range.

Table S5. Comparison of experimental vibrational frequencies of **2c** isolated in an argon matrix at 3 K and computed vibrational frequencies at the B3LYP/6-311++G(3df,3pd) level of theory (unscaled).

Assignment ^a	Sym.	$\tilde{\nu}_{\text{anharm.}} / \text{cm}^{-1}$	$I_{\text{rel.}} / \text{km mol}^{-1}$	$\tilde{\nu}_{\text{harm.}} / \text{cm}^{-1}$	$I_{\text{rel.}} / \text{km mol}^{-1}$	$\tilde{\nu}_{\text{exp.}} / \text{cm}^{-1}$	$I_{\text{rel.}}^{\text{b}}$
$\tau(\text{CC})$	a''	92.9	8.3	93.8	7.6	o.o.r.	o.o.r.
$\delta(\text{CC})$	a'	267.9	31.3	273.6	29.9	o.o.r.	o.o.r.
$\delta(\text{CN})$	a'	360.9	3.5	368.7	3.9	n.o.	n.o.
$\omega(\text{CCN})$	a''	410.5	4.7	416.4	8.4	n.o.	n.o.
$\delta(\text{CCN})$	a'	466.4	7.1	479.4	8.0	n.o.	n.o.
$\omega(\text{NH}_2)$	a''	539.5	145.7	531.2	157.3	521.9	s
$\delta(\text{CCO})$	a'	559.7	0.3	565.5	0.5	n.o.	n.o.
$\tau(\text{CN})$	a''	631.8	8.8	663.1	6.7	n.o.	n.o.
$\tau(\text{CO})$	a''	701.1	51.6	737.1	63.8	703.9	m
$\nu(\text{CC})$	a'	754.2	17.2	765.3	21.3	758.3	w
$\omega(\text{CCO})$	a''	792.2	18.0	799.7	6.1	n.o.	n.o.
$\delta(\text{CNH})$	a'	908.6	7.4	931.5	3.4	n.o.	n.o.
$\nu(\text{CO})$	a'	1166.1	0.5	1217.5	4.6	1066.7	w
$\delta(\text{CNH})$	a'	1273.7	22.7	1281.4	25.2	1273.2	m
$\delta(\text{COH})$	a'	1341.6	319.6	1397.6	446.1	1352.2	s
$\nu(\text{CN})$	a'	1405.6	71.1	1443.3	129.6	1428.4	m
$\delta(\text{NH}_2)$	a'	1577.4	208.2	1615.8	259.2	1580.1	vs
$\nu(\text{C=O})$	a'	1790.0	251.7	1821.4	284.3	1758.6	vs
$\nu(\text{OH})$	a'	3195.3	231.4	3455.5	217.5	3357.8	w
$\nu_{\text{s}}(\text{NH}_2)$	a'	3363.6	95.7	3533.4	122.2	3374.9	m
$\nu_{\text{as}}(\text{NH}_2)$	a'	3501.3	70.8	3684.5	83.0	3510.7	m

a: assignments (ν = stretching, δ = bending, ω = wagging, τ = twisting, ρ = rocking; s = symmetric, as = antisymmetric).

b: rel. experimental intensities (vw = very weak, w = weak, m = middle, s = strong, vs = very strong); n.o. = not observed; o.o.r. = out of range.

Table S6. Comparison of experimental vibrational frequencies of **2c-d₃** isolated in an argon matrix at 3 K and computed vibrational frequencies at the B3LYP/6-311++G(3df,3pd) level of theory (unscaled).

Assignment ^a	Sym.	$\tilde{\nu}_{\text{anharm.}} / \text{cm}^{-1}$	$I_{\text{rel.}} / \text{km mol}^{-1}$	$\tilde{\nu}_{\text{harm.}} / \text{cm}^{-1}$	$I_{\text{rel.}} / \text{km mol}^{-1}$	$\tilde{\nu}_{\text{exp.}} / \text{cm}^{-1}$	$I_{\text{rel.}}^{\text{b}}$
$\tau(\text{CC})$	a''	91.3	7.8	91.5	7.5	o.o.r.	o.o.r.
$\delta(\text{CC})$	a'	257.5	30.4	263.0	29.8	o.o.r.	o.o.r.
$\delta(\text{CN})$	a'	327.2	1.2	333.0	1.3	o.o.r.	o.o.r.
$\omega(\text{ND}_2)$	a''	352.4	25.3	352.8	32.1	n.o.	n.o.
$\omega(\text{CND})$	a''	437.5	27.7	455.8	53.3	439.8	s
$\delta(\text{CCO})$	a'	462.2	6.9	464.2	8.7	469.0	s
$\omega(\text{CND})$	a''	485.3	59.2	491.2	14.5	477.8	s
$\delta(\text{CCO})$	a''	526.0	0.3	532.1	0.8	519.7	s
$\tau(\text{CO})$	a'	526.4	4.7	539.9	22.8	n.o.	n.o.
$\nu(\text{CC})$	a'	734.8	14.7	743.3	22.6	738.3	s
$\omega(\text{CCO})$	a''	785.4	8.1	795.8	11.0	780.2	s
$\delta(\text{CND})$	a'	779.2	0.2	798.4	0.2	n.o.	n.o.
$\delta(\text{COD})$	a'	958.8	16.3	1004.1	52.8	974.7	s
$\delta(\text{ND}_2)$	a'	1095.5	1.2	1116.8	2.7	n.o.	n.o.
$\nu(\text{CS})$	a'	1169.7	35.3	1196.7	39.0	1177.4	s
$\nu(\text{CO})$	a'	1284.8	151.8	1315.0	245.9	1319.0	s
$\nu(\text{CN})$	a'	1452.8	250.0	1491.5	324.8	1465.5	s
$\nu(\text{C=O})$	a'	1781.0	214.6	1811.2	307.7	1775.9	s
$\nu(\text{OD})$	a'	2383.2	102.7	2515.0	113.2	2391.1	w
$\nu_{\text{s}}(\text{ND}_2)$	a'	2454.7	25.0	2552.8	101.3	2462.3	m
$\nu_{\text{as}}(\text{ND}_2)$	a'	2629.2	40.1	2728.9	47.2	2629.5	w

a: assignments (ν = stretching, δ = bending, ω = wagging, τ = twisting, ρ = rocking; s = symmetric, as = antisymmetric).

b: rel. experimental intensities (vw = very weak, w = weak, m = middle, s = strong, vs = very strong); n.o. = not observed; o.o.r. = out of range.

Table S7. Comparison of experimental vibrational frequencies of **2t** isolated in an argon matrix at 3 K and computed vibrational frequencies at the B3LYP/6-311++G(3df,3pd) level of theory (unscaled).

Assignment ^a	Sym.	$\tilde{\nu}_{\text{anharm.}} / \text{cm}^{-1}$	$I_{\text{rel.}} / \text{km mol}^{-1}$	$\tilde{\nu}_{\text{harm.}} / \text{cm}^{-1}$	$I_{\text{rel.}} / \text{km mol}^{-1}$	$\tilde{\nu}_{\text{exp.}} / \text{cm}^{-1}$	$I_{\text{rel.}}^{\text{b}}$
$\tau(\text{CC})$	a''	53.0	5.3	51.1	4.1	o.o.r.	o.o.r.
$\delta(\text{CCO})$	a'	243.2	6.5	244.9	6.4	o.o.r.	o.o.r.
$\delta(\text{CCN})$	a'	380.2	6.2	383.9	6.1	n.o.	n.o.
$\omega(\text{CCN})$	a''	386.4	89.4	393.0	66.4	n.o.	n.o.
$\omega(\text{NH}_2)$	a''	479.5	1.5	465.8	89.3	n.o.	n.o.
$\delta(\text{CCO})$	a'	507.9	34.6	475.1	2.3	n.o.	n.o.
$\delta(\text{CCO})$	a'	547.4	37.1	553.4	40.3	546.1	w
$\tau(\text{CO})$	a''	595.1	49.8	627.6	106.4	597.0	m
$\tau(\text{CN})$	a''	614.0	63.4	638.9	2.2	602.6	vw
$\nu(\text{CC})$	a'	733.6	23.7	746.5	26.1	738.7	w
$\omega(\text{CCO})$	a''	791.6	21.5	800.6	33.6	782.9	w
$\delta(\text{CNH})$	a'	922.3	10.0	944.4	7.9	947.7	vw
$\delta(\text{COH})$	a'	1145.3	156.0	1187.8	246.8	1183.0	m
$\delta(\text{CNH})$	a'	1259.7	6.8	1270.6	14.3	n.o.	n.o.
$\nu(\text{CS})$	a'	1347.0	47.9	1396.2	77.9	1361.9	w
$\nu(\text{CN})$	a'	1363.6	200.2	1405.5	176.5	1378.5	m
$\delta(\text{NH}_2)$	a'	1572.3	144.6	1607.0	268.2	1571.3	s
$\nu(\text{C=O})$	a'	1747.0	202.6	1777.3	272.6	1747.1	s
$\nu_{\text{s}}(\text{NH}_2)$	a'	3377.8	54.4	3550.1	96.2	3386.5	m
$\nu_{\text{as}}(\text{NH}_2)$	a'	3507.8	61.9	3695.9	73.8	3520.7	m
$\nu(\text{OH})$	a'	3577.0	85.5	3754.9	99.9	3557.1	m

a: assignments (ν = stretching, δ = bending, ω = wagging, τ = twisting, ρ = rocking; s = symmetric, as = antisymmetric).

b: rel. experimental intensities (vw = very weak, w = weak, m = middle, s = strong, vs = very strong); n.o. = not observed; o.o.r. = out of range.

Table S8. Comparison of experimental vibrational frequencies of **2t-d₃** isolated in an argon matrix at 3 K and computed vibrational frequencies at the B3LYP/6-311++G(3df,3pd) level of theory (unscaled).

Assignment ^a	Sym.	$\tilde{\nu}_{\text{anharm.}} / \text{cm}^{-1}$	$I_{\text{rel.}} / \text{km mol}^{-1}$	$\tilde{\nu}_{\text{harm.}} / \text{cm}^{-1}$	$I_{\text{rel.}} / \text{km mol}^{-1}$	$\tilde{\nu}_{\text{exp.}} / \text{cm}^{-1}$	$I_{\text{rel.}}^{\text{b}}$
$\tau(\text{CC})$	a''	51.6	4.6	50.4	4.0	o.o.r.	o.o.r.
$\delta(\text{CCO})$	a'	236.2	6.2	238.1	6.2	o.o.r.	o.o.r.
$\omega(\text{ND}_2)$	a''	327.5	71.5	314.6	78.8	o.o.r.	o.o.r.
$\delta(\text{CCN})$	a'	343.7	3.7	346.6	3.7	o.o.r.	o.o.r.
$\omega(\text{CCN})$	a''	387.8	0.7	388.2	2.6	n.o.	n.o.
$\tau(\text{CN})$	a''	440.9	8.2	456.7	10.3	n.o.	n.o.
$\delta(\text{CCO})$	a'	461.7	2.1	464.6	2.3	n.o.	n.o.
$\tau(\text{CO})$	a''	499.1	41.2	517.6	54.6	511.3	w
$\delta(\text{CCO})$	a'	513.1	42.9	519.0	47.0	517.0	vw
$\nu(\text{CC})$	a'	666.7	20.9	679.7	19.7	673.2	vw
$\omega(\text{CCO})$	a''	787.0	14.5	796.9	18.3	n.o.	n.o.
$\delta(\text{CND})$	a'	787.6	4.4	798.3	6.8	n.o.	n.o.
$\delta(\text{COD})$	a'	990.1	39.1	1017.8	57.1	1006.4	vw
$\delta(\text{ND}_2)$	a'	1088.8	0.7	1111.1	0.3	n.o.	n.o.
$\nu(\text{CS})$	a'	1168.3	40.0	1200.1	61.8	1187.9	w
$\nu(\text{CO})$	a'	1303.1	142.8	1334.3	199.9	1327.5	w
$\nu(\text{CN})$	a'	1413.9	206.5	1454.8	330.1	1432.6	s
$\nu(\text{C=O})$	a'	1737.5	255.2	1768.3	294.7	1740.7	s
$\nu_{\text{s}}(\text{ND}_2)$	a'	2458.8	47.0	2563.3	81.3	2470.1	m
$\nu(\text{OD})$	a'	2633.5	41.8	2731.3	59.1	2623.9	m
$\nu_{\text{as}}(\text{ND}_2)$	a'	2635.3	46.8	2738.4	44.3	2644.6	w

a: assignments (ν = stretching, δ = bending, ω = wagging, τ = twisting, ρ = rocking; s = symmetric, as = antisymmetric).

b: rel. experimental intensities (vw = very weak, w = weak, m = middle, s = strong, vs = very strong); n.o. = not observed; o.o.r. = out of range.

Matrix UV/VIS Spectra

UV/VIS spectra recorded after deposition of **2** (black spectrum in Fig. S29) show an absorption at 293.6 nm, which we assign to **2c** (compd. 276.1 nm with $f = 0.1343$ at B3LYP/6-311++G(3df,3pd)). After 4 min of irradiation at 254 nm the intensity of this absorption decreases. For **2t** we computed the absorbance maximum at 295.4 nm ($f = 0.1304$), which is in accord with a shift to higher wavelengths of the absorption in the experiment (red spectrum). Within 19 h **2c** reforms (the maximum shifts left), but does not reach its initial concentration (blue spectrum).

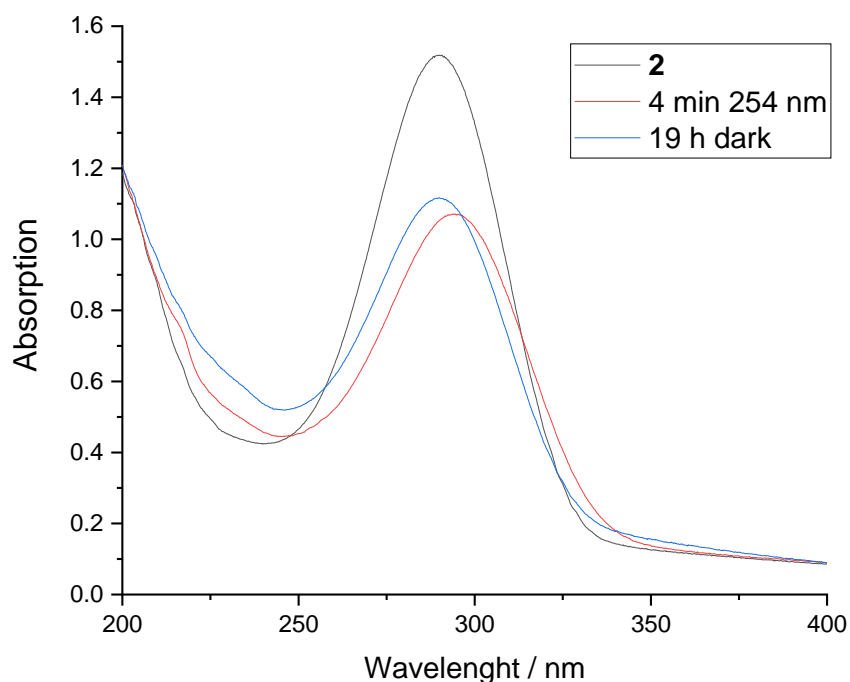


Fig. S29. Experimental matrix UV/Vis spectra. Black: After deposition. Red: After irradiation at 254 nm for 4 min. Blue: After keeping the matrix 19 h in the dark. The baseline of the blue spectrum is shifted to facilitate visual comparison.

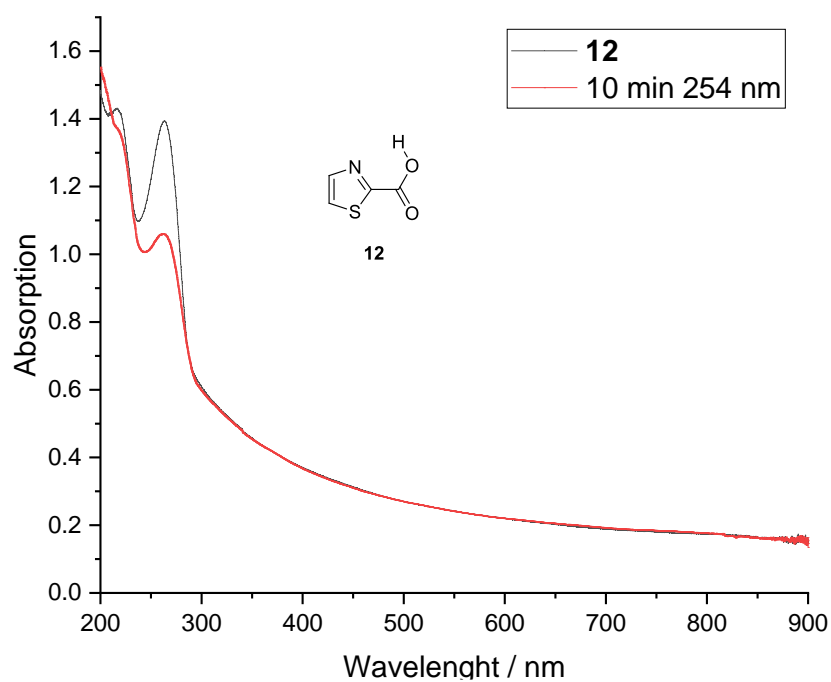


Fig. S30. Experimental matrix UV/Vis spectra of **12**. Black: After deposition. Red: After irradiation at 254 nm for 10 min. The baseline of the red spectrum is shifted to facilitate visual comparison.

Kinetic Analyses

Kinetic Measurements

To evaluate the kinetics of the reactions $1\mathbf{t}\text{-CO}_2 \rightarrow 2\mathbf{c}$ and $2\mathbf{t} \rightarrow 2\mathbf{c}$ we measured the time evolution of the corresponding matrix IR bands at different temperatures. The decay of the integral below the strongest band was measured and plotted to calculate k through exponential fitting. The band decay was evaluated *via* integration using a Python script (available at: https://github.com/prs-group/Spectra_Analyzer). The bands at 2336.1 and 2333.2 cm^{-1} (distinct matrix sites displaying different kinetics) were used for the evaluation of the decay of $1\mathbf{t}\text{-CO}_2$. The third band at 2330.4 cm^{-1} cannot be reliably evaluated due to its small intensity and long half-life.

We performed temperature dependent measurements of the band at 2336.1 cm^{-1} . The results are displayed in Table S9.

Table S9. Experimental rate constants measured at different temperatures. The band at 2336.1 cm^{-1} was used for the evaluation of the decay of $1\mathbf{t}\text{-CO}_2$. The values of the first reaction are plotted in an Arrhenius plot in the main text. The values of the second reaction are plotted in Fig. S26.

Reaction	Temperature / K	Experimental k / s^{-1}	Experimental $t_{1/2} / \text{h}$
$1\mathbf{t}\text{-CO}_2 \rightarrow 2\mathbf{c}$	3.5	4.53×10^{-4}	0.43
	5.3	4.64×10^{-4}	0.41
	7.2	9.10×10^{-4}	0.21
	10.0	2.00×10^{-3}	0.10
	12.2	4.51×10^{-3}	0.04
$2\mathbf{t} \rightarrow 2\mathbf{c}$	3.5	1.74×10^{-4}	1.11
	5.3	1.71×10^{-4}	1.13
	7.2	1.75×10^{-4}	1.10
	10.0	1.83×10^{-4}	1.05
	12.2	1.84×10^{-4}	1.05

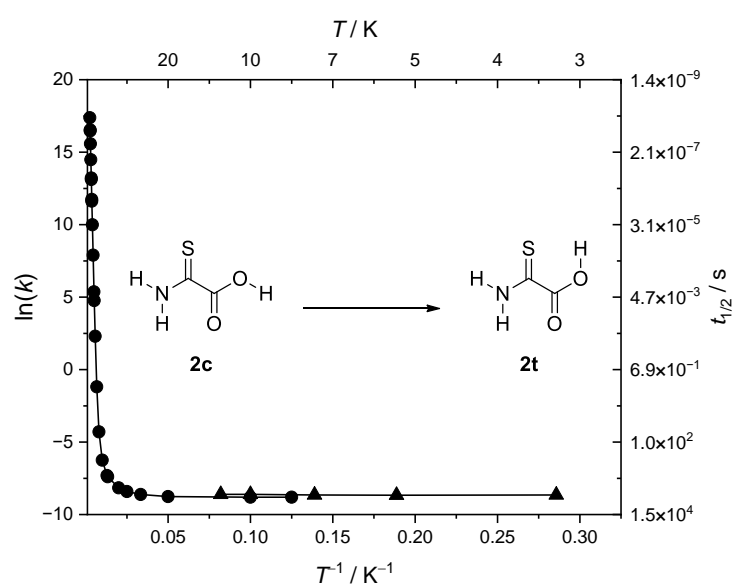


Fig. S31. Arrhenius plot of the $2\mathbf{t} \rightarrow 2\mathbf{c}$ reaction. Below 20 K the rotamerization is only feasible *via* QMT since this reaction is associated with a barrier of 9.9 kcal mol^{-1} at the CCSD(T)/cc-pVTZ level of theory (circles: computed rates; triangles: experimental rates).

Fig. S32 shows an example of the evaluation of the decay of **1t**-CO₂ (2336.1 cm⁻¹) at 3 K. A biexponential model is used for the fit function. A monoexponential function does not yield a good fit due to the presence of several matrix sites. To obtain k , t_1 and t_2 were scaled with A_1 and A_2 and the average of the resulting values was further used.

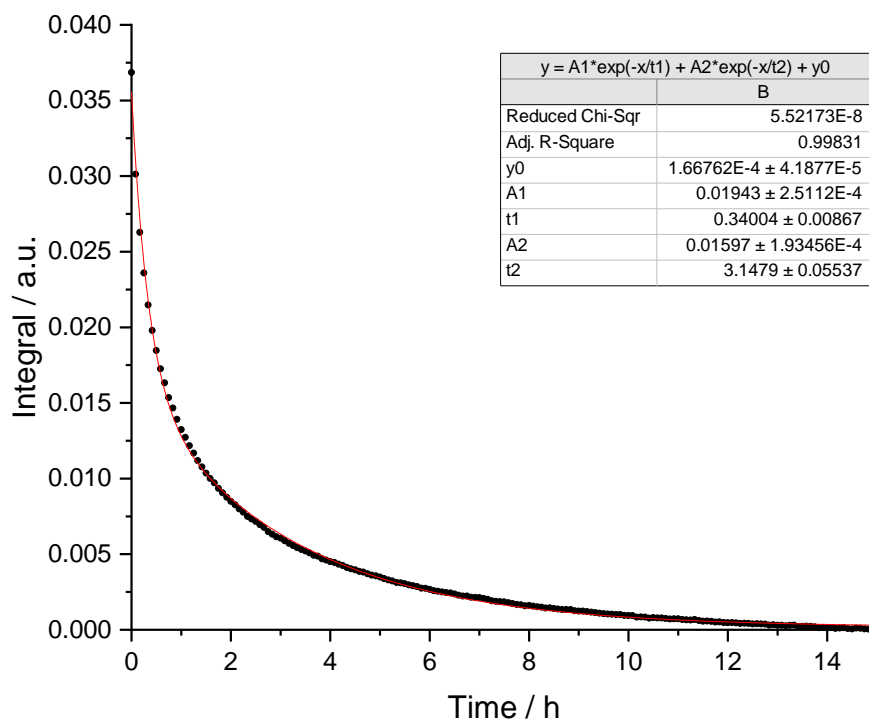


Fig. S32. Decay of the integral of the 2336.1 cm⁻¹ IR band of **1t**-CO₂ over time. Black: Measured values. Red: Biexponential fit function.

Fig. S33 to S35 show the evaluation of the 2333.2 cm⁻¹ band of **1t**-CO₂ compared to bands of **2c**. The resulting QMT half-life of the reaction at this matrix site amounts to ca. 90 h.

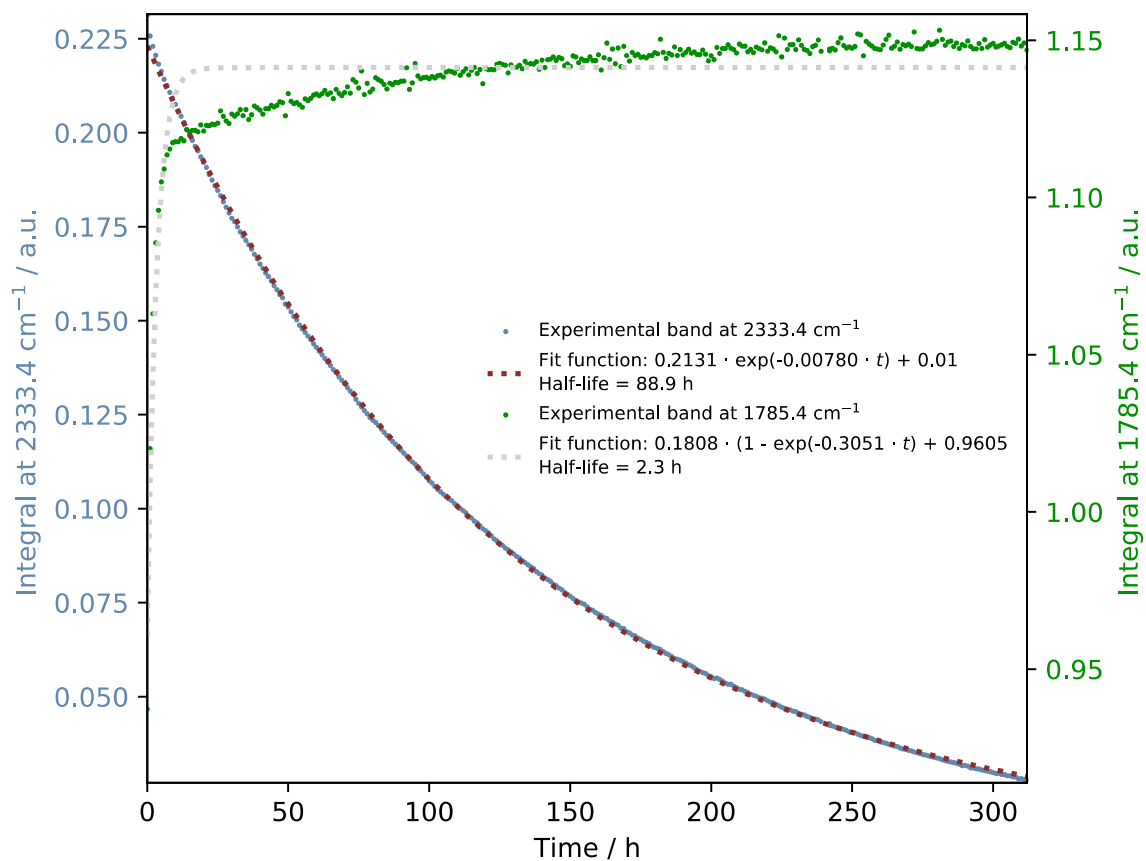


Fig. S33. Evaluation of the $\mathbf{1t}\text{-CO}_2 \rightarrow \mathbf{2c}$ reaction. The kinetics of $\mathbf{2c}$ are dominated by the reaction from $\mathbf{1t}\text{-CO}_2$ at the above-mentioned matrix site at 2336.1 cm^{-1} and from further side products present after photolysis (*vide supra*).

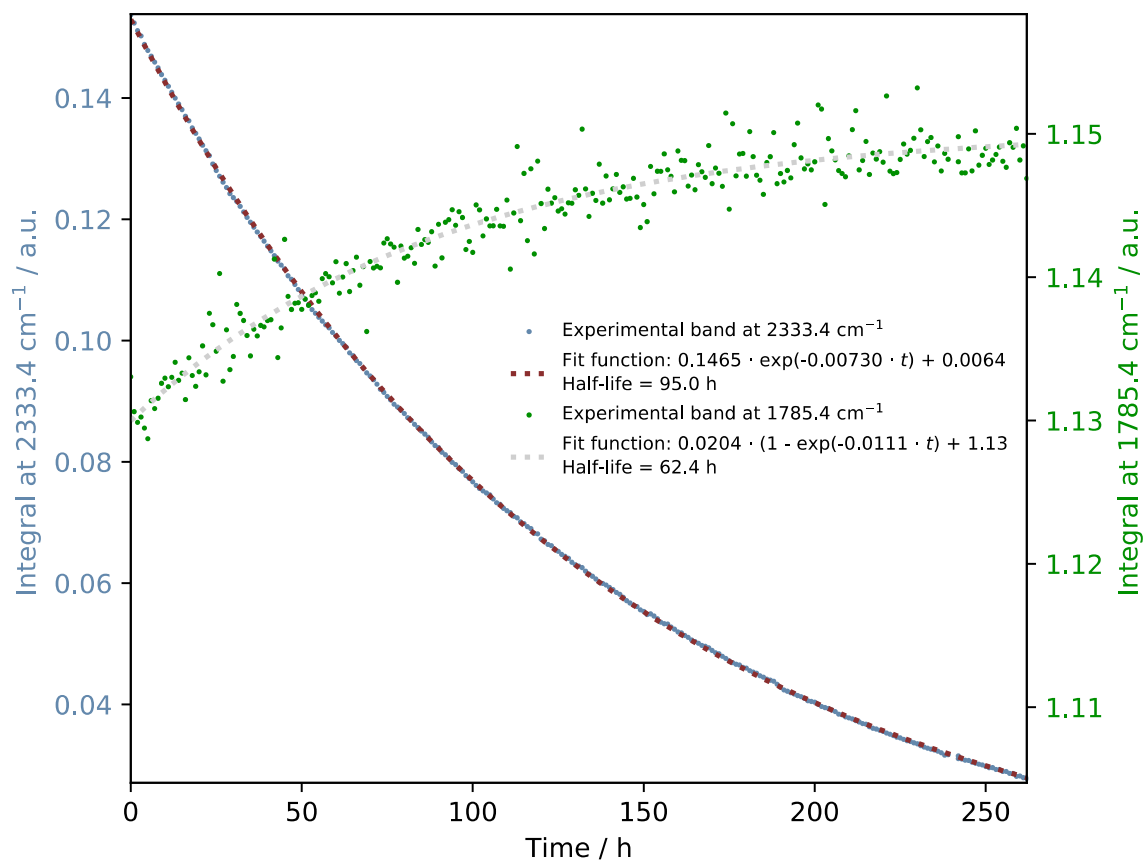


Fig. S34. Evaluation of the $\mathbf{1t}\text{-CO}_2 \rightarrow \mathbf{2c}$ (1785.4 cm^{-1}) reaction considering only the points recorded after 50 h when $\mathbf{1t}\text{-CO}_2$ (2333.2 cm^{-1}) $\rightarrow \mathbf{2c}$ is the dominant reaction (*cf.* Fig. S28).

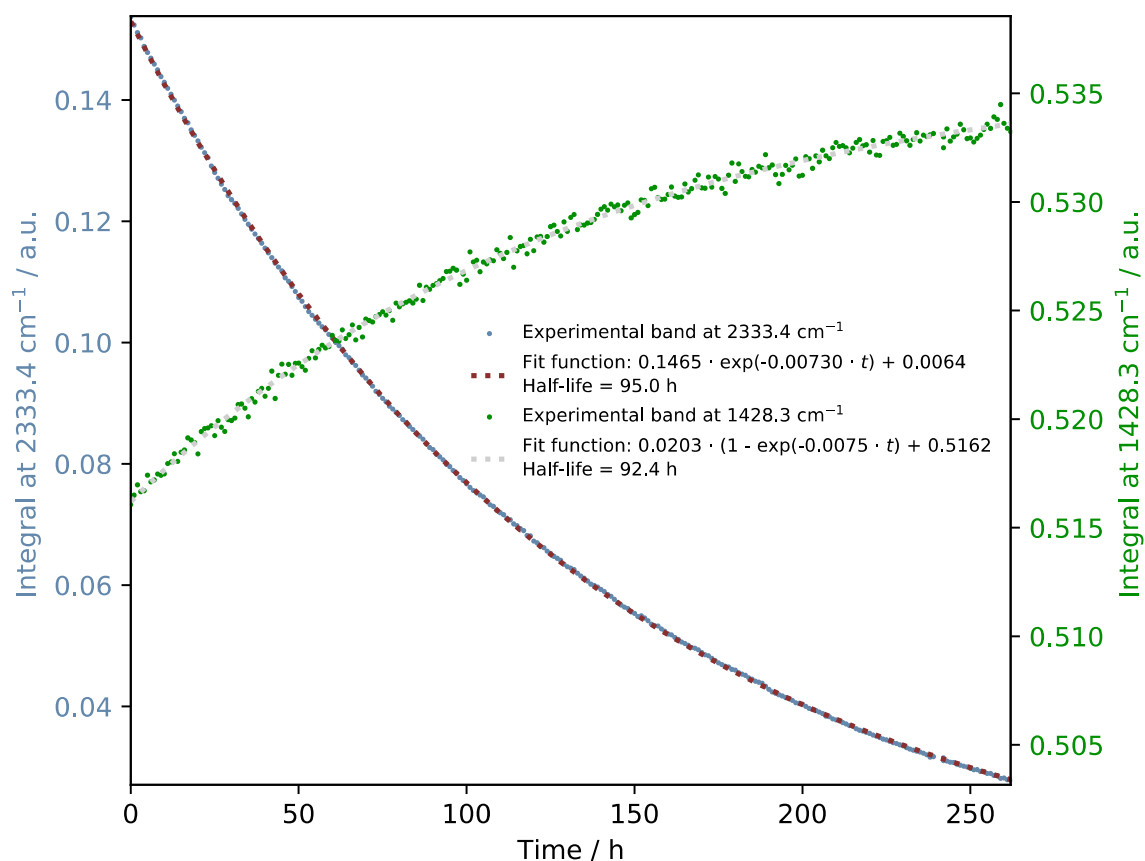


Fig. S35. Evaluation of the $\mathbf{1t}\text{-CO}_2 \rightarrow \mathbf{2c}$ (1428.3 cm^{-1}) reaction considering only the points recorded after 50 h when $\mathbf{1t}\text{-CO}_2$ (2333.2 cm^{-1}) $\rightarrow \mathbf{2c}$ is the dominant reaction (*cf.* Fig. S33).

We note that another way to assign the 2333.2 cm^{-1} band would be the *cis*-complex $\mathbf{1c}\text{-CO}_2$ (computed: 2271.7 cm^{-1}). This band disappears with a long half-life (ca. 90 h) and the hindered rotation of the CS bond to give $\mathbf{1t}\text{-CO}_2$ is associated with a barrier of $10.7\text{ kcal mol}^{-1}$ (CCSD(T)/cc-pVTZ + ZPVE). The overall $\mathbf{1c}\text{-CO}_2 \rightarrow \mathbf{1t}\text{-CO}_2 \rightarrow \mathbf{2c}$ reaction would represent a domino QMT process, for which only one other example has been reported (23). However, the experimental half-life is not in accordance at all with the computed half-life of the $\mathbf{1c}\text{-CO}_2 \rightarrow \mathbf{1t}\text{-CO}_2$ reaction (CVT/SCT//B3LYP/6-311+G(d,p): 5.23×10^{10} years at 10 K). Furthermore, the corresponding band also vanishes in the perdeuterated case providing another hint that these bands can indeed be assigned to different matrix sites of $\mathbf{1t}\text{-CO}_2$ instead of $\mathbf{1c}\text{-CO}_2$. Similar behavior has already been observed for other matrix-isolated compounds²³.

Kinetic Computations

Table S10. Computed rate constants at the CVT/SCT//B3LYP/6-311+G(d,p) level of theory. The values of the first reaction are plotted in an Arrhenius plot in the main text. The values of the second reaction are plotted in Fig. S26.

Reaction	Temperature / K	Computed k / s^{-1}	Computed $t_{1/2} / \text{h}$
1t-CO₂ → 2c	4.0	2.09×10^{-4}	0.92
	5.0	2.09×10^{-4}	0.92
	6.0	2.10×10^{-4}	0.92
	8.0	2.13×10^{-4}	0.90
	10.0	2.31×10^{-4}	0.83
2t → 2c	4.0	N.A.	N.A.
	5.0	N.A.	N.A.
	6.0	N.A.	N.A.
	8.0	1.50×10^{-4}	1.28
	10.0	1.50×10^{-4}	1.28

The computed rates of the reaction of **1t-CO₂** to **2c** vary over several orders of magnitude depending on the basis set used in the computations (Table S11). This is expected to be a result of significant changes in the CC distance between **1** and CO₂ for the different basis sets (Table S12). The shortening of the CC distance for smaller basis sets matches our expectations when considering the basis set superposition error (BSSE)²⁴. Thinking of the matrix cage, in which the complex forms, the complex might not reach its minimum gas-phase structure due to the restricted cage space (Fig. S36). In addition, different $t_{1/2}$ were measured at different matrix-sites, suggesting different geometries that result in markedly different tunneling rates. The changes in geometries caused by different basis sets can simulate the restrictions enforced by the matrix. B3LYP/6-311+G(d,p) simulates $t_{1/2}$ of the 2336.1 cm⁻¹ matrix-site very accurately presumably because the computed CC distance is smaller than, *e.g.*, compared to the B3LYP/6-311++G(3df,3pd) minimum, whose resulting computed $t_{1/2}$ fits well with the 2333.2 cm⁻¹ site (Table S11 and Fig. S37).

Table S11. Comparison of the computed half-lives of **1t-CO₂ → 2c** at different levels of theory with experimental half-lives at different matrix-sites.

Level of Theory	$\Delta E^\ddagger / \text{kcal mol}^{-1}$	k / h^{-1}	$t_{1/2} (\text{comp.})$	$t_{1/2} (\text{exp.})$
B3LYP/6-311++G(3df,3pd)	2.15	1.06×10^{-6}	7.6 d	3.8 d (2333.2 cm ⁻¹)
B3LYP/6-311+G(d,p)	1.85	2.09×10^{-4}	0.92 h	0.4 h (2336.1 cm ⁻¹)

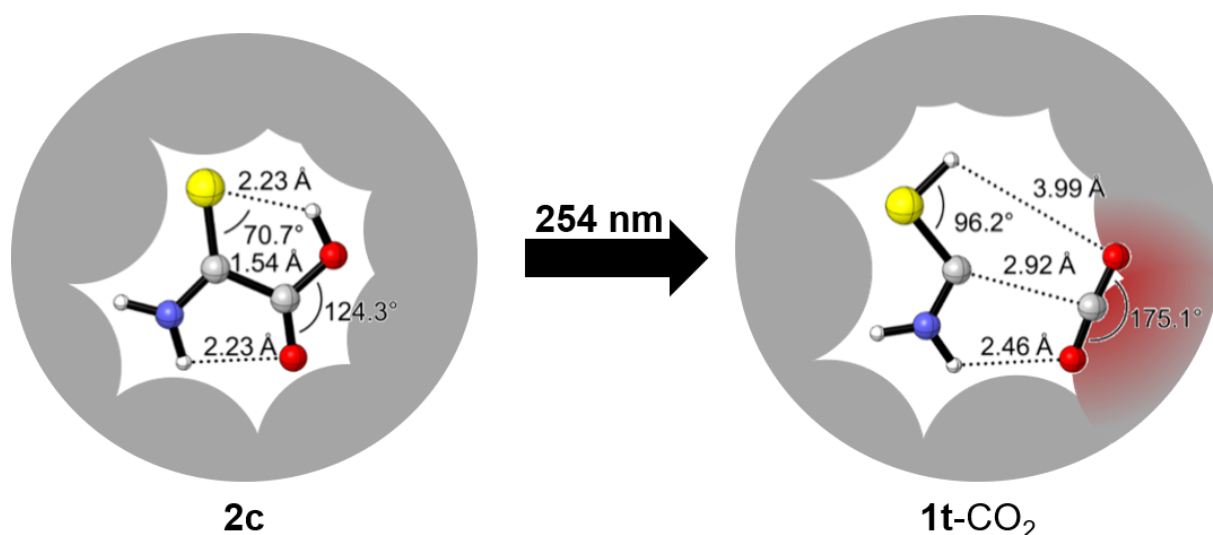


Fig. S36. The Ar matrix cage inhibits the system from reaching the minimum gas-phase geometry of **1t**-CO₂ after photolysis. Geometries were optimized at B3LYP/6-311++G(3df,3pd). The radius of the Ar atoms was approximated to 1.9 Å (Van-der-Waals-radius).²⁵

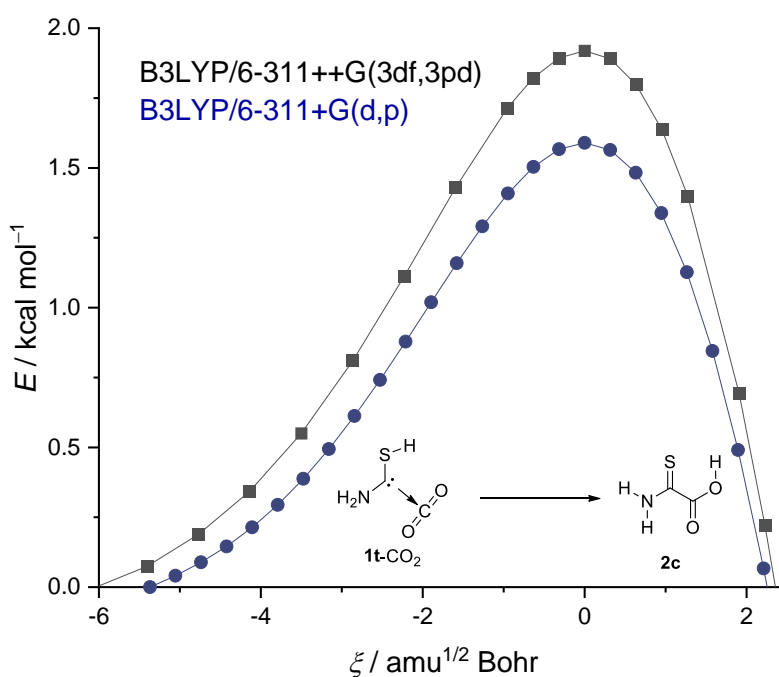


Fig. S37. **1t**-CO₂ → **2c** IRC curves at two different levels of theory (only energy values above 0 kcal mol⁻¹ are shown). The smaller basis set mimics the surrounding of the complex in the 2336.1 cm⁻¹ matrix cage better, while the larger basis set fits $t_{1/2}$ of the 2333.2 cm⁻¹ site. The different barrier widths and heights result from different C–C distances in **1t**-CO₂ (Table S12).

We conclude that a smaller C–C bond distance indeed better represents the minimum structure in the 2336.1 cm⁻¹ matrix-site than gas phase minimum structures obtained at higher levels of theory. As expected, the rotamerization of **2t** to **2c** was rather insensitive to changes in the basis set, because of the smaller influence on geometries of covalent bonds on the reaction rate. As this reaction does not exhibit noncovalently bound fragments, we also expect a smaller effect of the matrix cage on the geometries compared to the reaction from **1t**-CO₂ to **2c** (Table S12).

Table S12. Comparison of the influence of the level of theory on the C–C bond distance of **2c** and **1t**-CO₂.

Level of Theory	C–C distance 2c / Å	C–C distance 1t -CO ₂ / Å
B3LYP/6-311++G(3df,3pd)	1.540	3.005
B3LYP-D3BJ/6-311++G(3df,3pd)	1.538	2.851
B3LYP/6-311+G(d,p)	1.543	2.971
B3LYP/6-31+G(d,p)	1.543	2.942
CCSD(T)/cc-pVTZ	1.539	2.963

Approximating the thermal half-life with the Eyring equation gives $t_{1/2} \approx 1$ d with an activation barrier of 1.5 kcal mol⁻¹ at 20 K which is in a reasonably good agreement with a thermal reactivity that begins to influence the overall kinetics above ca. 8 K. The reaction barrier is strongly influenced by the C–C bond distance. The different matrix sites feature different C–C bond distances resulting in different kinetics. The molecule geometry in the matrix site featuring the fastest kinetics is best represented with a smaller C–C bond distance and a resulting activation energy of ca. 1.9 kcal mol⁻¹ whereas we observed a matrix site showing no reactivity even at 20 K. This matrix site might allow the molecule to reach a geometry featuring a longer C–C bond distance and an activation energy of ca. 4 kcal mol⁻¹. This is in agreement with no observable reaction.

NBO and QTAIM Analysis.

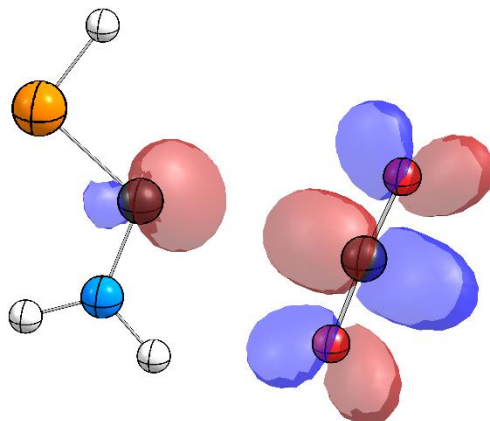


Fig. S38. Electron donation from the carbene lone pair to the π^* -CO₂ orbital results in an attractive interaction between **1t** and CO₂.

Table S13. Selected parameters obtained from a QTAIM analysis of **1t**-CO₂ at the B3LYP/6-311++G(3df,3pd) level of theory.

Entry	Type	Atoms	$\rho / e\text{\AA}^{-3}$	$-\nabla^2\rho / e\text{\AA}^{-5}$	$G(r) / \rho(r)$	$H(r) / e\text{\AA}^{-3}$
1	BCP1	C1 - O7	0.011169	+0.033811	+0.007124	-0.001328
2	BCP2	C1 - N3	0.345661	-0.902908	+0.329806	+0.555533
3	BCP3	N3 - H5	0.343694	-1.714455	+0.060493	+0.489107
4	BCP4	H4 - O7	0.009954	+0.039526	+0.008254	-0.001628
5	BCP5	N3 - H4	0.353381	-1.919840	+0.056557	+0.536517
6	BCP6	C1 - S6	0.212440	-0.405396	+0.069516	+0.170865
7	BCP7	C2 - O7	0.467088	-0.085893	+0.858614	+0.880088
8	BCP8	C2 - O8	0.474101	-0.005124	+0.898183	+0.899464
9	BCP9	S6 - H9	0.225051	-0.705425	+0.051033	+0.227389
10	RCP1	C1 - N3 - H4 - O7	0.008225	+0.035906	+0.007624	-0.001352

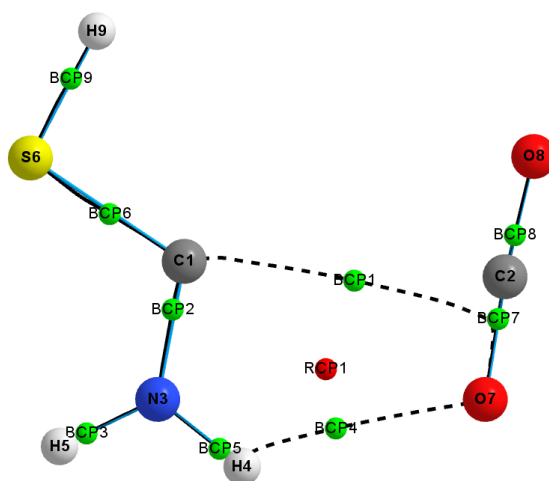


Fig. S39. BCP1 and BCP4 represent attractive interactions compared to hydrogen bonds in different systems showing resonance-assisted hydrogen bonds.²⁶

Table S14. Selected parameters obtained from a QTAIM analysis of **TS: 1t-CO₂ → 2c** at the B3LYP/6-311++G(3df,3pd) level of theory.

Entry	Type	Atoms	$\rho / e\text{\AA}^{-3}$	$-\nabla^2\rho / e\text{\AA}^{-5}$	$G(r) / \rho(r)$	$H(r) / e\text{\AA}^{-3}$
1	BCP1	C1 - C7	0.015865	+0.065980	+0.014056	-0.002439
2	BCP2	C1 - N2	0.065154	+0.052796	+0.028036	+0.014837
3	BCP3	N2 - H5	0.224839	-0.704291	+0.047381	+0.223454
4	BCP4	C1 - S3	0.348184	-1.943924	+0.053775	+0.539757
5	BCP5	N2 - H4	0.347666	-1.812744	+0.058621	+0.511807
6	BCP6	S3 - H6	0.213184	-0.414497	+0.072635	+0.176260
7	BCP7	H4 - O8	0.352877	-0.946339	+0.333683	+0.570268
8	BCP8	C7 - O8	0.442635	-0.334663	+0.737026	+0.820692
9	BCP9	C7 - O9	0.450880	-0.264327	+0.777743	+0.843825
10	RCP1	C1 - N2 - H4 - O8 - C7	0.015317	+0.078707	+0.016603	-0.003073

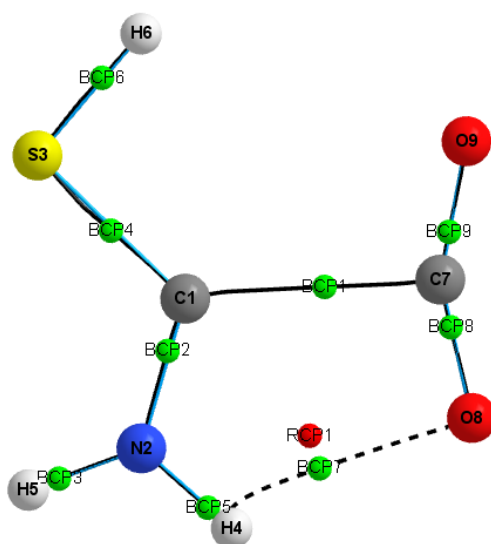


Fig. S40. BCPs and RCP of **TS: 1t-CO₂ → 2c**.

Computed Potential Energy Surfaces.

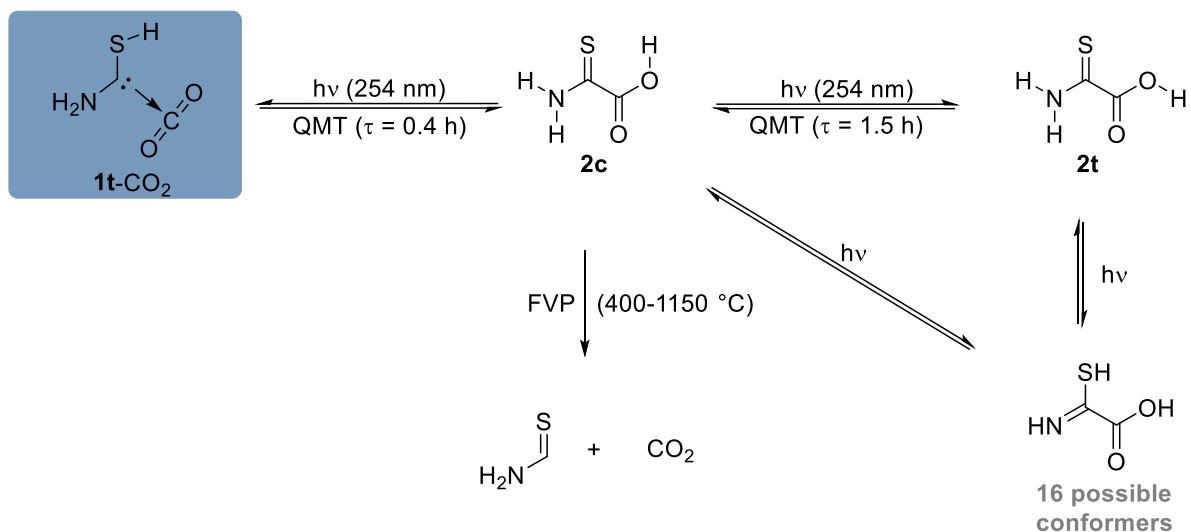


Fig. S41. Reaction network of 2.

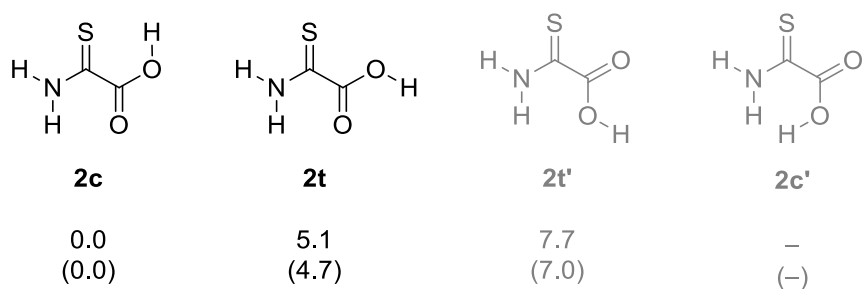


Fig. S42. There are three C_s symmetric conformers of 2-amino-2-thioxoacetic acid (2). Among them, 2c is the most stable one. Conceivable conformer 2c' could not be located as a local minimum structure even when its geometry was not restricted to the C_s point group. Energies including ZPVEs are given in kcal mol⁻¹ at the B3LYP/6-311++G(3df,3pd) (MP2/def2-QZVPP, in brackets) level of theory.

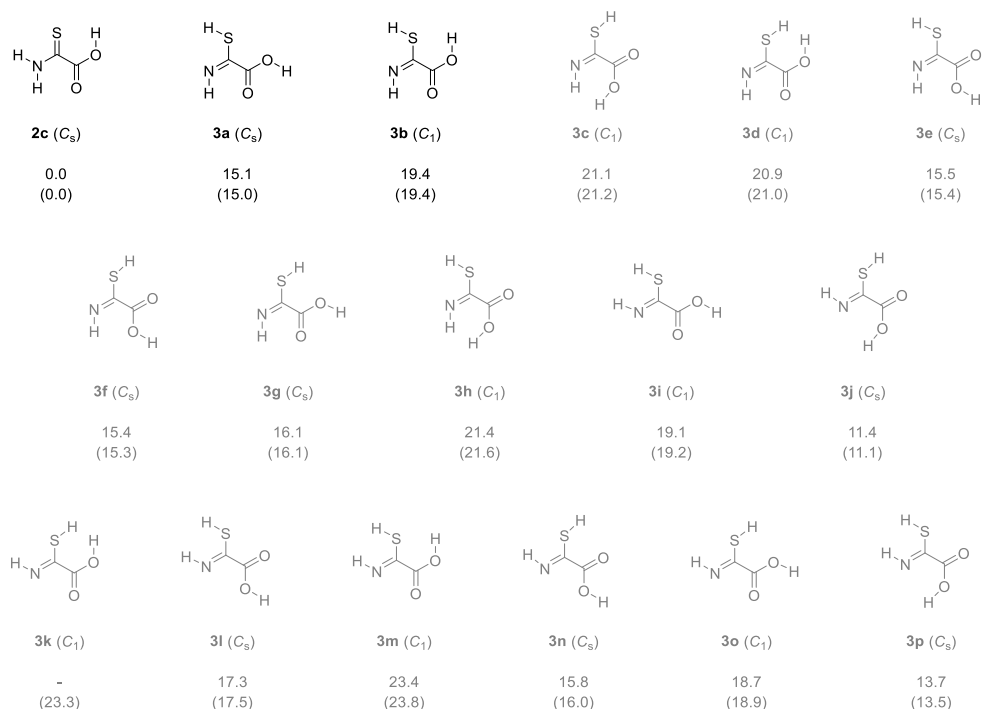


Fig. S43. There are 16 conformers of the thiolimine tautomer of **2**. Energies including ZPVEs are given in kcal mol⁻¹ with respect to **2c** at the B3LYP/6-311++G(3df,3pd) (MP2/def2-QZVPP, in brackets) level of theory. For C_1 symmetric conformers, the corresponding C_s geometries represent transition states of the respective rotamerization, which are associated with barriers <1 kcal mol⁻¹. **3k** could not be localized as a stationary point at the B3LYP/6-311++G(3df,3pd) level of theory.

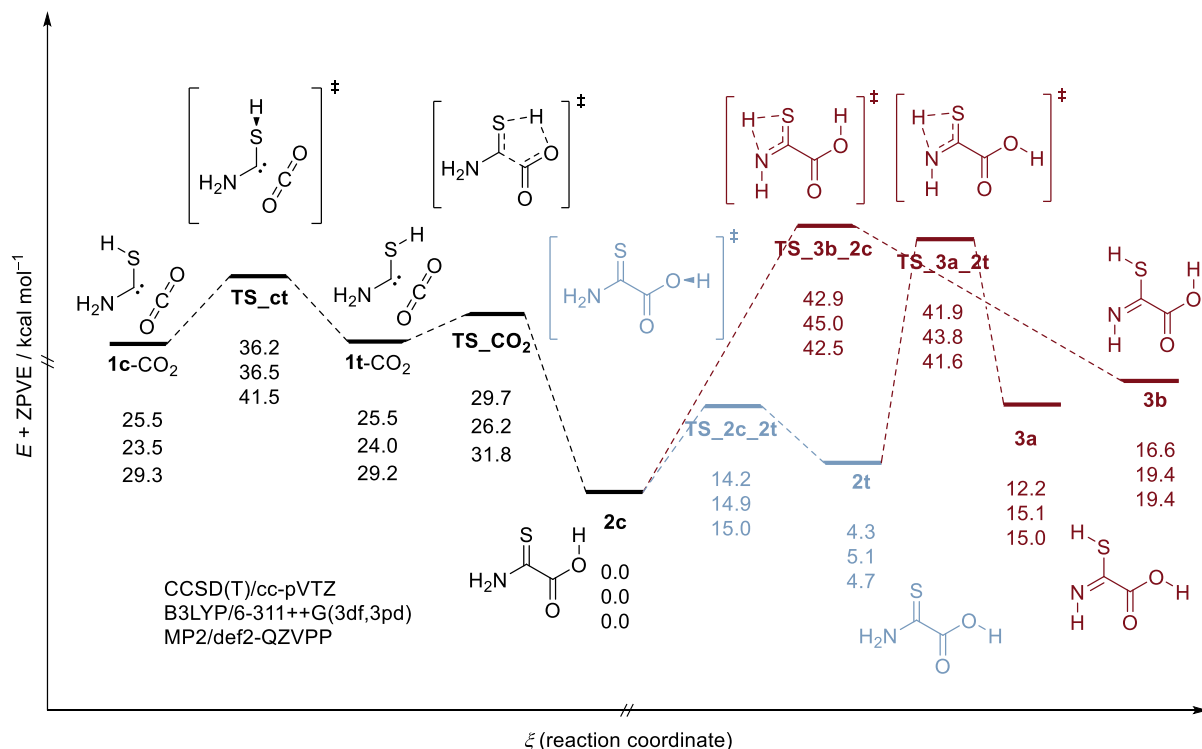


Fig. S44. PES of experimentally observed species. Black: Photodecarboxylation. Blue: Rotamerization. Red: Isomerization.

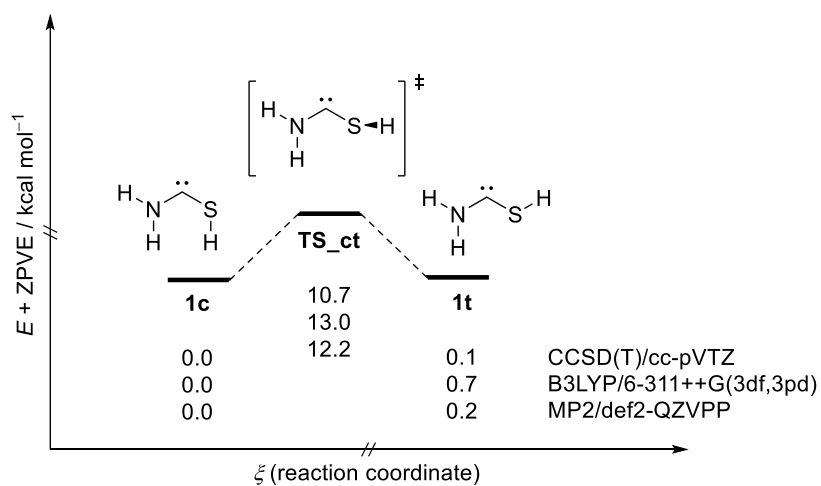


Fig. S45. PES of the rotamerization of free aminomercaptomethylene **1**.

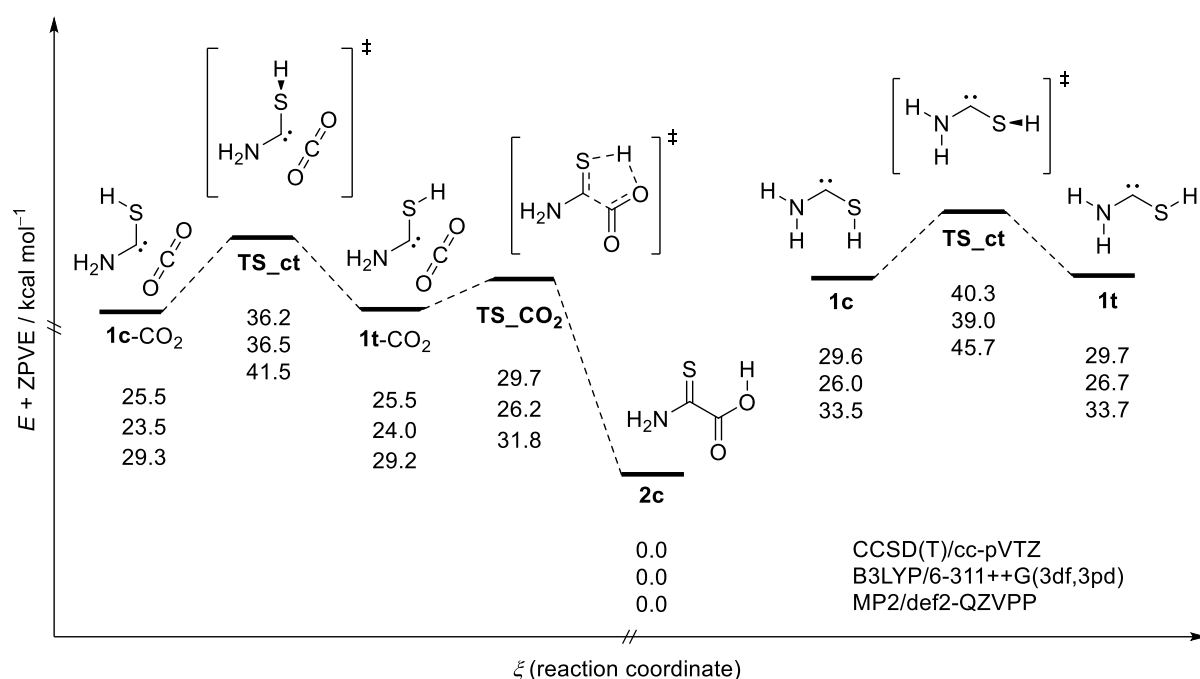


Fig. S46. Comparison of the PESs of **1-CO₂** (left) and free **1** (right). The energetics of the right PES were obtained by adding the energy of CO₂ computed at the respective level of theory. The complex is stabilized by ca. 4 kcal mol⁻¹ compared to free **1**.

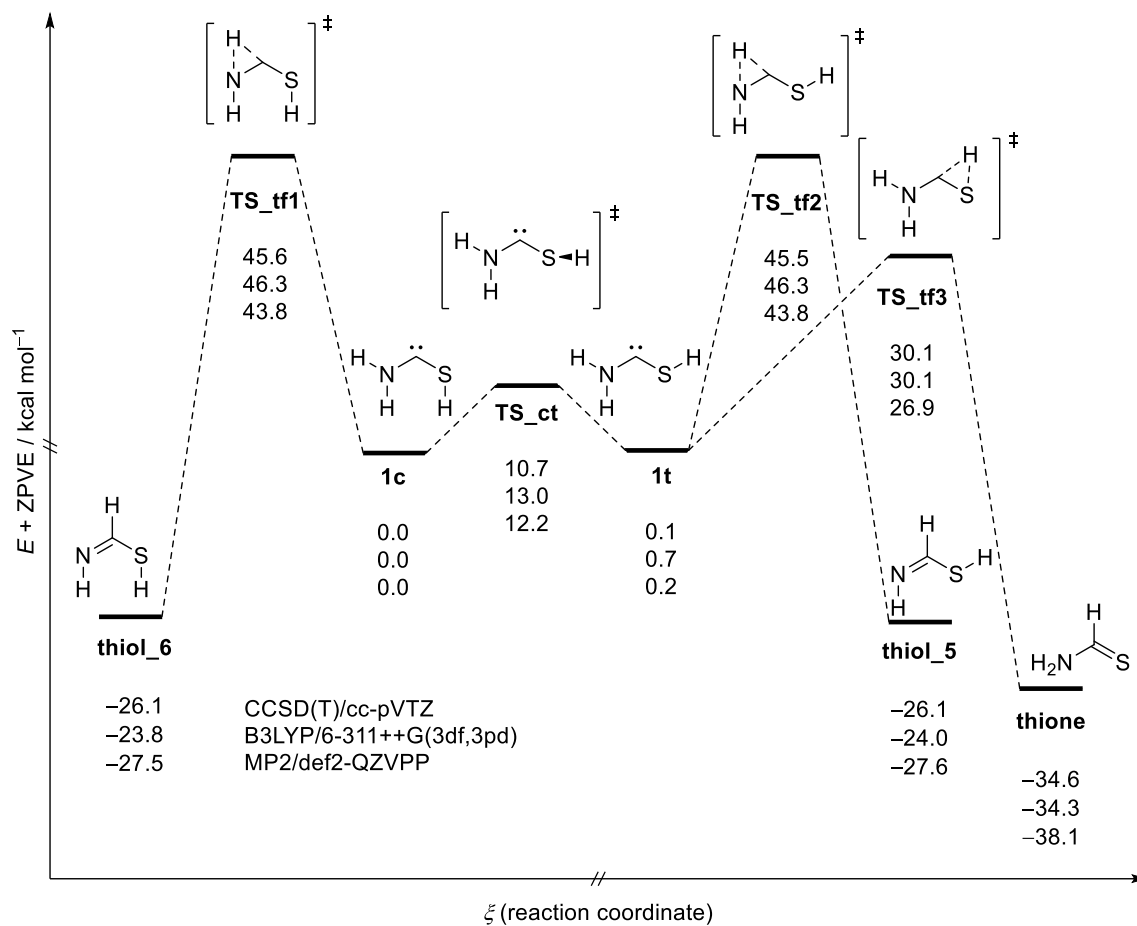


Fig. S47. Connection between free aminomercaptocarbene **1** and thioformamide. Note that **TS_tf3** is planar (C_s) at B3LYP/6-311++G(3df,3pd) and at MP2/def2-QZVPP while it bears C_1 symmetry at CCSD(T)/cc-pVTZ.

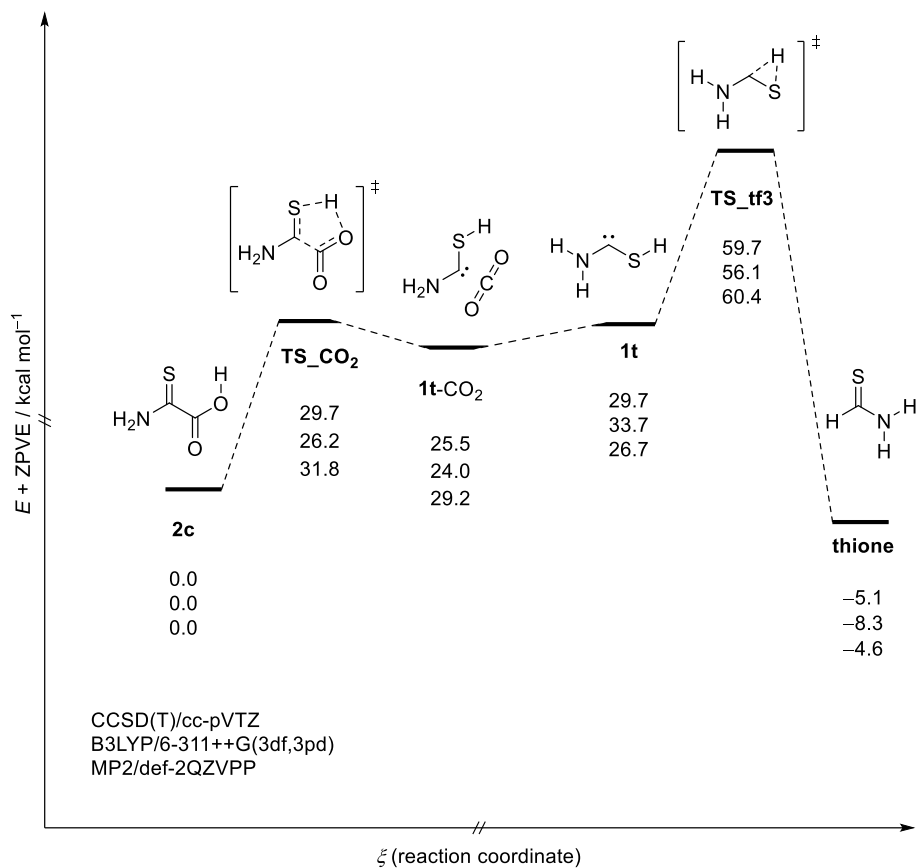


Fig. S48. PES of the pyrolysis of **2c** via **1t-CO₂** and **1t** to yield thioformamide (**thione**) at 0 K. Note that **TS_{tf3}** is planar (C_s) at B3LYP/6-311++G(3df,3pd) and at MP2/def2-QZVPP while it bears C_1 symmetry at CCSD(T)/cc-pVTZ. Some energies were corrected for CO₂ loss. CO₂ was computed at the respective level of theory.

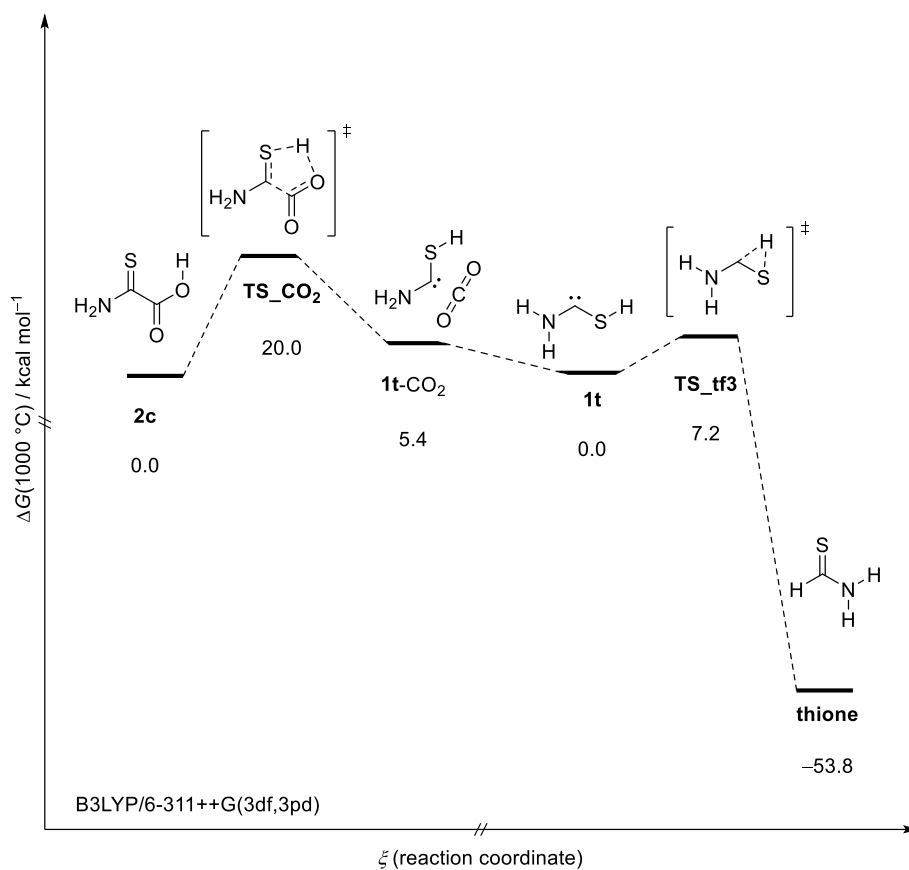


Fig. S49. PES of the pyrolysis of **2c** via **1t-CO₂** and **1t** to yield thioformamide (**thione**) at 1273.15 K (1000 °C). Some energies were corrected for CO₂ loss. CO₂ was computed at the same level of theory. The low activation barrier (**TS_tf3**) is presumably the reason for the absence of **1** in our pyrolysis experiments. For analogue PESs of related systems see below.

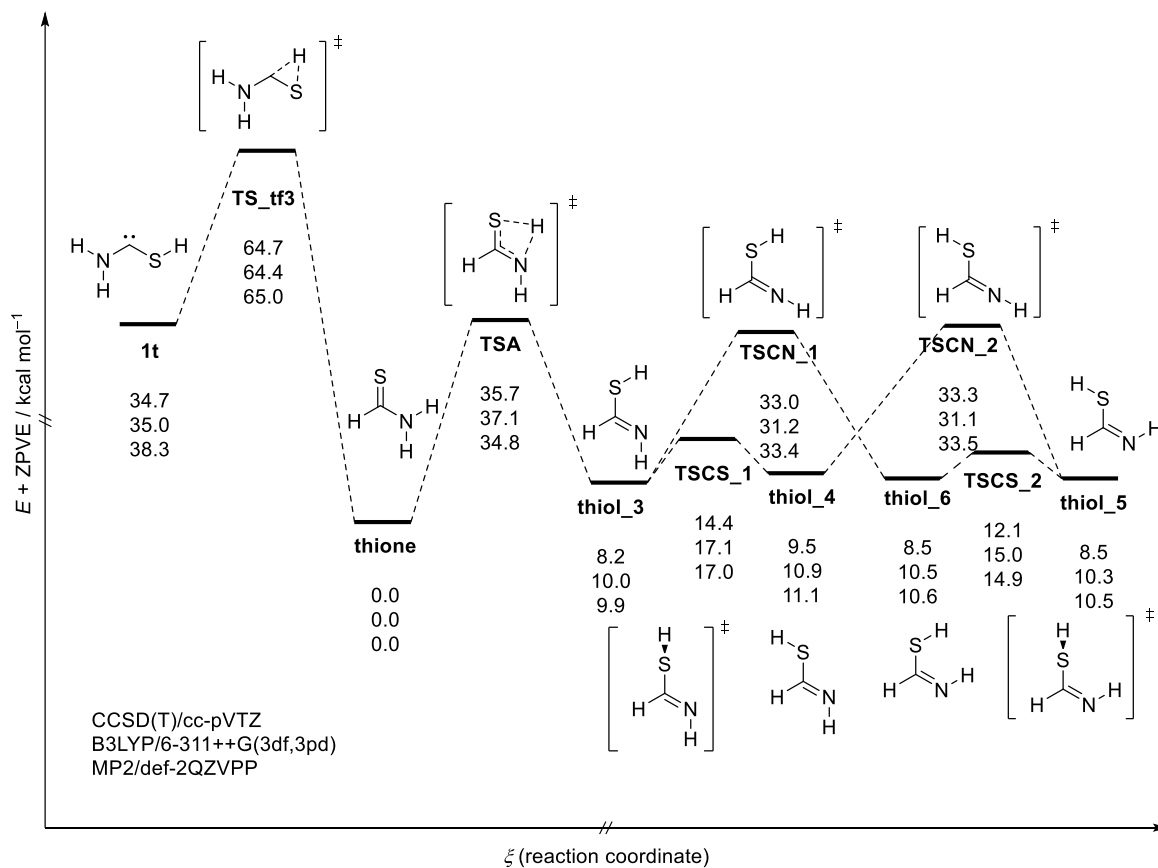


Fig. S50. PES of thioformamide and connection to **1**. Note that **TS_tf3** is planar (C_s) at B3LYP/6-311++G(3df,3pd) and at MP2/def2-QZVPP while it bears C_1 symmetry at CCSD(T)/cc-pVTZ.

Other Carbene-CO₂ Complexes

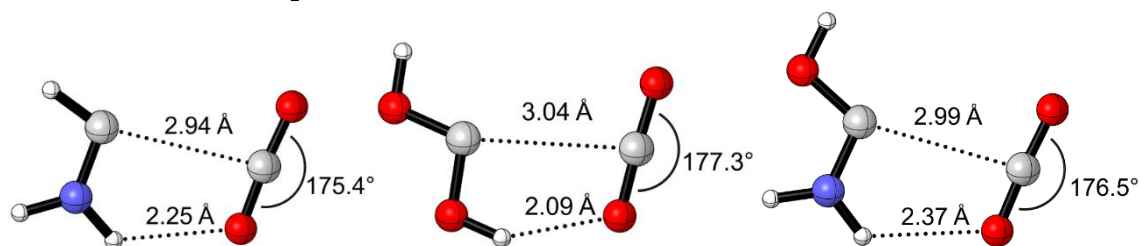


Fig. S51. Minimum geometries of aminomethylene-CO₂, dihydroxymethylene-CO₂, and aminohydroxymethylene-CO₂ complexes at the CCSD(T)/cc-pVTZ level of theory.

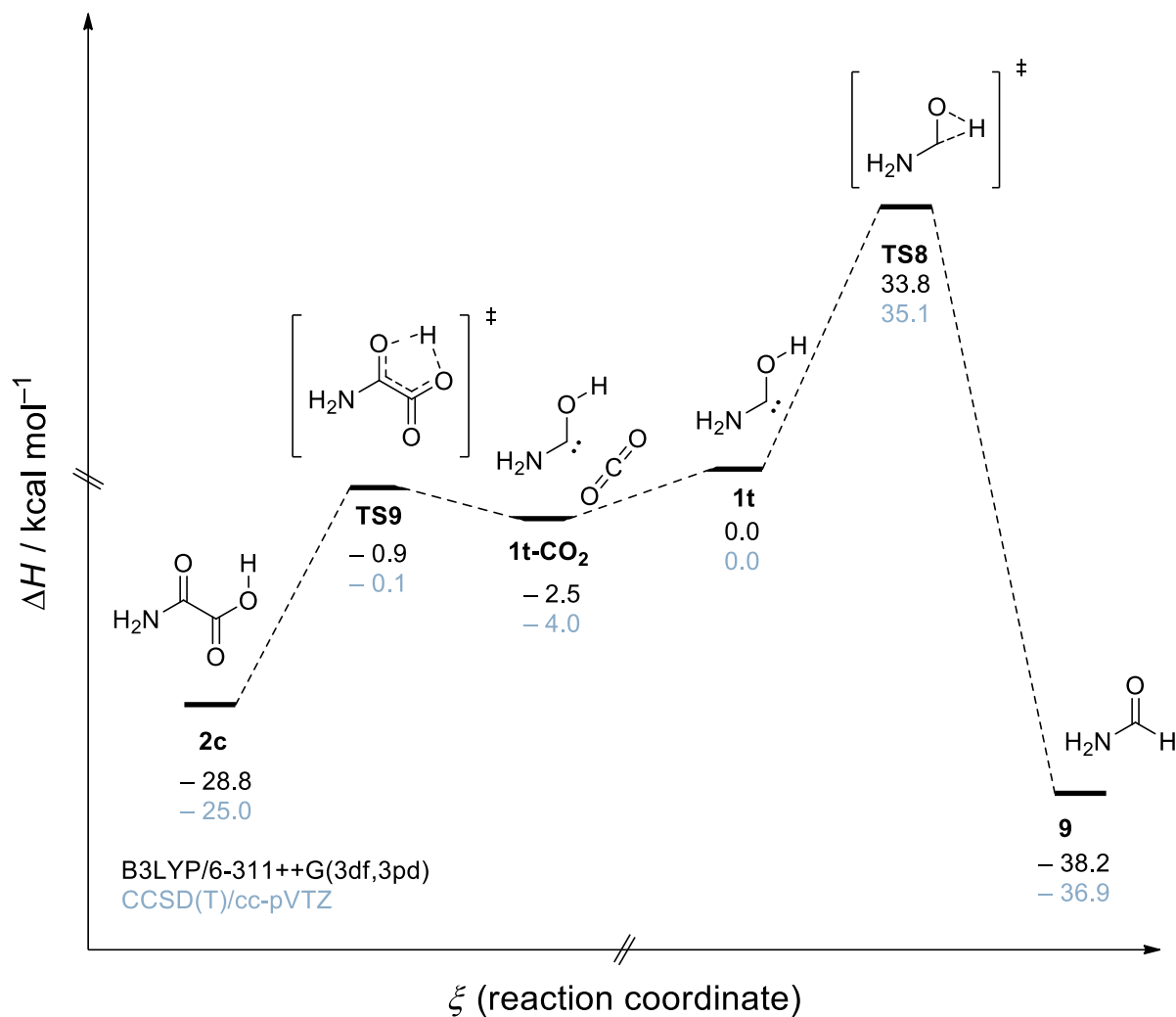


Fig. S52. PES around aminohydroxymethylene.²⁷ Some energies were corrected for CO₂ loss. CO₂ was computed at the same level of theory.

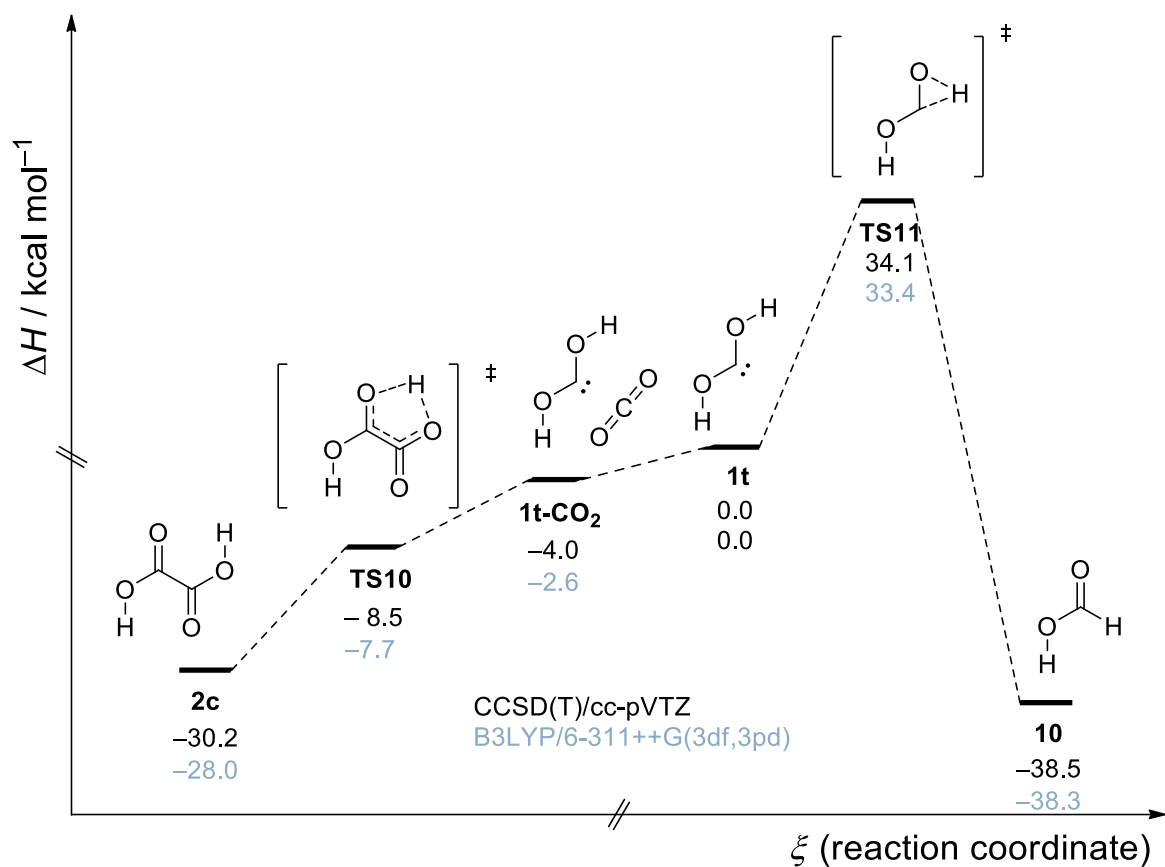


Fig. S53. PES around dihydroxycarbene.²⁸ Some energies were corrected for CO₂ loss. CO₂ was computed at the same level of theory (ZPVE was not considered, the reaction is pseudo-barrierless).

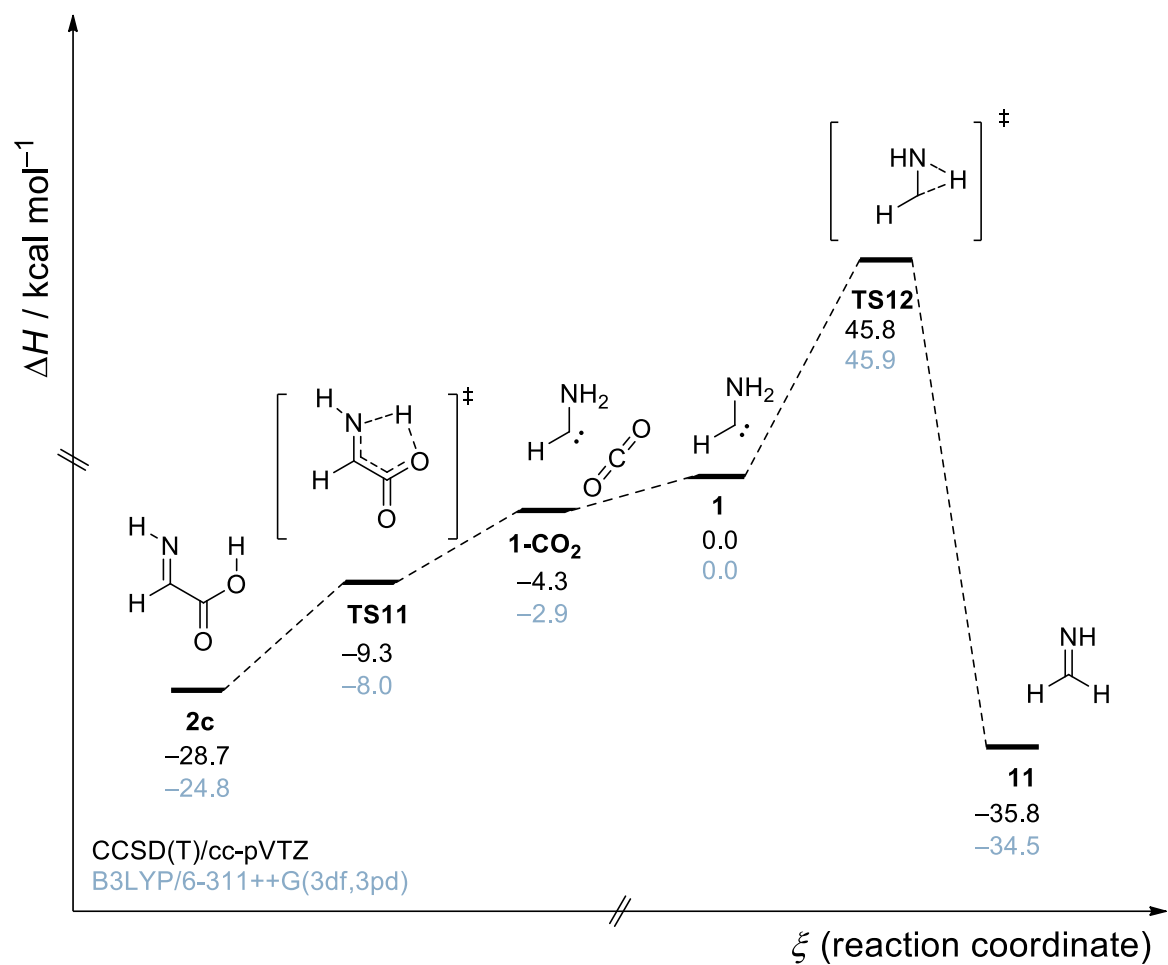


Fig. S54. PES around aminomethylene.²⁹ Some energies were corrected for CO₂ loss. CO₂ was computed at the same level of theory (ZPVE was not considered, the reaction is pseudo-barrierless).

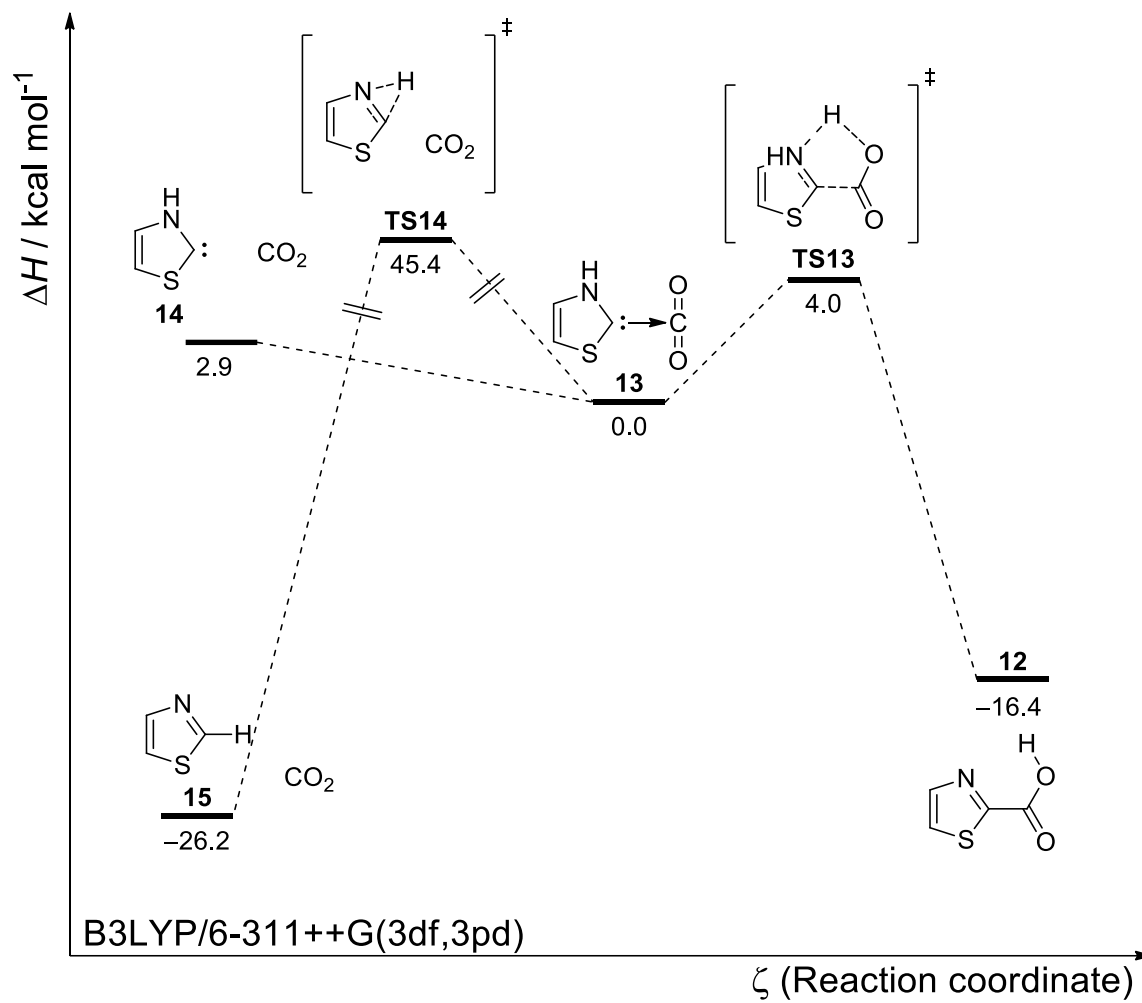


Fig. S55: PES of **13** at the B3LYP/6-311++G(3df,3pd) level of theory.

Tunneling Computations

Table S15. Overview of CVT/SCT tunneling half-lives at the B3LYP/6-311+G(d,p) level of theory. The symmetry number accounts for the degeneracy of the reaction path.

Reaction	Symmetry Number	Tunneling Half-Life
1t-CO₂ → 2c	1	0.92 h (4 K)
1t-CO₂-d₃ → 2c-d₃	1	4.32 h (4 K)
1t-¹³CO₂ → 2c-¹³C	1	1.55 h (4 K)
3a → 2t	1	433 a (30 K)
3b → 2c	1	1.61 a (20 K)
2t → 2c	2	1.28 h (8 K)
1t-CO₂ → 1c-CO₂	2	7.55 x 10 ¹⁰ a (10 K)
1c-CO₂ → 1t-CO₂	2	5.23 x 10 ¹⁰ a (10 K)
1c → thiol_6	2	1.00 x 10 ¹⁰ a (35 K)
1t → thiol_5	2	9.05 x 10 ⁹ a (35 K)
1t → thione	1	2.63 a (25 K)

Table S16. Computed rate constants in s^{-1} of the reaction $\mathbf{1t}\text{-CO}_2 \rightarrow \mathbf{2c}$ at the B3LYP/6-311+G(d,p) level of theory.

T / K	TST	CVT	CVT/ZCT	CVT/SCT
4.00	4.48×10^{-94}	6.08×10^{-95}	7.58×10^{-5}	2.09×10^{-4}
5.00	3.78×10^{-73}	7.64×10^{-74}	7.58×10^{-5}	2.09×10^{-4}
6.00	3.49×10^{-59}	9.19×10^{-60}	7.59×10^{-5}	2.10×10^{-4}
8.00	1.06×10^{-41}	3.89×10^{-42}	7.80×10^{-5}	2.13×10^{-4}
10.00	3.44×10^{-31}	1.54×10^{-31}	8.78×10^{-5}	2.31×10^{-4}
20.00	4.41×10^{-10}	2.92×10^{-10}	1.23×10^{-3}	1.99×10^{-3}
30.00	5.15×10^{-3}	3.88×10^{-3}	2.07×10^{-1}	2.36×10^{-1}
40.00	1.76×10^1	1.40×10^1	6.71×10^1	6.87×10^1
50.00	2.29×10^3	1.88×10^3	4.39×10^3	4.43×10^3
75.00	1.42×10^6	1.20×10^6	1.61×10^6	1.61×10^6
77.36	2.09×10^6	1.77×10^6	2.31×10^6	2.32×10^6
100.00	3.33×10^7	2.82×10^7	3.19×10^7	3.20×10^7
125.00	2.14×10^8	1.79×10^8	1.88×10^8	1.88×10^8
150.00	7.22×10^8	5.94×10^8	5.98×10^8	5.98×10^8
175.00	1.70×10^9	1.38×10^9	1.34×10^9	1.34×10^9
194.70	2.84×10^9	2.26×10^9	2.17×10^9	2.17×10^9
200.00	3.21×10^9	2.54×10^9	2.42×10^9	2.42×10^9
225.00	5.23×10^9	4.06×10^9	3.78×10^9	3.78×10^9
250.00	7.70×10^9	5.85×10^9	5.35×10^9	5.35×10^9
273.15	1.03×10^{10}	7.69×10^9	6.91×10^9	6.91×10^9
275.00	1.05×10^{10}	7.84×10^9	7.03×10^9	7.03×10^9
298.15	1.34×10^{10}	9.79×10^9	8.64×10^9	8.64×10^9
300.00	1.37×10^{10}	9.95×10^9	8.76×10^9	8.77×10^9
325.00	1.70×10^{10}	1.21×10^{10}	1.05×10^{10}	1.05×10^{10}
350.00	2.05×10^{10}	1.43×10^{10}	1.21×10^{10}	1.22×10^{10}
373.15	2.38×10^{10}	1.62×10^{10}	1.36×10^{10}	1.36×10^{10}
375.00	2.41×10^{10}	1.64×10^{10}	1.37×10^{10}	1.37×10^{10}
400.00	2.77×10^{10}	1.84×10^{10}	1.52×10^{10}	1.52×10^{10}

Table S17. Computed rate constants in s^{-1} of the reaction $\mathbf{1t}\text{-CO}_2\text{-}d_3 \rightarrow \mathbf{2c}\text{-}d_3$ at the B3LYP/6-311+G(d,p) level of theory.

T / K	TST	CVT	CVT/ZCT	CVT/SCT
4.00	4.73×10^{-94}	7.56×10^{-95}	2.50×10^{-5}	4.64×10^{-5}
5.00	3.95×10^{-73}	9.09×10^{-74}	2.50×10^{-5}	4.64×10^{-5}
6.00	3.62×10^{-59}	1.06×10^{-59}	2.51×10^{-5}	4.65×10^{-5}
8.00	1.09×10^{-41}	4.34×10^{-42}	2.60×10^{-5}	4.84×10^{-5}
10.00	3.52×10^{-31}	1.68×10^{-31}	3.01×10^{-5}	5.67×10^{-5}
20.00	4.44×10^{-10}	3.04×10^{-10}	6.08×10^{-4}	9.91×10^{-4}
30.00	5.12×10^{-3}	3.94×10^{-3}	1.59×10^{-1}	1.81×10^{-1}
40.00	1.74×10^1	1.41×10^1	6.78×10^1	6.94×10^1
50.00	2.24×10^3	1.86×10^3	4.91×10^3	4.96×10^3
75.00	1.37×10^6	1.17×10^6	1.88×10^6	1.89×10^6
77.36	2.02×10^6	1.72×10^6	2.71×10^6	2.72×10^6
100.00	3.21×10^7	2.72×10^7	3.67×10^7	3.68×10^7
125.00	2.05×10^8	1.72×10^8	2.11×10^8	2.11×10^8
150.00	6.91×10^8	5.71×10^8	6.58×10^8	6.58×10^8
175.00	1.63×10^9	1.32×10^9	1.45×10^9	1.45×10^9
194.70	2.72×10^9	2.17×10^9	2.32×10^9	2.32×10^9
200.00	3.07×10^9	2.44×10^9	2.59×10^9	2.59×10^9
225.00	5.01×10^9	3.90×10^9	4.00×10^9	4.00×10^9
250.00	7.39×10^9	5.62×10^9	5.61×10^9	5.61×10^9
273.15	9.92×10^9	7.39×10^9	7.20×10^9	7.20×10^9
275.00	1.01×10^{10}	7.54×10^9	7.32×10^9	7.33×10^9
298.15	1.29×10^{10}	9.42×10^9	8.95×10^9	8.95×10^9
300.00	1.32×10^{10}	9.58×10^9	9.08×10^9	9.08×10^9
325.00	1.64×10^{10}	1.17×10^{10}	1.08×10^{10}	1.08×10^{10}
350.00	1.98×10^{10}	1.38×10^{10}	1.25×10^{10}	1.25×10^{10}
373.15	2.30×10^{10}	1.57×10^{10}	1.40×10^{10}	1.40×10^{10}
375.00	2.32×10^{10}	1.58×10^{10}	1.41×10^{10}	1.41×10^{10}
400.00	2.68×10^{10}	1.78×10^{10}	1.55×10^{10}	1.55×10^{10}

Table S18. Computed rate constants in s^{-1} of the reaction $\mathbf{1t}\text{-}^{13}\text{CO}_2 \rightarrow \mathbf{2c}\text{-}^{13}\text{CO}_2$ at the B3LYP/6-311+G(d,p) level of theory.

T / K	TST	CVT	CVT/ZCT	CVT/SCT
4.00	7.74×10^{-95}	1.01×10^{-95}	3.60×10^{-5}	1.24×10^{-4}
5.00	9.28×10^{-74}	1.82×10^{-74}	3.60×10^{-5}	1.24×10^{-4}
6.00	1.08×10^{-59}	2.78×10^{-60}	3.61×10^{-5}	1.24×10^{-4}
8.00	4.41×10^{-42}	1.59×10^{-42}	3.71×10^{-5}	1.26×10^{-4}
10.00	1.70×10^{-31}	7.50×10^{-32}	4.19×10^{-5}	1.34×10^{-4}
20.00	3.10×10^{-10}	2.04×10^{-10}	6.48×10^{-4}	1.01×10^{-3}
30.00	4.06×10^{-3}	3.04×10^{-3}	1.36×10^{-1}	1.52×10^{-1}
40.00	1.47×10^1	1.17×10^1	5.02×10^1	5.14×10^1
50.00	1.98×10^3	1.62×10^3	3.46×10^3	3.49×10^3
75.00	1.29×10^6	1.08×10^6	1.36×10^6	1.36×10^6
77.36	1.90×10^6	1.60×10^6	1.96×10^6	1.97×10^6
100.00	3.09×10^7	2.60×10^7	2.80×10^7	2.81×10^7
125.00	2.00×10^8	1.67×10^8	1.69×10^8	1.69×10^8
150.00	6.83×10^8	5.62×10^8	5.48×10^8	5.48×10^8
175.00	1.62×10^9	1.31×10^9	1.24×10^9	1.24×10^9
194.70	2.72×10^9	2.16×10^9	2.02×10^9	2.02×10^9
200.00	3.07×10^9	2.43×10^9	2.26×10^9	2.26×10^9
225.00	5.02×10^9	3.90×10^9	3.56×10^9	3.56×10^9
250.00	7.42×10^9	5.64×10^9	5.06×10^9	5.06×10^9
273.15	9.97×10^9	7.42×10^9	6.56×10^9	6.56×10^9
275.00	1.02×10^{10}	7.57×10^9	6.68×10^9	6.68×10^9
298.15	1.30×10^{10}	9.46×10^9	8.23×10^9	8.23×10^9
300.00	1.32×10^{10}	9.62×10^9	8.35×10^9	8.35×10^9
325.00	1.65×10^{10}	1.17×10^{10}	1.00×10^{10}	1.00×10^{10}
350.00	1.99×10^{10}	1.38×10^{10}	1.16×10^{10}	1.16×10^{10}

Table S19. Computed rate constants in s^{-1} of the reaction **3a** \rightarrow **2t** at the B3LYP/6-311+G(d,p) level of theory.

T / K	TST	CVT	CVT/ZCT	CVT/SCT
4.00	0.00	0.00	NaN	NaN
5.00	0.00	0.00	NaN	NaN
6.00	0.00	0.00	NaN	NaN
8.00	0.00	0.00	NaN	NaN
10.00	0.00	0.00	NaN	NaN
20.00	0.00	0.00	NaN	NaN
30.00	3.12×10^{-195}	3.12×10^{-195}	1.14×10^{-14}	7.32×10^{-11}
40.00	1.71×10^{-143}	1.71×10^{-143}	1.69×10^{-14}	9.45×10^{-11}
50.00	2.00×10^{-112}	2.00×10^{-112}	2.78×10^{-14}	1.26×10^{-10}
75.00	6.02×10^{-71}	6.02×10^{-71}	1.35×10^{-13}	2.79×10^{-10}
77.36	2.03×10^{-68}	2.03×10^{-68}	1.60×10^{-13}	3.03×10^{-10}
100.00	3.62×10^{-50}	3.61×10^{-50}	8.64×10^{-13}	6.89×10^{-10}
125.00	1.11×10^{-37}	1.11×10^{-37}	6.22×10^{-12}	1.92×10^{-9}
150.00	2.41×10^{-29}	2.40×10^{-29}	4.78×10^{-11}	6.07×10^{-9}
175.00	2.20×10^{-23}	2.19×10^{-23}	3.80×10^{-10}	2.13×10^{-8}
194.70	9.18×10^{-20}	9.15×10^{-20}	1.97×10^{-9}	6.10×10^{-8}
200.00	6.54×10^{-19}	6.52×10^{-19}	3.07×10^{-9}	8.18×10^{-8}
225.00	1.98×10^{-15}	1.98×10^{-15}	2.50×10^{-8}	3.45×10^{-7}
250.00	1.22×10^{-12}	1.21×10^{-12}	2.04×10^{-7}	1.59×10^{-6}
273.15	1.63×10^{-10}	1.62×10^{-10}	1.43×10^{-6}	6.98×10^{-6}
275.00	2.33×10^{-10}	2.31×10^{-10}	1.67×10^{-6}	7.88×10^{-6}
298.15	1.38×10^{-8}	1.37×10^{-8}	1.17×10^{-5}	3.66×10^{-6}
300.00	1.86×10^{-8}	1.84×10^{-8}	1.36×10^{-5}	4.15×10^{-5}
325.00	7.56×10^{-7}	7.51×10^{-7}	1.09×10^{-5}	2.31×10^{-4}
350.00	1.82×10^{-5}	1.80×10^{-5}	8.41×10^{-4}	1.35×10^{-3}
373.15	2.36×10^{-4}	2.34×10^{-4}	5.17×10^{-3}	7.02×10^{-3}
375.00	2.86×10^{-4}	2.83×10^{-4}	5.96×10^{-3}	7.99×10^{-3}
400.00	3.19×10^{-3}	3.16×10^{-3}	3.76×10^{-2}	4.52×10^{-2}

Table S20. Computed rate constants in s^{-1} of the reaction **3b** \rightarrow **2c** at the B3LYP/6-311+G(d,p) level of theory.

T / K	TST	CVT	CVT/ZCT	CVT/SCT
4.00	0.00	0.00	NaN	NaN
5.00	0.00	0.00	NaN	NaN
6.00	0.00	0.00	NaN	NaN
8.00	0.00	0.00	NaN	NaN
10.00	0.00	0.00	NaN	NaN
20.00	7.48×10^{-265}	7.42×10^{-265}	1.13×10^{-11}	1.97×10^{-8}
30.00	1.08×10^{-172}	1.08×10^{-172}	2.90×10^{-11}	3.12×10^{-8}
40.00	1.47×10^{-126}	1.47×10^{-126}	7.05×10^{-11}	5.37×10^{-8}
50.00	7.53×10^{-99}	7.52×10^{-99}	1.48×10^{-10}	8.88×10^{-8}
75.00	7.53×10^{-62}	7.53×10^{-62}	6.72×10^{-10}	2.51×10^{-7}
77.36	1.36×10^{-59}	1.36×10^{-59}	7.65×10^{-10}	2.74×10^{-7}
100.00	2.59×10^{-43}	2.59×10^{-43}	2.60×10^{-9}	5.98×10^{-7}
125.00	3.56×10^{-32}	3.56×10^{-32}	1.04×10^{-8}	1.37×10^{-6}
150.00	9.68×10^{-25}	9.67×10^{-25}	4.57×10^{-8}	3.22×10^{-6}
175.00	2.00×10^{-19}	1.99×10^{-19}	2.23×10^{-8}	8.15×10^{-6}
194.70	3.38×10^{-16}	3.37×10^{-16}	8.24×10^{-7}	1.82×10^{-5}
200.00	1.94×10^{-15}	1.94×10^{-15}	1.18×10^{-6}	2.28×10^{-5}
225.00	2.47×10^{-12}	2.46×10^{-12}	6.67×10^{-6}	7.23×10^{-5}
250.00	7.51×10^{-10}	7.50×10^{-10}	3.98×10^{-5}	2.59×10^{-4}
273.15	5.90×10^{-8}	5.89×10^{-8}	2.16×10^{-4}	9.32×10^{-4}
275.00	8.11×10^{-8}	8.08×10^{-8}	2.48×10^{-4}	1.04×10^{-4}
298.15	3.07×10^{-6}	3.06×10^{-6}	1.39×10^{-3}	4.04×10^{-3}
300.00	4.01×10^{-6}	4.00×10^{-6}	1.59×10^{-3}	4.52×10^{-3}
325.00	1.09×10^{-4}	1.09×10^{-4}	1.02×10^{-2}	2.11×10^{-2}
350.00	1.85×10^{-3}	1.84×10^{-3}	6.34×10^{-2}	1.03×10^{-2}
373.15	1.82×10^{-2}	1.81×10^{-2}	3.21×10^{-1}	4.45×10^{-1}
375.00	2.16×10^{-2}	2.15×10^{-2}	3.64×10^{-1}	5.00×10^{-1}
400.00	1.85×10^{-1}	1.84×10^{-1}	1.87×10^0	2.32×10^0

Table S21. Computed rate constants in s^{-1} of the reaction $2\mathbf{t} \rightarrow 2\mathbf{c}$ at the B3LYP/6-311+G(d,p) level of theory.

T / K	TST	CVT	CVT/ZCT	CVT/SCT
4.00	0.00	0.00	NaN	NaN
5.00	0.00	0.00	NaN	NaN
6.00	0.00	0.00	NaN	NaN
8.00	5.19×10^{-261}	5.19×10^{-261}	1.89×10^{-6}	1.50×10^{-4}
10.00	1.30×10^{-206}	1.30×10^{-206}	1.89×10^{-6}	1.50×10^{-4}
20.00	1.04×10^{-97}	1.04×10^{-97}	2.00×10^{-6}	1.57×10^{-4}
30.00	2.43×10^{-61}	2.43×10^{-61}	2.33×10^{-6}	1.81×10^{-4}
40.00	4.03×10^{-43}	4.03×10^{-43}	2.92×10^{-6}	2.23×10^{-4}
50.00	3.61×10^{-32}	3.61×10^{-32}	3.87×10^{-6}	2.86×10^{-4}
75.00	1.61×10^{-17}	1.61×10^{-17}	1.02×10^{-5}	6.16×10^{-4}
77.36	1.26×10^{-16}	1.26×10^{-16}	1.15×10^{-5}	6.71×10^{-4}
100.00	3.70×10^{-10}	3.70×10^{-10}	5.45×10^{-5}	1.94×10^{-3}
125.00	1.02×10^{-5}	1.02×10^{-5}	1.32×10^{-3}	1.36×10^{-2}
150.00	9.56×10^{-3}	9.56×10^{-3}	1.07×10^{-1}	3.04×10^{-1}
175.00	1.30×10^0	1.30×10^0	5.95×10^0	9.98×10^0
194.70	2.59×10^1	2.59×10^1	8.24×10^1	1.17×10^2
200.00	5.25×10^1	5.25×10^1	1.55×10^2	2.13×10^2
225.00	9.44×10^2	9.44×10^2	2.15×10^3	2.68×10^3
250.00	9.60×10^3	9.60×10^3	1.85×10^4	2.18×10^4
273.15	5.66×10^4	5.66×10^4	9.75×10^5	1.11×10^5
275.00	6.44×10^4	6.44×10^4	1.10×10^5	1.25×10^5
298.15	2.84×10^5	2.84×10^5	4.47×10^5	4.97×10^5
300.00	3.16×10^5	3.16×10^5	4.96×10^5	5.50×10^5
325.00	1.22×10^6	1.22×10^6	1.79×10^6	1.95×10^6
350.00	3.89×10^6	3.89×10^6	5.43×10^6	5.83×10^6
373.15	9.95×10^6	9.95×10^6	1.33×10^7	1.42×10^7
375.00	1.07×10^7	1.07×10^7	1.43×10^7	1.52×10^7
400.00	2.58×10^7	2.58×10^7	3.34×10^7	3.53×10^7

Table S22. Computed rate constants in s^{-1} of the reaction $\mathbf{1t}\text{-CO}_2 \rightarrow \mathbf{1c}\text{-CO}_2$ at the B3LYP/6-311+G(d,p) level of theory.

T / K	TST	CVT	CVT/ZCT	CVT/SCT
4.00	0.00	0.00	NaN	NaN
5.00	0.00	0.00	NaN	NaN
6.00	0.00	0.00	NaN	NaN
8.00	0.00	0.00	NaN	NaN
10.00	2.64×10^{-257}	2.62×10^{-257}	8.40×10^{-22}	4.20×10^{-19}
20.00	6.86×10^{-123}	6.84×10^{-123}	8.77×10^{-22}	4.39×10^{-19}
30.00	5.26×10^{-78}	5.25×10^{-78}	9.67×10^{-22}	4.83×10^{-19}
40.00	1.60×10^{-55}	1.60×10^{-55}	1.13×10^{-21}	5.54×10^{-19}
50.00	5.23×10^{-42}	5.22×10^{-42}	1.57×10^{-21}	6.95×10^{-19}
75.00	6.17×10^{-24}	6.17×10^{-24}	2.57×10^{-19}	1.73×10^{-17}
77.36	7.83×10^{-23}	7.82×10^{-23}	6.63×10^{-19}	3.37×10^{-17}
100.00	7.35×10^{-15}	7.34×10^{-15}	7.97×10^{-14}	2.46×10^{-13}
125.00	2.15×10^{-9}	2.15×10^{-9}	5.82×10^{-9}	8.76×10^{-9}
150.00	9.78×10^{-6}	9.77×10^{-6}	1.61×10^{-5}	2.02×10^{-5}
175.00	4.08×10^{-3}	4.07×10^{-3}	5.30×10^{-3}	6.12×10^{-3}
194.70	1.60×10^{-1}	1.60×10^{-1}	1.88×10^{-1}	2.09×10^{-11}
200.00	3.80×10^{-1}	3.80×10^{-1}	4.38×10^{-1}	4.83×10^{-1}
225.00	1.31×10^1	1.31×10^1	1.40×10^1	1.50×10^1
250.00	2.22×10^2	2.22×10^2	2.28×10^2	2.41×10^2
273.15	1.94×10^3	1.94×10^3	1.94×10^3	2.02×10^3
275.00	2.27×10^3	2.27×10^3	2.27×10^3	2.36×10^3
298.15	1.38×10^4	1.38×10^4	1.36×10^4	1.40×10^4
300.00	1.58×10^4	1.57×10^4	1.55×10^4	1.60×10^4
325.00	8.14×10^4	8.14×10^4	7.90×10^4	8.11×10^4
350.00	3.33×10^5	3.33×10^5	3.21×10^5	3.28×10^5
373.15	1.04×10^6	1.04×10^6	9.96×10^5	1.01×10^6
375.00	1.13×10^6	1.13×10^6	1.08×10^6	1.10×10^6
400.00	3.30×10^6	3.30×10^6	3.15×10^6	3.20×10^6

Table S23. Computed rate constants in s^{-1} of the reaction $\mathbf{1c}\text{-CO}_2 \rightarrow \mathbf{1t}\text{-CO}_2$ at the B3LYP/6-311+G(d,p) level of theory.

T / K	TST	CVT	CVT/ZCT	CVT/SCT
4.00	0.00	0.00	NaN	NaN
5.00	0.00	0.00	NaN	NaN
6.00	0.00	0.00	NaN	NaN
8.00	0.00	0.00	NaN	NaN
10.00	2.91×10^{-250}	2.89×10^{-250}	8.02×10^{-22}	4.03×10^{-19}
20.00	2.25×10^{-119}	2.25×10^{-119}	1.03×10^{-21}	4.85×10^{-19}
30.00	1.15×10^{-75}	1.15×10^{-75}	1.79×10^{-21}	7.37×10^{-19}
40.00	9.00×10^{-54}	8.99×10^{-54}	3.72×10^{-21}	1.31×10^{-18}
50.00	1.30×10^{-40}	1.30×10^{-40}	9.81×10^{-21}	2.76×10^{-18}
75.00	5.16×10^{-23}	5.16×10^{-23}	2.13×10^{-18}	1.39×10^{-16}
77.36	6.13×10^{-22}	6.13×10^{-22}	5.17×10^{-18}	2.58×10^{-16}
100.00	3.56×10^{-14}	3.56×10^{-14}	4.23×10^{-13}	1.23×10^{-12}
125.00	7.52×10^{-9}	7.52×10^{-9}	2.60×10^{-8}	3.65×10^{-8}
150.00	2.75×10^{-5}	2.75×10^{-5}	6.14×10^{-5}	7.36×10^{-5}
175.00	9.86×10^{-3}	9.86×10^{-3}	1.75×10^{-2}	1.97×10^{-2}
194.70	3.54×10^{-1}	3.54×10^{-1}	5.62×10^{-1}	6.15×10^{-1}
200.00	8.24×10^{-1}	8.23×10^{-1}	1.28×10^0	1.39×10^0
225.00	2.60×10^1	2.60×10^1	3.68×10^1	3.92×10^1
250.00	4.13×10^2	4.13×10^2	5.49×10^2	5.77×10^2
273.15	3.43×10^3	3.42×10^3	4.36×10^3	4.54×10^3
275.00	3.99×10^3	3.99×10^3	5.07×10^3	5.28×10^3
298.15	2.33×10^4	2.33×10^4	2.86×10^4	2.96×10^4
300.00	2.66×10^4	2.66×10^4	3.25×10^4	3.36×10^4
325.00	1.32×10^5	1.32×10^5	1.58×10^5	1.62×10^5
350.00	5.25×10^5	5.25×10^5	6.12×10^5	6.27×10^5
373.15	1.60×10^6	1.60×10^6	1.83×10^6	1.87×10^6
375.00	1.73×10^6	1.73×10^6	1.99×10^6	2.03×10^6
400.00	4.95×10^6	4.95×10^6	5.58×10^6	5.68×10^6

Table S24. Computed rate constants in s^{-1} of the reaction **1c** \rightarrow **thiol_6** at the B3LYP/6-311+G(d,p) level of theory.

T / K	TST	CVT	CVT/ZCT	CVT/SCT
0.10	NaN	NaN	NaN	NaN
8.00	0.00×10^0	0.00×10^0	NaN	NaN
10.00	0.00×10^0	0.00×10^0	NaN	NaN
15.00	0.00×10^0	0.00×10^0	NaN	NaN
20.00	0.00×10^0	0.00×10^0	NaN	NaN
25.00	0.00×10^0	0.00×10^0	NaN	NaN
30.00	0.00×10^0	0.00×10^0	NaN	NaN
35.00	2.11×10^{-276}	2.07×10^{-276}	4.04×10^{-21}	2.19×10^{-18}
40.00	2.32×10^{-240}	2.27×10^{-240}	4.04×10^{-21}	2.19×10^{-18}
45.00	2.52×10^{-212}	2.48×10^{-212}	4.04×10^{-21}	2.19×10^{-18}
50.00	6.86×10^{-190}	6.75×10^{-190}	4.04×10^{-21}	2.19×10^{-18}
200.00	3.78×10^{-38}	3.77×10^{-38}	1.86×10^{-20}	4.38×10^{-18}
250.00	5.75×10^{-28}	5.72×10^{-28}	1.11×10^{-18}	2.71×10^{-17}
300.00	3.66×10^{-21}	3.65×10^{-21}	2.19×10^{-16}	1.30×10^{-15}
350.00	2.72×10^{-16}	2.71×10^{-16}	7.84×10^{-14}	2.08×10^{-13}

Table S25. Computed rate constants in s^{-1} of the reaction **1t** \rightarrow **thiol_5** at the B3LYP/6-311+G(d,p) level of theory.

T / K	TST	CVT	CVT/ZCT	CVT/SCT
0.10	NaN	NaN	NaN	NaN
8.00	0.00×10^0	0.00×10^0	NaN	NaN
10.00	0.00×10^0	0.00×10^0	NaN	NaN
15.00	0.00×10^0	0.00×10^0	NaN	NaN
20.00	0.00×10^0	0.00×10^0	NaN	NaN
25.00	0.00×10^0	0.00×10^0	NaN	NaN
30.00	0.00×10^0	0.00×10^0	NaN	NaN
35.00	2.96×10^{-274}	2.96×10^{-274}	3.56×10^{-21}	2.43×10^{-18}
40.00	1.75×10^{-238}	1.75×10^{-238}	3.56×10^{-21}	2.43×10^{-18}
45.00	1.18×10^{-210}	1.18×10^{-210}	3.56×10^{-21}	2.43×10^{-18}
50.00	2.18×10^{-188}	2.18×10^{-188}	3.56×10^{-21}	2.43×10^{-18}
200.00	9.03×10^{-38}	9.03×10^{-38}	2.05×10^{-20}	5.32×10^{-18}
250.00	1.15×10^{-27}	1.15×10^{-27}	1.59×10^{-18}	4.02×10^{-17}
300.00	6.54×10^{-21}	6.54×10^{-21}	3.56×10^{-16}	2.16×10^{-15}
350.00	4.47×10^{-16}	4.47×10^{-16}	1.28×10^{-13}	3.47×10^{-13}

Table S26. Computed rate constants in s^{-1} of the reaction **1t** \rightarrow **thione** at the B3LYP/6-311+G(d,p) level of theory.

T / K	TST	CVT	CVT/ZCT	CVT/SCT
0.10	NaN	NaN	NaN	NaN
8.00	0.00×10^0	0.00×10^0	NaN	NaN
10.00	0.00×10^0	0.00×10^0	NaN	NaN
15.00	0.00×10^0	0.00×10^0	NaN	NaN
20.00	0.00×10^0	0.00×10^0	NaN	NaN
25.00	4.15×10^{-243}	3.07×10^{-243}	6.81×10^{-10}	8.37×10^{-9}
30.00	1.12×10^{-200}	8.68×10^{-201}	6.81×10^{-10}	8.38×10^{-9}
35.00	2.33×10^{-170}	1.87×10^{-170}	6.83×10^{-10}	8.40×10^{-9}
40.00	1.31×10^{-147}	1.07×10^{-147}	6.86×10^{-10}	8.43×10^{-9}
45.00	6.60×10^{-130}	5.48×10^{-130}	6.90×10^{-10}	8.48×10^{-9}
50.00	9.72×10^{-116}	8.16×10^{-116}	6.95×10^{-10}	8.55×10^{-9}
200.00	1.28×10^{-19}	1.01×10^{-19}	3.00×10^{-9}	2.73×10^{-8}
250.00	4.01×10^{-13}	3.10×10^{-13}	3.33×10^{-8}	1.60×10^{-7}
300.00	9.00×10^{-9}	6.78×10^{-9}	1.60×10^{-6}	3.95×10^{-6}
350.00	1.18×10^{-5}	8.72×10^{-6}	1.59×10^{-4}	2.42×10^{-4}

Cartesian Coordinates of Computed Structures

In this section the Cartesian coordinates of the computed geometries are given in Angstrom at the CCSD(T)/cc-pVTZ, the B3LYP/6-311++G(3df,3pd), and the MP2/def2-QZVPP levels of theory. Electronic and zero-point vibrational energies (ZPVEs) are provided for each structure. For transition states, the imaginary frequency is given additionally.

For CCSD(T)/cc-pVTZ and B3LYP/6-311++G(3df,3pd) geometries of thioformamide and its thiolimine tautomers see: https://chemistry-europe.onlinelibrary.wiley.com/action/downloadSupplement?doi=10.1002%2Fchem.202005188&file=chem202005188-s1-Supporting_Information_for_Accepted_Article.pdf.

CCSD(T)/cc-pVTZ

1c

16	-1.005899507	-0.048274946	0.000000000
1	-0.766159617	-1.393207595	0.000000000
6	0.581687068	0.632616933	0.000000000
7	1.567991390	-0.247507122	0.000000000
1	1.448259211	-1.258290352	0.000000000
1	2.516616239	0.089453308	0.000000000

E = -492.177533201648714 au

ZPVE = 25.2367 kcal mol⁻¹

1t

16	-0.978456306	0.131779804	0.000000000
1	-1.686738109	-1.003338591	0.000000000
6	0.596885928	-0.661189097	0.000000000
7	1.559959702	0.252271146	0.000000000
1	1.432294040	1.260180970	0.000000000
1	2.513181392	-0.069880920	0.000000000

E = -492.177819346771571 au

ZPVE = 25.5404 kcal mol⁻¹

TS: 1t → 1c

16	-1.019924969	-0.074382959	-0.042768317
1	-1.036412296	-0.301683913	1.280904541
6	0.680699195	0.688452917	0.020387781
7	1.545166732	-0.300411882	-0.008783273
1	1.287772674	-1.284663213	-0.064812873
1	2.530510200	-0.077203627	0.019967297

E = -492.159698956876639 au

ZPVE = 24.7388 kcal mol⁻¹

$\nu_i = 391.3i$ cm⁻¹

1c-CO₂

6	0.764236820	-0.157585318	0.000000000
7	0.748140735	-1.476673929	0.000000000
16	2.327113903	0.575855794	0.000000000
1	-0.148528396	-1.938837880	0.000000000
1	1.574368368	-2.069769535	0.000000000
1	3.167683720	-0.499265907	0.000000000
6	-2.217841140	0.201818503	0.000000000
8	-2.203764548	-0.968898185	0.000000000
8	-2.301738499	1.361461802	0.000000000

E = -680.512402831025042 au

ZPVE = 33.2153 kcal mol⁻¹

1t-CO₂

6	0.731983541	-0.146292045	0.000000000
7	0.742864515	-1.470185930	0.000000000
16	2.371756496	0.490645917	0.000000000
1	-0.150276343	-1.938308386	0.000000000
1	1.567464388	-2.062715835	0.000000000
1	2.003363801	1.777208468	0.000000000
6	-2.210241911	0.205855697	0.000000000
8	-2.212974318	-0.964782927	0.000000000
8	-2.284740876	1.366573744	0.000000000

E = -680.512969882841276 au

ZPVE = 33.5207 kcal mol⁻¹

TS: 1t-CO₂ → 1c-CO₂

6	0.712835865	-0.088204756	0.006853581
7	0.724794895	-1.399024962	0.014659337
16	2.477073622	0.496512582	0.035385458
1	-0.167216222	-1.878216710	0.001274269
1	1.573025385	-1.961911659	0.039506569
1	2.609723129	0.367501545	-1.295021455
6	-2.293345038	0.193298389	-0.003177503
8	-2.236056542	-0.976548103	-0.012303980
8	-2.417133250	1.348840888	0.005009165

E = -680.494478242239893 au

ZPVE = 32.7021 kcal mol⁻¹

$\nu_i = 394.9i$ cm⁻¹

TS: 1t-CO₂ → 2c

6	0.453625666	-0.377034990	0.000000000
7	0.500542389	-1.686027545	0.000000000
16	1.955123982	0.480386996	0.000000000
1	-0.401664482	-2.148286680	0.000000000
1	1.334632066	-2.260667243	0.000000000
1	1.363759193	1.686138551	0.000000000
6	-1.585719474	0.308820656	0.000000000
8	-2.130120554	-0.750714076	0.000000000
8	-1.511541100	1.489279756	0.000000000

E = -680.506474541059561 au

ZPVE = 33.6575 kcal mol⁻¹

$\nu_i = 214.4i$ cm⁻¹

CO₂

8	0.000000000	0.000000000	1.166288734
6	0.000000000	0.000000000	0.000000000
8	0.000000000	0.000000000	-1.166288734

E = -188.327217847799375 au

ZPVE = 7.2380 kcal mol⁻¹

Trans-2-Amino-2-thioxoacetic acid (2t)

16	-1.749606440	0.433982924	0.000000000
6	-0.349044250	-0.431241034	0.000000000
6	1.044500521	0.189922175	0.000000000
8	1.042353072	1.523634795	0.000000000
8	2.049641029	-0.488473115	0.000000000
7	-0.245801811	-1.769978526	0.000000000
1	0.671958992	-2.186447101	0.000000000
1	-1.079593239	-2.330185993	0.000000000
1	1.974240378	1.786309047	0.000000000

E = -680.552608465715139 au

ZPVE = 37.2399 kcal mol⁻¹

Cis-2-Amino-2-thioacetic acid (**2c**)

16	-1.725048134	0.384411123	0.000000000
6	-0.323751974	-0.466125272	0.000000000
6	1.048064403	0.232202813	0.000000000
8	0.996607281	1.556940905	0.000000000
8	2.072503211	-0.407949774	0.000000000
7	-0.175586425	-1.790436534	0.000000000
1	0.765932309	-2.155634221	0.000000000
1	-0.977091605	-2.396576502	0.000000000
1	0.042678711	1.784121190	0.000000000

E = -680.559917124698927 au

ZPVE = 37.5291 kcal mol⁻¹

3a

7	-0.285193072	1.843295997	0.000000000
6	-0.252159526	0.569088877	0.000000000
1	0.683387739	2.177910192	0.000000000
16	-1.714913506	-0.430626273	0.000000000
1	-2.519357933	0.644688752	0.000000000
6	1.074111962	-0.172316951	0.000000000
8	2.136849149	0.397655594	0.000000000
8	0.925303272	-1.507372850	0.000000000
1	1.816740369	-1.885161400	0.000000000

E = -680.536555058892645 au

ZPVE = 35.1017 kcal mol⁻¹

3b

7	-0.293886819	1.830979550	-0.185011320
6	-0.244648400	0.569197167	-0.038052639
1	0.670896499	2.173872368	-0.233606688
6	1.087284147	-0.180672802	0.015859315
16	-1.716940038	-0.426357157	0.108641973
8	2.114381648	0.405021418	0.228383979
8	1.050055591	-1.507599444	-0.203078924
1	-2.530875693	0.552453370	-0.314432459
1	0.156225787	-1.768294367	-0.465245747

E = -680.529285495559293 au

ZPVE = 34.8678 kcal mol⁻¹

TS: 3a → 2t

7	-0.545309942	1.666460947	0.000000000
6	-0.283307206	0.390066150	0.000000000
1	0.228527783	2.330308757	0.000000000
16	-1.754397209	-0.492185934	0.000000000
6	1.140481040	-0.109196048	0.000000000
8	2.086011133	0.641947471	0.000000000
8	1.219776874	-1.444993352	0.000000000
1	2.163700698	-1.662466341	0.000000000
1	-1.830777838	1.192437382	0.000000000

E = -680.486257311029703 au

ZPVE = 33.1731 kcal mol⁻¹

$\nu_i = 1834.7i$ cm⁻¹

TS: 3b → 2c

7	-0.535065235	1.683032582	0.000000000
6	-0.265212143	0.413746181	0.000000000
1	0.241874845	2.344027646	0.000000000
6	1.152421596	-0.122996186	0.000000000
16	-1.743982704	-0.478999101	0.000000000
8	2.099122335	0.618401984	0.000000000
8	1.266343642	-1.458037698	0.000000000
1	-1.837046535	1.175963168	0.000000000
1	0.379129215	-1.845230934	0.000000000

E = -680.484444459190854 au

ZPVE = 33.0679 kcal mol⁻¹

$\nu_i = 1809.3i$ cm⁻¹

TS: 2t → 2c

16	-1.726531227	-0.451745171	0.088423931
6	-0.347733017	0.439800709	-0.050892654
6	1.048228120	-0.178775120	0.012799443
8	1.111537584	-1.510578442	-0.243661368
8	2.016726061	0.505335173	0.230588838
7	-0.275560940	1.774435902	-0.175625764
1	0.628971193	2.216417272	-0.133192263
1	-1.119543792	2.319303654	-0.147809244
1	1.103007718	-2.013314286	0.577101578

E = -680.535066092372745 au

ZPVE = 36.1632 kcal mol⁻¹

$\nu_i = 630.8243i$ cm⁻¹

TS_tf1

16	-1.033314550	-0.041467943	-0.007131140
1	-0.750884127	-1.370442215	-0.025741272
6	0.599434213	0.553628757	0.056519744
7	1.673869455	-0.247743151	0.027477624
1	1.495318521	-1.253396024	-0.152348881
1	1.641572492	0.789627570	-0.650437411

E = -492.098393717232113 au

ZPVE = 21.1683 kcal mol⁻¹

$\nu_i = 1947.7i$ cm⁻¹

TS_tf2

16	-1.006708307	0.123799134	0.010392194
1	-1.664869817	-1.039970166	-0.081189258
6	0.609414882	-0.574153690	-0.051374210
7	1.670220561	0.249359422	-0.031142060
1	1.491348882	1.256681955	0.121345894
1	1.647336650	-0.772432130	0.674565767

E = -492.098890642865570 au

ZPVE = 21.3554 kcal mol⁻¹

$\nu_i = 1962.7i$ cm⁻¹

TS_tf3 (C₁)

16	-1.034695872	0.113835080	-0.001361589
6	0.580687315	-0.578041365	-0.049982797
7	1.612761844	0.245013797	0.015863967
1	1.492021122	1.253890106	0.040912725
1	2.549790641	-0.121840823	0.028432064
1	-0.539717417	-1.265002161	0.348567144

E = -492.125707736241168 au

ZPVE = 22.8172 kcal mol⁻¹

$\nu_i = 1675.3i$ cm⁻¹

Dihydroxymethylene-CO₂ complex

6	-1.233521005	0.244812128	0.000000000
8	-1.439011622	-1.061722013	0.000000000
1	-0.556945195	-1.455413286	0.000000000
8	-2.443992075	0.793662372	0.000000000
1	-2.295643001	1.744319462	0.000000000
6	1.795052897	0.033007441	0.000000000
8	1.499734145	-1.100473091	0.000000000
8	2.141725723	1.141898092	0.000000000

E = -377.770921524285484 au

ZPVE = 29.3267 kcal mol⁻¹

Aminomethylene-CO₂ complex

6	1.523656375	0.903530819	0.000000000
7	2.127790005	-0.263185918	0.000000000
1	3.131349098	-0.413314192	0.000000000
1	2.324724165	1.666467583	0.000000000
1	1.560876692	-1.100930030	0.000000000
6	-1.225804897	-0.146637545	0.000000000
8	-1.841930561	0.839433029	0.000000000
8	-0.686477837	-1.186463447	0.000000000

E = -282.751367779795260 au

ZPVE = 33.3169 kcal mol⁻¹

Aminohydroxymethylene-CO₂ complex

8	0.134948738	-0.457339162	-2.339184787
6	0.134948738	0.674838866	-2.045037203
8	0.134948738	1.816983235	-1.822755290
7	0.134948738	-1.702657334	0.451326069
1	0.134948738	-1.970561408	-0.516103728
1	0.134948738	-2.423572035	1.163763301
6	0.134948738	-0.408119364	0.742142365
8	0.134948738	-0.293929961	2.091436420
1	0.134948738	0.648304706	2.274412855

E = - 357.918469840371245 au

ZPVE = 36.8402 kcal mol⁻¹

B3LYP/6-311++G(3df,3pd)

1c

16	-0.817218000	-0.664046000	0.000000000
1	1.890043000	-0.034037000	0.000000000
7	1.312938000	0.807884000	0.000000000
1	0.179138000	-1.611507000	0.000000000
6	0.000000000	0.822233000	0.000000000
1	1.815747000	1.681696000	0.000000000

E = -492.8651962 au

ZPVE = 0.0398879 au

1t

16	-0.686639000	-0.754320000	0.000000000
1	1.909980000	-0.015395000	0.000000000
7	1.318715000	0.814690000	0.000000000
1	-1.967943000	-0.361547000	0.000000000
6	0.000000000	0.841768000	0.000000000
1	1.813171000	1.692633000	0.000000000

E = -492.8646319 au

ZPVE = 0.0404994 au

TS: 1t → 1c

16	1.061708000	0.064293000	-0.082802000
1	-1.304380000	1.234184000	-0.104572000
7	-1.514363000	0.237843000	-0.011880000
1	1.125777000	0.328314000	1.233410000
6	-0.619240000	-0.706342000	0.040169000
1	-2.492749000	-0.018036000	0.038134000

E = -492.8436498 au

ZPVE = 0.0391178 au

$\nu_i = 430.8i \text{ cm}^{-1}$

1c-CO₂

6	0.000000000	0.783724000	0.000000000
6	0.202798000	-2.285058000	0.000000000
7	1.290388000	1.014531000	0.000000000
1	1.922283000	0.226578000	0.000000000
1	1.720209000	1.939023000	0.000000000
16	-1.067412000	2.102900000	0.000000000
8	1.341745000	-2.048211000	0.000000000
8	-0.912113000	-2.590744000	0.000000000
1	-0.250458000	3.205913000	0.000000000

E = -681.5306927 au

ZPVE = 0.0527453 au

1t-CO₂

6	0.000000000	0.750306000	0.000000000
6	0.257571000	-2.243605000	0.000000000
7	1.282377000	1.045480000	0.000000000
1	1.938971000	0.278412000	0.000000000
1	1.689526000	1.978612000	0.000000000
16	-1.018951000	2.153516000	0.000000000
8	1.398272000	-2.014847000	0.000000000
8	-0.856337000	-2.555215000	0.000000000
1	-2.182813000	1.488648000	0.000000000

E = -681.5305073 au

ZPVE = 0.0533081 au

TS: 1t-CO₂ → 1c-CO₂

6	0.709992000	0.081566000	-0.018631000
6	-2.358308000	-0.215477000	0.005530000
7	0.724929000	1.380858000	-0.016937000
1	-0.164650000	1.867906000	0.003430000
1	1.572184000	1.950973000	-0.038781000
16	2.443936000	-0.554807000	-0.070546000
8	-2.297287000	0.946770000	0.019173000
8	-2.489802000	-1.363427000	-0.006712000
1	2.601608000	-0.471259000	1.261553000

E = -681.5091572 au

ZPVE = 0.0519173 au

$\nu_i = 434.0i \text{ cm}^{-1}$

TS: 1t-CO₂ → 2c

6	0.000000000	0.593013000	0.000000000
6	0.726751000	-1.533180000	0.000000000
7	1.018012000	1.409220000	0.000000000
1	1.935708000	0.978061000	0.000000000
1	0.982344000	2.423876000	0.000000000
16	-1.577231000	1.258355000	0.000000000
8	1.885864000	-1.303370000	0.000000000
8	-0.256086000	-2.175401000	0.000000000
1	-2.207160000	0.071010000	0.000000000

E = -681.5270882 au

ZPVE = 0.0534466 au

$\nu_i = 151.3i \text{ cm}^{-1}$

CO₂

6	0.000000000	0.000000000	0.000000000
8	0.000000000	0.000000000	1.159059000
8	0.000000000	0.000000000	-1.159059000

E = -188.6604007 au

ZPVE = 0.0117227 au

2t

16	1.616811000	0.828342000	0.000000000
6	-0.626739000	-0.846785000	0.000000000
6	0.000000000	0.545814000	0.000000000
7	-0.957156000	1.481269000	0.000000000
8	0.256440000	-1.841295000	0.000000000
8	-1.823339000	-1.008626000	0.000000000
1	-1.925889000	1.198726000	0.000000000
1	-0.702598000	2.453758000	0.000000000
1	-0.244775000	-2.669645000	0.000000000

E = -681.5663854 au

ZPVE = 0.0591648 au

2c

16	1.647072000	0.659813000	0.000000000
6	-0.712272000	-0.818713000	0.000000000
6	0.000000000	0.546802000	0.000000000
7	-0.871153000	1.547726000	0.000000000
8	0.090793000	-1.867056000	0.000000000
8	-1.913012000	-0.890483000	0.000000000
1	-1.857050000	1.323597000	0.000000000
1	-0.559280000	2.503828000	0.000000000
1	1.012634000	-1.526738000	0.000000000

E = -681.5738753 au

ZPVE = 0.0594046 au

3a

7	-0.481077000	1.789468000	0.000000000
1	2.065415000	1.597581000	0.000000000
16	1.737763000	0.294520000	0.000000000
6	0.000000000	0.621986000	0.000000000
1	-1.501954000	1.744757000	0.000000000
6	-0.908277000	-0.601295000	0.000000000
8	-2.105213000	-0.520155000	0.000000000
8	-0.229714000	-1.757566000	0.000000000
1	-0.871054000	-2.483308000	0.000000000

E = -681.5469988 au

ZPVE = 0.0556568 au

3b

7	0.300169000	1.811820000	0.199710000
6	0.235923000	0.565795000	0.034944000
6	-1.104239000	-0.178112000	-0.026260000
8	-2.120541000	0.404383000	-0.262108000
16	1.690093000	-0.448676000	-0.134060000
8	-1.083415000	-1.497404000	0.220083000
1	-0.641439000	2.204518000	0.262614000
1	2.542113000	0.503007000	0.279406000
1	-0.201798000	-1.793376000	0.489063000

E = -681.5397071 au

ZPVE = 0.0552246 au

2t'

16	-1.571855000	0.985251000	0.000000000
6	0.380446000	-0.956901000	0.000000000
6	0.000000000	0.522910000	0.000000000
7	1.050151000	1.360216000	0.000000000
8	1.729933000	-1.125663000	0.000000000
8	-0.387122000	-1.870417000	0.000000000
1	1.994780000	1.013594000	0.000000000
1	0.879813000	2.351879000	0.000000000
1	1.898867000	-2.078418000	0.000000000

E = -681.5618741 au

ZPVE = 0.0587476 au

2* (zwitterion)

16	1.678014000	-0.438029000	-0.000192000
1	0.774981000	2.428461000	0.000371000
8	-0.912158000	-1.617597000	-0.000146000
6	0.226950000	0.444294000	0.000055000
6	-1.121244000	-0.407963000	0.000009000
1	2.527539000	0.613866000	-0.000053000
8	-2.112209000	0.330444000	0.000154000
7	0.051401000	1.726112000	0.000273000
1	-0.949856000	1.962599000	0.000388000

E = - 681.475634 au

ZPVE = 0.0551773 au

3c

7	0.250321000	1.775723000	-0.294939000
1	1.267349000	-1.531639000	0.170131000
16	1.794704000	-0.296535000	0.154429000
6	0.257991000	0.524907000	-0.084836000
1	-0.678714000	2.155185000	-0.466688000
6	-0.985435000	-0.371974000	-0.044115000
8	-0.974986000	-1.524817000	-0.360277000
8	-2.118891000	0.231826000	0.356178000
1	-1.940476000	1.117299000	0.696758000

E = -681.537135 au

ZPVE = 0.0552831 au

3d

7	-0.263520000	1.814415000	-0.245238000
1	-1.355423000	-1.237127000	0.976114000
16	-1.769524000	-0.322111000	0.081843000
6	-0.225598000	0.575969000	-0.027893000
1	0.684026000	2.185446000	-0.341717000
6	1.100021000	-0.192647000	0.036439000
8	2.116838000	0.355552000	0.343709000
8	1.059938000	-1.488843000	-0.303940000
1	0.167680000	-1.729047000	-0.596649000

E = -681.5374791 au

ZPVE = 0.0554331 au

3e

7	-0.563727000	1.726889000	0.000000000
1	1.988870000	1.703433000	0.000000000
16	1.754338000	0.380675000	0.000000000
6	0.000000000	0.595519000	0.000000000
1	-1.578049000	1.632400000	0.000000000
6	-0.720603000	-0.740980000	0.000000000
8	-0.162784000	-1.802996000	0.000000000
8	-2.057337000	-0.592601000	0.000000000
1	-2.449559000	-1.477313000	0.000000000

E = -681.5463785 au

ZPVE = 0.0556955 au

3f

7	-0.598721000	1.719157000	0.000000000
1	1.842555000	-0.787309000	0.000000000
16	1.761654000	0.553242000	0.000000000
6	0.000000000	0.605169000	0.000000000
1	-1.609093000	1.598714000	0.000000000
6	-0.705463000	-0.747671000	0.000000000
8	-0.153925000	-1.814478000	0.000000000
8	-2.041708000	-0.604515000	0.000000000
1	-2.431038000	-1.490425000	0.000000000

E = -681.5466142 au

ZPVE = 0.0557245 au

3g

7	-0.513189000	1.776993000	0.000000000
1	1.817808000	-0.858972000	0.000000000
16	1.761625000	0.479061000	0.000000000
6	0.000000000	0.622925000	0.000000000
1	-1.531759000	1.709022000	0.000000000
6	-0.896302000	-0.614484000	0.000000000
8	-2.093194000	-0.531789000	0.000000000
8	-0.233153000	-1.782167000	0.000000000
1	-0.891139000	-2.492971000	0.000000000

E = -681.5453992 au

ZPVE = 0.055652 au

3h

7	-0.284049000	1.763685000	-0.302808000
6	-0.255139000	0.515101000	-0.084200000
6	0.996192000	-0.360469000	-0.046037000
8	0.985337000	-1.508789000	-0.374142000
16	-1.712466000	-0.443505000	0.164727000
8	2.125820000	0.247086000	0.364964000
1	0.636852000	2.162221000	-0.481180000
1	-2.525526000	0.625058000	0.108608000
1	1.940903000	1.128833000	0.711436000

E = -681.536557 au

ZPVE = 0.0552241 au

3i

7	0.303355000	1.838027000	0.047027000
1	2.587407000	0.361713000	-0.029416000
16	1.631910000	-0.583150000	-0.025775000
6	0.272813000	0.578242000	0.012336000
1	1.244615000	2.224010000	0.055930000
6	-1.104810000	-0.081030000	-0.003254000
8	-2.140018000	0.510388000	-0.063648000
8	-1.006225000	-1.425236000	0.058740000
1	-1.904143000	-1.786000000	0.041464000

E = -681.5403508 au

ZPVE = 0.0553023 au

3j

7	-0.742465000	1.596404000	0.000000000
1	1.793485000	-0.839987000	0.000000000
16	1.751564000	0.506386000	0.000000000
6	0.000000000	0.567602000	0.000000000
1	-0.251478000	2.486388000	0.000000000
6	-0.732680000	-0.784075000	0.000000000
8	-0.164997000	-1.841118000	0.000000000
8	-2.052088000	-0.650778000	0.000000000
1	-2.237017000	0.310599000	0.000000000

E = -681.5533085 au

ZPVE = 0.0560519 au

3l

7	-0.617082000	1.708974000	0.000000000
1	2.108059000	1.560238000	0.000000000
16	1.750458000	0.264988000	0.000000000
6	0.000000000	0.608597000	0.000000000
1	-0.004792000	2.521863000	0.000000000
6	-0.776389000	-0.696322000	0.000000000
8	-0.229353000	-1.768229000	0.000000000
8	-2.099844000	-0.525598000	0.000000000
1	-2.499113000	-1.407765000	0.000000000

E = -681.5435001 au

ZPVE = 0.055639 au

3m

7	0.318995000	1.781820000	0.413320000
1	2.591748000	0.223941000	0.158266000
16	1.601738000	-0.583335000	-0.256030000
6	0.260225000	0.568812000	0.089916000
1	1.264066000	2.154645000	0.472668000
6	-1.121499000	-0.080494000	-0.041733000
8	-2.034465000	0.449080000	-0.590718000
8	-1.233089000	-1.307862000	0.509119000
1	-0.408514000	-1.577620000	0.936005000

E = -681.5330168 au

ZPVE = 0.0549181 au

3n

7	-0.653783000	1.688297000	0.000000000
1	1.784255000	-0.881842000	0.000000000
16	1.766499000	0.462083000	0.000000000
6	0.000000000	0.606827000	0.000000000
1	-0.059320000	2.515773000	0.000000000
6	-0.757751000	-0.716494000	0.000000000
8	-0.217633000	-1.793487000	0.000000000
8	-2.080947000	-0.550670000	0.000000000
1	-2.477300000	-1.434070000	0.000000000

E = -681.5457088 au

ZPVE = 0.0555533 au

3o

7	0.351863000	1.797004000	0.287113000
1	1.077796000	-1.665608000	-0.204883000
16	1.719093000	-0.490195000	-0.149227000
6	0.293350000	0.554482000	0.075873000
1	1.305265000	2.151940000	0.343715000
6	-1.098837000	-0.058489000	-0.026914000
8	-2.063650000	0.534959000	-0.404915000
8	-1.121688000	-1.352305000	0.363325000
1	-2.035968000	-1.659434000	0.277973000

E = -681.5408091 au

ZPVE = 0.0552121 au

3p

7	-0.704254000	1.613380000	0.000000000
1	2.042009000	1.632745000	0.000000000
16	1.747365000	0.321060000	0.000000000
6	0.000000000	0.560421000	0.000000000
1	-0.187649000	2.488066000	0.000000000
6	-0.753351000	-0.769794000	0.000000000
8	-0.188103000	-1.826354000	0.000000000
8	-2.074956000	-0.627120000	0.000000000
1	-2.257848000	0.332608000	0.000000000

E = -681.5496327 au

ZPVE = 0.0560287 au

TS: 3a → 2t

7	-0.553040000	1.650315000	0.000000000
1	0.777303000	2.050636000	0.000000000
16	1.701224000	0.651251000	0.000000000
6	0.000000000	0.478950000	0.000000000
1	-1.568700000	1.731296000	0.000000000
6	-0.827846000	-0.783869000	0.000000000
8	-2.029436000	-0.765969000	0.000000000
8	-0.083756000	-1.892962000	0.000000000
1	-0.684292000	-2.653195000	0.000000000

E = -681.4982053 au

ZPVE = 0.0525787 au

$\nu_i = 1781.7i \text{ cm}^{-1}$

TS: 3b → 2c

7	-0.447468000	1.688336000	0.000000000
6	0.000000000	0.478905000	0.000000000
6	-0.906491000	-0.738830000	0.000000000
8	-2.097748000	-0.626609000	0.000000000
16	1.721528000	0.510901000	0.000000000
8	-0.293540000	-1.926832000	0.000000000
1	-1.454378000	1.846499000	0.000000000
1	0.943278000	1.963684000	0.000000000
1	0.668186000	-1.815884000	0.000000000

E = -681.4960935 au

ZPVE = 0.052377 au

$\nu_i = 1753.9i \text{ cm}^{-1}$

TS: 2t → 2c

16	-1.698863000	-0.564936000	0.085910000
6	1.053172000	-0.146295000	0.006351000
6	-0.374940000	0.399405000	-0.046785000
7	-0.383811000	1.732833000	-0.148971000
8	1.189057000	-1.461795000	-0.275745000
8	1.980418000	0.579583000	0.233111000
1	0.489791000	2.236867000	-0.127286000
1	-1.258078000	2.229594000	-0.130477000
1	1.211593000	-2.018276000	0.509672000

E = -681.5489329 au

ZPVE = 0.0573238 au

$\nu_i = 645.4i \text{ cm}^{-1}$

TS_tf1

16	-1.069114000	-0.001109000	-0.008314000
1	1.520492000	-1.230071000	-0.148061000
7	1.639323000	-0.220111000	0.055332000
1	-0.860747000	-1.346980000	-0.070446000
6	0.558425000	0.546688000	0.087063000
1	1.620276000	0.855444000	-0.558173000

E = -492.7850248 au

ZPVE = 0.0334823 au

$\nu_i = 1905.6i \text{ cm}^{-1}$

TS_tf2

16	-1.027628000	-0.160366000	-0.019896000
1	1.569715000	-1.216160000	-0.122936000
7	1.654041000	-0.200717000	0.058822000
1	-1.715088000	0.985399000	0.098903000
6	0.564460000	0.556178000	0.083972000
1	1.622366000	0.864569000	-0.573223000

E = -492.7853887 au

ZPVE = 0.0338407 au

$\nu_i = 1912.7i \text{ cm}^{-1}$

TS_tf3

16	-0.713971000	-0.828328000	0.000000000
1	1.939808000	0.099630000	0.000000000
7	1.305198000	0.898196000	0.000000000
1	-1.372062000	0.511474000	0.000000000
6	0.000000000	0.756317000	0.000000000
1	1.719407000	1.816866000	0.000000000

E = -492.8132748 au

ZPVE = 0.0359615 au

$\nu_i = 1661.1i \text{ cm}^{-1}$

Dimer_A

8	1.537867000	0.563932000	0.000000000
6	1.804427000	-0.633929000	0.000000000
8	0.924062000	-1.590241000	0.000000000
8	-1.537662000	-0.563769000	0.000000000
6	-1.804376000	0.634053000	0.000000000
6	3.263968000	-1.086052000	0.000000000
8	-0.924105000	1.590463000	0.000000000
16	3.723482000	-2.660704000	0.000000000
7	4.088464000	-0.031072000	0.000000000
6	-3.263963000	1.085986000	0.000000000
1	0.000000000	-1.211828000	0.000000000
16	-3.723679000	2.660580000	0.000000000
7	-4.088304000	0.030884000	0.000000000
1	-0.000025000	1.212168000	0.000000000
1	3.706395000	0.902293000	0.000000000
1	-3.706112000	-0.902431000	0.000000000
1	5.082886000	-0.179040000	0.000000000
1	-5.082745000	0.178714000	0.000000000

E = -13623.15587 au

ZPVE = 0.1200014 au

Dimer_B

8	-3.465631000	-3.065196000	0.000000000
6	-3.477367000	-1.863865000	0.000000000
8	-4.582005000	-1.138235000	0.000000000
8	1.502211000	-0.601178000	0.000000000
6	1.789950000	0.585044000	0.000000000
6	-2.158785000	-1.064586000	0.000000000
8	0.924464000	1.565635000	0.000000000
16	-2.183787000	0.601932000	0.000000000
7	-1.102501000	-1.847044000	0.000000000
6	3.254007000	1.026603000	0.000000000
1	-4.323352000	-0.193086000	0.000000000
16	3.732220000	2.595518000	0.000000000
7	4.067531000	-0.037234000	0.000000000
1	0.000000000	1.213848000	0.000000000
1	-1.267887000	-2.845625000	0.000000000
1	3.674305000	-0.965746000	0.000000000
1	-0.155806000	-1.465947000	0.000000000
1	5.063464000	0.099919000	0.000000000

E = -1363.156321 au

ZPVE = 0.1199167 au

Dimer_C

8	3.055860000	-3.385665000	0.000000000
6	3.223715000	-2.191216000	0.000000000
8	4.419094000	-1.608038000	0.000000000
8	-3.055540000	3.385734000	0.000000000
6	-3.223580000	2.191309000	0.000000000
6	2.048583000	-1.210620000	0.000000000
8	-4.419053000	1.608319000	0.000000000
16	2.256910000	0.430994000	0.000000000
7	0.894935000	-1.863042000	0.000000000
6	-2.048616000	1.210539000	0.000000000
1	5.083135000	-2.312814000	0.000000000
16	-2.257186000	-0.431047000	0.000000000
7	-0.894861000	1.862785000	0.000000000
1	-5.082978000	2.313205000	0.000000000
1	0.918467000	-2.873294000	0.000000000
1	-0.918265000	2.873040000	0.000000000
1	0.000044000	-1.373312000	0.000000000
1	0.000000000	1.372950000	0.000000000

E = -1363.146604 au

ZPVE = 0.1198165 au

12

1	0.282673000	2.459435000	0.000000000
8	-0.689372000	2.457996000	0.000000000
7	1.258804000	0.538686000	0.000000000
6	2.065644000	-0.559016000	0.000000000
1	3.137533000	-0.436602000	0.000000000
6	-1.109099000	1.185000000	0.000000000
6	0.000000000	0.193625000	0.000000000
8	-2.268962000	0.877515000	0.000000000
6	1.407453000	-1.756788000	0.000000000
16	-0.286187000	-1.506720000	0.000000000
1	1.829850000	-2.747117000	0.000000000

E = -757.722007 au

ZPVE = 0.0703586 kcal mol⁻¹

13

1	-0.455864000	-1.586925000	0.000000000
8	1.837324000	-2.115617000	0.000000000
7	-0.841614000	-0.652466000	0.000000000
6	-2.214025000	-0.434170000	0.000000000
1	-2.895869000	-1.269125000	0.000000000
6	2.584064000	-1.223094000	0.000000000
6	0.000000000	0.394431000	0.000000000
8	3.382026000	-0.387101000	0.000000000
6	-2.506074000	0.879658000	0.000000000
16	-1.013368000	1.775698000	0.000000000
1	-3.481690000	1.332948000	0.000000000

E = -757.695887 au

ZPVE = 0.0678521 kcal mol⁻¹

14

6	-1.323468000	0.096245000	0.000000000
16	0.000000000	1.188298000	0.000000000
6	0.631874000	-1.245448000	0.000000000
7	-0.754949000	-1.122887000	0.000000000
6	1.232931000	-0.042126000	0.000000000
1	-1.342642000	-1.943203000	0.000000000
1	1.089675000	-2.221498000	0.000000000
1	2.289587000	0.160121000	0.000000000

E = -569.042598 au

ZPVE = 0.055214 kcal mol⁻¹

15

6	-1.200856000	-0.066080000	0.000000000
16	0.000000000	1.180195000	0.000000000
6	0.638707000	-1.262643000	0.000000000
7	-0.731766000	-1.275462000	0.000000000
6	1.217914000	-0.030246000	0.000000000
1	-2.252256000	0.177206000	0.000000000
1	1.175675000	-2.198751000	0.000000000
1	2.264352000	0.220474000	0.000000000

E = -569.088892 au

ZPVE = 0.0550984 kcal mol⁻¹

TS13

1	1.859955000	0.080054000	0.000000000
8	1.836898000	1.525048000	0.000000000
7	0.981489000	-0.679794000	0.000000000
6	0.589277000	-1.989031000	0.000000000
1	1.316036000	-2.784010000	0.000000000
6	0.569542000	1.643365000	0.000000000
6	0.000000000	0.191848000	0.000000000
8	-0.181741000	2.594902000	0.000000000
6	-0.764067000	-2.112930000	0.000000000
16	-1.519490000	-0.554810000	0.000000000
1	-1.344333000	-3.019642000	0.000000000

E = -569.042598 au

ZPVE = 0.048762 kcal mol⁻¹

$\nu_i = 0.0661858i$ cm⁻¹

TS14

6	-0.013893000	1.285906000	0.087554000
16	1.196197000	0.040457000	-0.014481000
6	-1.238026000	-0.686659000	-0.024702000
7	-1.251243000	0.699602000	0.081112000
6	0.007838000	-1.212527000	-0.006794000
1	-1.015696000	1.621216000	-0.693508000
1	-2.168900000	-1.230754000	-0.041703000
1	0.268622000	-2.255312000	0.062769000

E = -568.974921 au

ZPVE = 0.0486441 kcal mol⁻¹

$\nu_i = 1712.2614i$ cm⁻¹

TS15

6	0.245788000	0.474431000	0.000003000
6	-1.029133000	-0.464469000	-0.000011000
7	-0.166079000	1.686776000	0.000011000
1	-1.352676000	1.423057000	0.000004000
1	0.433621000	2.499218000	0.000035000
16	1.807927000	-0.204238000	0.000009000
8	-2.052707000	0.285417000	-0.000002000
8	-0.874184000	-1.669156000	-0.000026000
1	1.269977000	-1.451757000	-0.000004000

E = -681.481012 au

ZPVE = 0.0518805 kcal mol⁻¹

$\nu_i = 1261.9511i$ cm⁻¹

TS16

1	-0.232957000	1.906505000	-0.000006000
8	-2.298033000	1.171295000	0.000016000
7	0.419380000	1.126470000	0.000001000
6	1.796252000	1.243196000	-0.000012000
1	2.261139000	2.215105000	-0.000029000
6	-2.133307000	-0.014538000	-0.000015000
6	-0.108032000	-0.092138000	0.000023000
8	-2.570269000	-1.113386000	-0.000060000
6	2.393386000	0.033473000	-0.000001000
16	1.177765000	-1.207070000	0.000026000
1	3.448537000	-0.177011000	-0.000006000

E = -757.687524 au

ZPVE = 0.0681282 kcal mol⁻¹

$\nu_i = 179.4305i$ cm⁻¹

MP2/def2-QZVPP

1c

16	-0.816373000	-0.652355000	0.000000000
1	1.855796000	-0.080885000	0.000000000
7	1.311851000	0.778341000	0.000000000
1	0.189096000	-1.565862000	0.000000000
6	0.000000000	0.833128000	0.000000000
1	1.834114000	1.637272000	0.000000000

E = -492.1747052 au

ZPVE = 0.0407957 au

1t

16	-0.685971000	-0.741129000	0.000000000
1	1.879503000	-0.056737000	0.000000000
7	1.317561000	0.788508000	0.000000000
1	-1.953503000	-0.338475000	0.000000000
6	0.000000000	0.846500000	0.000000000
1	1.826611000	1.654725000	0.000000000

E = -492.1749769 au

ZPVE = 0.0413122 au

TS: 1t → 1c

16	1.068342000	0.061592000	-0.082248000
1	-1.308180000	1.238115000	-0.129510000
7	-1.517791000	0.241460000	-0.014780000
1	1.101437000	0.379443000	1.229442000
6	-0.627207000	-0.713621000	0.046631000
1	-2.498947000	-0.011524000	0.039706000

E = -492.1543923 au
ZPVE = 0.0399709 au
 $\nu_i = 421.3i \text{ cm}^{-1}$

1c-CO₂

6	0.000000000	0.727909000	0.000000000
6	0.156735000	-2.224730000	0.000000000
7	1.292867000	0.943409000	0.000000000
1	1.907182000	0.144417000	0.000000000
1	1.727197000	1.862033000	0.000000000
16	-1.011488000	2.088152000	0.000000000
8	1.308392000	-2.014057000	0.000000000
8	-0.971295000	-2.506721000	0.000000000
1	-0.137821000	3.126406000	0.000000000

E = -680.5512359 au
ZPVE = 0.053554 au

1t-CO₂

6	0.000000000	0.705695000	0.000000000
6	0.202959000	-2.197568000	0.000000000
7	1.288904000	0.969943000	0.000000000
1	1.919836000	0.184422000	0.000000000
1	1.709889000	1.892929000	0.000000000
16	-0.949597000	2.147808000	0.000000000
8	1.354760000	-1.988058000	0.000000000
8	-0.923318000	-2.488304000	0.000000000
1	-2.127795000	1.530254000	0.000000000

E = -680.5518426 au
ZPVE = 0.0540646 au

TS: 1t-CO₂ → 1c-CO₂

6	0.664910000	0.064282000	-0.018213000
6	-2.284958000	-0.217791000	0.006048000
7	0.679817000	1.364598000	-0.021008000
1	-0.210861000	1.844532000	0.003768000
1	1.530097000	1.923487000	-0.051335000
16	2.390707000	-0.538006000	-0.068413000
8	-2.238705000	0.952645000	0.021092000
8	-2.404315000	-1.373692000	-0.007608000
1	2.535174000	-0.422683000	1.254335000

E = -680.5309307 au
ZPVE = 0.0527052 au
 $\nu_i = 423.5i \text{ cm}^{-1}$

TS: 1t-CO₂ → 2c

6	0.000000000	0.567537000	0.000000000
6	0.691964000	-1.541260000	0.000000000
7	1.040198000	1.354940000	0.000000000
1	1.938435000	0.888162000	0.000000000
1	1.029670000	2.367284000	0.000000000
16	-1.539317000	1.301901000	0.000000000
8	1.856543000	-1.310051000	0.000000000
8	-0.302627000	-2.174049000	0.000000000
1	-2.203532000	0.144700000	0.000000000

E = -680.547686 au

ZPVE = 0.0540389 au

$\nu_i = 194.9i \text{ cm}^{-1}$

CO₂

6	0.000000000	0.000000000	0.000000000
8	0.000000000	0.000000000	1.166283000
8	0.000000000	0.000000000	-1.166283000

E = -188.3685783 au

ZPVE = 0.0115804 au

2t

16	1.605510000	0.828889000	0.000000000
6	-0.617555000	-0.842832000	0.000000000
6	0.000000000	0.543910000	0.000000000
7	-0.967747000	1.470361000	0.000000000
8	0.277390000	-1.826609000	0.000000000
8	-1.818260000	-1.014175000	0.000000000
1	-1.929590000	1.171180000	0.000000000
1	-0.719514000	2.443235000	0.000000000
1	-0.232537000	-2.649375000	0.000000000

E = -680.5963501 au

ZPVE = 0.0594597 au

2c

16	1.634390000	0.669038000	0.000000000
6	-0.699624000	-0.818462000	0.000000000
6	0.000000000	0.543301000	0.000000000
7	-0.886796000	1.532176000	0.000000000
8	0.115859000	-1.857558000	0.000000000
8	-1.905448000	-0.901345000	0.000000000
1	-1.865286000	1.283669000	0.000000000
1	-0.585945000	2.490440000	0.000000000
1	1.023022000	-1.481753000	0.000000000

E = -680.6040706 au
ZPVE = 0.0597681 au

2t'

16	-1.563611000	0.978479000	0.000000000
6	0.375675000	-0.949732000	0.000000000
6	0.000000000	0.522016000	0.000000000
7	1.055615000	1.353775000	0.000000000
8	1.725002000	-1.113196000	0.000000000
8	-0.397679000	-1.866571000	0.000000000
1	1.994234000	0.996676000	0.000000000
1	0.885254000	2.344130000	0.000000000
1	1.876350000	-2.068470000	0.000000000

E = -680.5921744 au
ZPVE = 0.0589776 au

2 (Zwitterion)

16	1.678985000	-0.408518000	-0.000082000
1	0.700428000	2.438514000	0.000870000
8	-0.873536000	-1.632133000	0.000322000
6	0.220806000	0.439772000	0.000011000
6	-1.095363000	-0.418997000	-0.000114000
1	2.484531000	0.664158000	-0.000537000
8	-2.102180000	0.312426000	-0.000286000
7	0.003109000	1.712898000	0.000131000
1	-1.017420000	1.876328000	0.000386000

E = -680.500358 au
ZPVE = 0.0558367 au

3a

7	-0.495587000	1.787902000	0.000000000
1	2.013263000	1.610423000	0.000000000
16	1.722339000	0.306446000	0.000000000
6	0.000000000	0.614219000	0.000000000
1	-1.514594000	1.696357000	0.000000000
6	-0.894671000	-0.607257000	0.000000000
8	-2.097338000	-0.533949000	0.000000000
8	-0.199368000	-1.752672000	0.000000000
1	-0.845310000	-2.474037000	0.000000000

E = -680.5763523 au
ZPVE = 0.0560141 au

3b

7	0.303011000	1.812351000	0.196208000
6	0.238633000	0.554299000	0.032258000
6	-1.095547000	-0.179949000	-0.024907000
8	-2.115455000	0.410166000	-0.254309000
16	1.678611000	-0.445701000	-0.130840000
8	-1.072773000	-1.500054000	0.213856000
1	-0.653947000	2.170061000	0.253832000
1	2.506275000	0.522832000	0.268617000
1	-0.183881000	-1.775138000	0.477058000

E = -680.5690439 au

ZPVE = 0.0556249 au

3c

7	-0.254093000	1.780743000	-0.292674000
1	-1.230586000	-1.515162000	0.161816000
16	-1.779235000	-0.297503000	0.153257000
6	-0.259694000	0.518963000	-0.083494000
1	0.686863000	2.130767000	-0.465266000
6	0.976919000	-0.370753000	-0.043421000
8	0.965208000	-1.531155000	-0.353731000
8	2.108065000	0.240119000	0.350105000
1	1.900599000	1.118265000	0.690558000

E = -680.5662319 au

ZPVE = 0.055744 au

3d

7	-0.261043000	1.818320000	-0.238353000
1	-1.330494000	-1.222057000	0.964967000
16	-1.756106000	-0.316713000	0.078755000
6	-0.227936000	0.567413000	-0.023540000
1	0.702619000	2.150925000	-0.326305000
6	1.090123000	-0.196703000	0.034273000
8	2.113979000	0.357192000	0.328649000
8	1.040986000	-1.495258000	-0.293377000
1	0.140028000	-1.709426000	-0.576841000

E = -680.566686 au

ZPVE = 0.0558894 au

3e

7	-0.576400000	1.726603000	0.000000000
1	1.938992000	1.711668000	0.000000000
16	1.737482000	0.391099000	0.000000000
6	0.000000000	0.589185000	0.000000000
1	-1.586542000	1.588170000	0.000000000
6	-0.708118000	-0.743712000	0.000000000
8	-0.137303000	-1.805059000	0.000000000
8	-2.044259000	-0.598079000	0.000000000
1	-2.416160000	-1.491384000	0.000000000

E = -680.5758308 au

ZPVE = 0.0560373 au

3f

7	-0.613242000	1.718406000	0.000000000
1	1.810934000	-0.772496000	0.000000000
16	1.743845000	0.561244000	0.000000000
6	0.000000000	0.600308000	0.000000000
1	-1.618166000	1.553800000	0.000000000
6	-0.692064000	-0.749216000	0.000000000
8	-0.129147000	-1.816317000	0.000000000
8	-2.027358000	-0.608011000	0.000000000
1	-2.397173000	-1.501983000	0.000000000

E = -680.5760157 au

ZPVE = 0.0560828 au

3g

7	-0.530878000	1.775397000	0.000000000
1	1.788533000	-0.840083000	0.000000000
16	1.743658000	0.490214000	0.000000000
6	0.000000000	0.617385000	0.000000000
1	-1.546232000	1.658647000	0.000000000
6	-0.880742000	-0.619855000	0.000000000
8	-2.083313000	-0.546498000	0.000000000
8	-0.201204000	-1.777459000	0.000000000
1	-0.864093000	-2.483294000	0.000000000

E = -680.5746694 au

ZPVE = 0.0560113 au

3h

7	0.291319000	1.766283000	0.300341000
6	0.257002000	0.506780000	0.081927000
6	-0.989499000	-0.359023000	0.044973000
8	-0.979030000	-1.514905000	0.367473000
16	1.697981000	-0.443599000	-0.163649000
8	-2.116201000	0.258343000	-0.358004000
1	-0.641168000	2.137987000	0.478800000
1	2.491752000	0.629328000	-0.096078000
1	-1.900683000	1.132249000	-0.703877000

E = -680.5656139 au

ZPVE = 0.0556612 au

3i

7	0.303073000	1.837489000	0.092949000
1	2.555165000	0.368778000	-0.054694000
16	1.615543000	-0.580463000	-0.051191000
6	0.276403000	0.567596000	0.023404000
1	1.256621000	2.194639000	0.108748000
6	-1.094747000	-0.082142000	-0.006245000
8	-2.129727000	0.511474000	-0.124646000
8	-0.992378000	-1.421781000	0.115892000
1	-1.895093000	-1.768695000	0.081441000

E = -680.5693267 au

ZPVE = 0.0556582 au

3j

7	-0.763306000	1.588652000	0.000000000
1	1.760084000	-0.824578000	0.000000000
16	1.733973000	0.515290000	0.000000000
6	0.000000000	0.562846000	0.000000000
1	-0.260899000	2.472597000	0.000000000
6	-0.717896000	-0.785341000	0.000000000
8	-0.137075000	-1.841670000	0.000000000
8	-2.036865000	-0.656768000	0.000000000
1	-2.200720000	0.309254000	0.000000000

E = -680.5831062 au

ZPVE = 0.0564362 au

3k

7	-0.345787000	1.768507000	0.451027000
1	-1.025822000	-1.400125000	-0.960775000
16	-1.666155000	-0.500733000	-0.208450000
6	-0.270953000	0.556509000	0.082027000
1	-1.311637000	2.092316000	0.495752000
6	1.105444000	-0.068855000	-0.048043000
8	1.987746000	0.421743000	-0.689311000
8	1.258471000	-1.238154000	0.609902000
1	0.439770000	-1.454637000	1.074393000

E = -680.5625698 au

ZPVE = 0.0553733 au

3l

7	-0.637854000	1.702938000	0.000000000
1	2.061601000	1.574032000	0.000000000
16	1.732479000	0.279601000	0.000000000
6	0.000000000	0.601709000	0.000000000
1	-0.008998000	2.504257000	0.000000000
6	-0.761336000	-0.701265000	0.000000000
8	-0.200319000	-1.771866000	0.000000000
8	-2.084378000	-0.534310000	0.000000000
1	-2.461697000	-1.425717000	0.000000000

E = -680.5724038 au

ZPVE = 0.0559701 au

3m

7	-0.313534000	1.785635000	0.403700000
1	-2.559073000	0.239824000	0.168217000
16	-1.588581000	-0.575087000	-0.251845000
6	-0.262188000	0.559232000	0.083446000
1	-1.269541000	2.133827000	0.450233000
6	1.112162000	-0.085183000	-0.037664000
8	2.039165000	0.455916000	-0.563876000
8	1.207395000	-1.323595000	0.490464000
1	0.368327000	-1.574571000	0.897775000

E = -680.5617232 au

ZPVE = 0.0553483 au

3n

7	-0.675493000	1.681750000	0.000000000
1	1.754605000	-0.862139000	0.000000000
16	1.747639000	0.474647000	0.000000000
6	0.000000000	0.600941000	0.000000000
1	-0.065420000	2.498657000	0.000000000
6	-0.742114000	-0.720376000	0.000000000
8	-0.189345000	-1.796785000	0.000000000
8	-2.064534000	-0.557751000	0.000000000
1	-2.439243000	-1.450220000	0.000000000

E = -680.5747306 au

ZPVE = 0.055905 au

3o

7	-0.339292000	1.805063000	0.255225000
1	-1.059090000	-1.641247000	-0.184617000
16	-1.708925000	-0.479531000	-0.132802000
6	-0.293847000	0.546837000	0.064442000
1	-1.301739000	2.138976000	0.300225000
6	1.090180000	-0.065944000	-0.023114000
8	2.072221000	0.539298000	-0.351020000
8	1.089257000	-1.374190000	0.317545000
1	2.008862000	-1.666900000	0.242477000

E = -680.569837 au

ZPVE = 0.055613 au

3p

7	-0.723332000	1.606481000	0.000000000
1	1.999465000	1.641237000	0.000000000
16	1.730219000	0.332340000	0.000000000
6	0.000000000	0.554656000	0.000000000
1	-0.193404000	2.473832000	0.000000000
6	-0.739170000	-0.772198000	0.000000000
8	-0.160324000	-1.827850000	0.000000000
8	-2.060792000	-0.634850000	0.000000000
1	-2.222301000	0.328969000	0.000000000

E = -680.5791465 au

ZPVE = 0.0564207 au

TS: 3a → 2t

7	-0.582726000	1.644380000	0.000000000
1	0.735336000	2.039656000	0.000000000
16	1.680198000	0.666332000	0.000000000
6	0.000000000	0.476038000	0.000000000
1	-1.601105000	1.688910000	0.000000000
6	-0.806675000	-0.789779000	0.000000000
8	-2.014744000	-0.788218000	0.000000000
8	-0.042003000	-1.883773000	0.000000000
1	-0.644293000	-2.642168000	0.000000000

E = -680.5308174 au

ZPVE = 0.0527743 au

$\nu_i = 1677.6i \text{ cm}^{-1}$

TS: 3b → 2c

7	-0.472961000	1.685822000	0.000000000
6	0.000000000	0.475355000	0.000000000
6	-0.888189000	-0.744811000	0.000000000
8	-2.087065000	-0.645210000	0.000000000
16	1.704185000	0.522666000	0.000000000
8	-0.256571000	-1.921829000	0.000000000
1	-1.485761000	1.807137000	0.000000000
1	0.908922000	1.950654000	0.000000000
1	0.698827000	-1.768141000	0.000000000

E = -680.5292074 au

ZPVE = 0.0525923 au

$\nu_i = 1642.9i \text{ cm}^{-1}$

TS: 2t → 2c

16	-1.695794000	-0.549165000	0.079334000
6	1.043531000	-0.155346000	0.004095000
6	-0.373228000	0.398476000	-0.042913000
7	-0.361436000	1.734036000	-0.138470000
8	1.160254000	-1.476431000	-0.262308000
8	1.985067000	0.567905000	0.213468000
1	0.522209000	2.216167000	-0.109755000
1	-1.228949000	2.239453000	-0.112033000
1	1.185117000	-1.997811000	0.545360000

E = -680.5781340 au

ZPVE = 0.057676 au

$\nu_i = 645.7i \text{ cm}^{-1}$

TS_tf1

16	-1.062167000	0.004973000	0.008553000
1	1.488241000	1.231309000	0.147892000
7	1.622731000	0.225387000	-0.055251000
1	-0.796888000	1.329544000	0.058156000
6	0.548605000	-0.561930000	-0.079521000
1	1.652575000	-0.846557000	0.520986000

E = -492.0981027 au
ZPVE = 0.0340052 au
 $\nu_i = 1960.2i \text{ cm}^{-1}$

TS_tf2

16	1.017966000	-0.160681000	0.018967000
1	-1.547915000	-1.217194000	0.120491000
7	-1.641222000	-0.205305000	-0.058662000
1	1.707792000	0.973331000	-0.095707000
6	-0.551991000	0.565412000	-0.075637000
1	-1.646838000	0.859419000	0.536188000

E = -492.0984322 au
ZPVE = 0.034361 au
 $\nu_i = 1986.8i \text{ cm}^{-1}$

TS_tf3

16	-0.716751000	-0.810416000	0.000000000
1	1.909166000	0.042766000	0.000000000
7	1.311120000	0.864908000	0.000000000
1	-1.367249000	0.515578000	0.000000000
6	0.000000000	0.764005000	0.000000000
1	1.748258000	1.769925000	0.000000000

E = -492.1275722 au
ZPVE = 0.0365519 au
 $\nu_i = 1620.3i \text{ cm}^{-1}$

Thione

7	1.330983000	0.802448000	0.000000000
6	0.000000000	0.634644000	0.000000000
1	1.926568000	-0.007874000	0.000000000
1	1.742164000	1.717298000	0.000000000
16	-0.777812000	-0.794576000	0.000000000
1	-0.540615000	1.578796000	0.000000000

E = -492.238718 au
ZPVE = 0.0440399 au

Thiol_3

7	1.245587000	1.028209000	0.000000000
6	0.000000000	0.763452000	0.000000000
1	1.382203000	2.036530000	0.000000000
16	-0.618461000	-0.868078000	0.000000000
1	-0.800316000	1.503421000	0.000000000
1	0.594382000	-1.428880000	0.000000000

E = -492.2195021 au
ZPVE = 0.0406766 au

Thiol_4

7	1.234072000	1.066505000	0.000000000
6	0.000000000	0.759631000	0.000000000
1	1.339909000	2.077746000	0.000000000
16	-0.460985000	-0.929124000	0.000000000
1	-0.828546000	1.466699000	0.000000000
1	-1.774112000	-0.701787000	0.000000000

E = -492.2175519 au
ZPVE = 0.0405699 au

Thiol_5

7	1.192685000	1.222924000	0.000000000
6	0.000000000	0.787060000	0.000000000
1	1.873791000	0.464151000	0.000000000
16	-0.475578000	-0.909316000	0.000000000
1	-0.822441000	1.495162000	0.000000000
1	-1.790893000	-0.693096000	0.000000000

E = -492.2184924 au
ZPVE = 0.040527 au

Thiol_6

7	1.196450000	1.214503000	0.000000000
6	0.000000000	0.787389000	0.000000000
1	1.870863000	0.450594000	0.000000000
16	-0.625037000	-0.857851000	0.000000000
1	-0.812525000	1.508974000	0.000000000
1	0.567094000	-1.459803000	0.000000000

E = -492.2185178 au
ZPVE = 0.0407071 au

TSCS_1

7	-1.578847000	-0.413777000	-0.017927000
6	-0.645635000	0.444508000	0.019968000
1	-2.479031000	0.064320000	0.036113000
16	1.063755000	-0.068417000	-0.083832000
1	-0.801146000	1.520412000	0.079972000
1	1.185827000	-0.260669000	1.230916000

E = -492.2074113 au

ZPVE = 0.0397467 au

$\nu_i = 340.2i \text{ cm}^{-1}$

TSCS_2

7	-1.682807000	-0.255690000	-0.004878000
6	-0.659725000	0.488931000	0.024631000
1	-1.407008000	-1.234060000	-0.089647000
16	1.049814000	-0.070131000	-0.083360000
1	-0.789848000	1.563760000	0.091406000
1	1.137832000	-0.351367000	1.218362000

E = -492.2109126 au

ZPVE = 0.0399207 au

$\nu_i = 278.6i \text{ cm}^{-1}$

TSCN_1

6	0.000000000	0.796212000	0.000000000
1	-0.861978000	1.476932000	0.000000000
16	-0.628611000	-0.890486000	0.000000000
7	1.174666000	1.144174000	0.000000000
1	0.579957000	-1.456462000	0.000000000
1	2.117143000	1.440820000	0.000000000

E = -492.1792425 au

ZPVE = 0.0377611 au

$\nu_i = 1095.5i \text{ cm}^{-1}$

TSCN_2

6	0.628154000	0.478618000	0.000000000
16	-1.038825000	-0.195839000	0.000000000
1	0.612836000	1.576810000	0.000000000
7	1.634300000	-0.219575000	0.000000000
1	-1.659625000	0.985537000	0.000000000
1	2.458964000	-0.763611000	0.000000000

E = -492.1790216 au

ZPVE = 0.0376988 au

$\nu_i = 1087.5i \text{ cm}^{-1}$

TSA

7	1.296333000	0.661865000	0.000000000
6	0.000000000	0.788099000	0.000000000
1	1.900986000	1.479079000	0.000000000
16	-0.712158000	-0.743832000	0.000000000
1	-0.530241000	1.733921000	0.000000000
1	0.949455000	-0.673346000	0.000000000

E = -492.1769829 au

ZPVE = 0.0377055 au

$\nu_i = 1635.3i \text{ cm}^{-1}$

B3LYP/6-311+G(d,p)

1c-CO₂

6	0.000000000	0.762382000	0.000000000
6	0.229366000	-2.267592000	0.000000000
7	1.286520000	1.038645000	0.000000000
1	1.694123000	1.976362000	0.000000000
1	1.941721000	0.266708000	0.000000000
16	-1.100790000	2.075320000	0.000000000
8	1.368345000	-2.020402000	0.000000000
8	-0.882970000	-2.589188000	0.000000000
1	-0.288042000	3.189275000	0.000000000

E = -681.449215 au

ZPVE = 0.052679403 kcal mol⁻¹

1t-CO₂

6	0.000000000	0.732302000	0.000000000
6	0.300463000	-2.223287000	0.000000000
7	1.273189000	1.081417000	0.000000000
1	1.648413000	2.030492000	0.000000000
1	1.958481000	0.336550000	0.000000000
16	-1.071975000	2.117748000	0.000000000
8	1.440363000	-1.980358000	0.000000000
8	-0.809738000	-2.554995000	0.000000000
1	-2.215392000	1.407791000	0.000000000

E = -681.449729 au

ZPVE = 0.053256863 kcal mol⁻¹

TS_1t-CO₂ to 2c

6	0.000000000	0.595067000	0.000000000
6	-0.760501000	-1.523544000	0.000000000
7	-0.991252000	1.450564000	0.000000000
1	-0.922962000	2.466227000	0.000000000
1	-1.925303000	1.050798000	0.000000000
16	1.609440000	1.220826000	0.000000000
8	-1.918106000	-1.278881000	0.000000000
8	0.218086000	-2.176155000	0.000000000
1	2.199159000	0.006960000	0.000000000

E = -681.446691 au

ZPVE = 0.053348622 kcal mol⁻¹

$\nu_i = 143.3086i$ cm⁻¹

2t

6	0.000000000	0.544939000	0.000000000
6	-0.630997000	-0.847577000	0.000000000
7	-0.957565000	1.486065000	0.000000000
1	-0.698657000	2.459839000	0.000000000
1	-1.930633000	1.209978000	0.000000000
16	1.624496000	0.827272000	0.000000000
8	-1.830664000	-1.007767000	0.000000000
8	0.252712000	-1.844663000	0.000000000
1	-0.250090000	-2.673368000	0.000000000

E = -681.480888 au

ZPVE = 0.059087391 kcal mol⁻¹

2c

6	0.000000000	0.546277000	0.000000000
6	-0.717404000	-0.820195000	0.000000000
7	-0.869886000	1.553419000	0.000000000
1	-0.551904000	2.510061000	0.000000000
1	-1.860008000	1.337806000	0.000000000
16	1.655005000	0.659290000	0.000000000
8	-1.920295000	-0.888284000	0.000000000
8	0.084946000	-1.873168000	0.000000000
1	1.008250000	-1.535327000	0.000000000

E = -681.546313514 au

ZPVE = 0.059254514 kcal mol⁻¹

3a

6	0.000000000	0.620526000	0.000000000
6	-0.915228000	-0.599834000	0.000000000
7	-0.472923000	1.794673000	0.000000000
1	2.071608000	1.597548000	0.000000000
1	-1.496340000	1.756369000	0.000000000
16	1.747072000	0.288021000	0.000000000
8	-2.114667000	-0.510138000	0.000000000
8	-0.240712000	-1.760226000	0.000000000
1	-0.883554000	-2.486196000	0.000000000

E = -681.463710 au

ZPVE = 0.055528355 kcal mol⁻¹

3b

6	-0.015171000	0.612028000	0.084654000
6	-0.953765000	-0.605374000	0.111520000
7	-0.439262000	1.783096000	-0.114148000
1	2.141736000	1.473860000	-0.077535000
1	-1.457140000	1.769565000	-0.229063000
16	1.724460000	0.264715000	0.346334000
8	-2.130531000	-0.467239000	0.284206000
8	-0.399402000	-1.813716000	-0.090092000
1	0.540053000	-1.735615000	-0.315875000

E = -681.455813 au

ZPVE = 0.055071577 kcal mol⁻¹

TS_3a to 2t

6	0.000000000	0.477371000	0.000000000
6	-0.833733000	-0.783809000	0.000000000
7	-0.549247000	1.654378000	0.000000000
1	0.786046000	2.051283000	0.000000000
1	-1.566898000	1.741263000	0.000000000
16	1.710049000	0.648685000	0.000000000
8	-2.038170000	-0.760572000	0.000000000
8	-0.091663000	-1.896529000	0.000000000
1	-0.694146000	-2.656714000	0.000000000

E = -681.418568 au

ZPVE = 0.052475973 kcal mol⁻¹

$\nu_i = 1778.4355i$ cm⁻¹

TS_3b to 2c

6	0.000000000	0.477040000	0.000000000
6	-0.911517000	-0.741238000	0.000000000
7	-0.446406000	1.690303000	0.000000000
1	0.948148000	1.966437000	0.000000000
1	-1.455288000	1.851550000	0.000000000
16	1.731111000	0.513694000	0.000000000
8	-2.104377000	-0.622400000	0.000000000
8	-0.302770000	-1.934537000	0.000000000
1	0.660488000	-1.828518000	0.000000000

E = -681.415591 au

ZPVE = 0.052186925 kcal mol⁻¹

$\nu_i = 1751.2527i$ cm⁻¹

TS_2t to 2c

6	0.372735000	0.400223000	-0.047382000
6	-1.056359000	-0.147591000	0.010427000
7	0.381851000	1.736563000	-0.162963000
1	1.258631000	2.233924000	-0.148193000
1	-0.491197000	2.246374000	-0.143053000
16	1.705199000	-0.565025000	0.092732000
8	-1.984733000	0.576031000	0.252739000
8	-1.193145000	-1.461351000	-0.292316000
1	-1.198808000	-2.029071000	0.486617000

E = -681.465050 au

ZPVE = 0.057230692 kcal mol⁻¹

$\nu_i = 648.4266i$ cm⁻¹

TS_1c-CO₂ to 1t-CO₂

6	0.695768000	0.089047000	-0.012703000
6	-2.351659000	-0.217038000	0.005952000
7	0.728474000	1.393061000	-0.021349000
1	1.579834000	1.960000000	-0.066550000
1	-0.159172000	1.888453000	0.001515000
16	2.438683000	-0.565609000	-0.069610000
8	-2.288498000	0.947105000	0.022001000
8	-2.488230000	-1.366222000	-0.008743000
1	2.610262000	-0.429253000	1.262678000

E = -681.430170 au

ZPVE = 0.051853034 kcal mol⁻¹

$\nu_i = 420.8355i$ cm⁻¹

References

1. A. D. Becke, *J. Chem. Phys.*, 1988, **88**, 1053.
2. C. Lee, W. Yang, R. G. Parr, *Phys. Rev. B*, 1988, **37**, 785.
3. A. D. McLean, G. S. Chandler, *J. Chem. Phys.*, 1980, **72**, 5639.
4. R. Krishnan, J. S. Binkley, R. Seeger, J. A. Pople, *J. Chem. Phys.*, 1980, **72**, 650.
5. C. Møller, M. S. Plesset, *Phys. Rev.*, 1934, **46**, 618.
6. M. Head-Gordon, J. A. Pople, M. J. Frisch, *Phys. Lett.*, 1988, **153**, 503.
7. F. Weigend, R. Ahlrichs, *Phys. Chem. Chem. Phys.*, 2005, **7**, 3297.
8. F. Weigend, *Phys. Chem. Chem. Phys.*, 2006, **8**, 1057.
9. G. D. Purvis III, R. J. Bartlett, *J. Chem. Phys.*, 1982, **76**, 1910.
10. K. Raghavachari, G. W. Trucks, J. A. Pople, M. Head-Gordon, *Chem. Phys. Lett.*, 1989, **157**, 479
11. Thom H. Dunning Jr., *J. Chem. Phys.*, 1989, **90**, 1007.
12. K. A. Peterson, D. E. Woon, Thom H. Dunning Jr., *J. Chem. Phys.*, 1994, **100**, 7410.
13. D. E. Woon, Thom H. Dunning Jr., *J. Chem. Phys.*, 1995, **103**, 4572.
14. Rick A. Kendall, Thom H. Dunning Jr., Robert J. Harrison, *J. Chem. Phys.*, 1992, **96**, 6796.
15. T. A. Keith, AIMAll. (TK Gristmill Software, USA, 2019).
16. R. F. Bader, *Acc. Chem. Res.*, 1985, **18**, 9.
17. B. Bernhardt, F. Dressler, A. K. Eckhardt, J. Becker, P. R. Schreiner, *Chem. Eur. J.*, 2021, **27**, 6732.
18. H. Rostkowska, L. Lapinski, M. J. Nowak, *Phys. Chem. Chem. Phys.*, 2018, **20**, 13994.
19. S. Góbi, I. Reva, I. P. Csonka, C. M. Nunes, G. Tarczay, R. Fausto, *Phys. Chem. Chem. Phys.*, 2019, **21**, 24935.
20. H. Rostkowska, L. Lapinski, A. Khvorostov, M. J. Nowak, *J. Phys. Chem. A*, 2003, **107**, 6373.
21. L. Lapinski, H. Rostkowska, A. Khvorostov, M. Yaman, R. Fausto, M. J. Nowak, *J. Phys. Chem. A*, 2004, **108**, 5551.
22. G. Maier, J. Endres, H. P. Reisenauer, *Angew. Chem. Int. Ed.*, 1997, **36**, 1709.
23. P. R. Schreiner, J. P. Wagner, H. P. Reisenauer, D. Gerbig, D. Ley, J. n. Sarka, A. G. Császár, A. Vaughn, W. D. Allen, *J. Am. Chem. Soc.*, 2015, **137**, 7828.
24. B. Liu, A. McLean, *J. Chem. Phys.*, 1973, **59**, 4557.
25. J. Vogt, S. Alvarez, *Inorg. Chem.*, 2014, **53**, 9260.

26. Y. Mo, *J. Phys. Chem. A*, 2012, **116**, 5240.
27. M. R. B. Bernhardt, H. P. Reisenauer, P. R. Schreiner, *J. Phys. Chem. A*, 2021, **125**, 7023.
28. P. R. Schreiner, H. P. Reisenauer, *Angew. Chem. Int. Ed.*, 2008, **120**, 7179.
29. A. K. Eckhardt, P. R. Schreiner, *Angew. Chem. Int. Ed.*, 2018, **57**, 5248.

Full Citations for Electronic Structure Codes

Gaussian 16

Gaussian 16, Revision A.03; Frisch, M. J.; Trucks, G. W.; Schlegel, H. B.; Scuseria, G. E.; Robb, M. A.; Cheeseman, J. R.; Scalmani, G.; Barone, V.; Petersson, G. A.; Nakatsuji, H.; Li, X.; Caricato, M.; Marenich, A. V.; Bloino, J.; Janesko, B. G.; Gomperts, R.; Mennucci, B.; Hratchian, H. P.; Ortiz, J. V.; Izmaylov, A. F.; Sonnenberg, J. L.; Williams-Young, D.; Ding, F.; Lipparini, F.; Egidi, F.; Goings, J.; Peng, B.; Petrone, A.; Henderson, T.; Ranasinghe, D.; Zakrzewski, V. G.; Gao, J.; Rega, N.; Zheng, G.; Liang, W.; Hada, M.; Ehara, M.; Toyota, K.; Fukuda, R.; Hasegawa, J.; Ishida, M.; Nakajima, T.; Honda, Y.; Kitao, O.; Nakai, H.; Vreven, T.; Throssell, K.; Montgomery, J. A., Jr.; Peralta, J. E.; Ogliaro, F.; Bearpark, M. J.; Heyd, J. J.; Brothers, E. N.; Kudin, K. N.; Staroverov, V. N.; Keith, T. A.; Kobayashi, R.; Normand, J.; Raghavachari, K.; Rendell, A. P.; Burant, J. C.; Iyengar, S. S.; Tomasi, J.; Cossi, M.; Millam, J. M.; Klene, M.; Adamo, C.; Cammi, R.; Ochterski, J. W.; Martin, R. L.; Morokuma, K.; Farkas, O.; Foresman, J. B.; Fox, D. J., Gaussian Inc., Wallingford CT **2016**.

Cfour

Coupled-Cluster techniques for Computational Chemistry, a quantum-chemical program package by Stanton, J.F.; Gauss, J.; Harding, M.E.; Szalay, P.G. with contributions from Auer, A.A.; Bartlett, R.J.; Benedikt, U.; Berger, C.; Bernholdt, D.E.; Bomble, Y.J.; Christiansen, O.; Heckert, M.; Heun, O.; Huber, C.; Jagau, T.-C.; Jonsson, D.; Jusélius, J.; Klein, K.; Lauderdale, W.J.; Matthews, D.A.; Metzroth, T.; O'Neill, D.P.; Price, D.R.; Prochnow, E.; Ruud, K.; Schiffmann, F.; Stopkowitz, S.; Tajti, A.; Vázquez, J.; Wang, F.; Watts, J.D. and the integral packages MOLECULE (Almlöf, J. and Taylor, P.R.), PROPS (Taylor, P.R.), ABACUS (Helgaker, T.; Jensen, H.J. Aa.; Jørgensen, P. and Olsen, J.), and ECP routines by Mitin, A. V. and van Wüllen, C. For the current version, see <http://www.cfour.de>.

Polyrate 2017-C

POLYRATE 2017-C; Zheng, J.; Bao, J. L.; Meana-Pañeda, R.; Zhang, S.; Lynch, B. J.; Corchado, J. C.; Chuang, Y.-Y.; Fast, P. L.; Hu, W.-P.; Liu, Y.-P.; Lynch, G. C.; Nguyen, K. A.; Jackels, C. F.; Ramos, A. F.; Ellingson, B. A.; Melissas, V. S.; Vill, J.; Rossi, I.; Coitio, E. L.; Pu, J.; Albu, T. V.; Steckler, R.; Garrett, B. C.; Isaacson, A. D.; Truhlar, D. G., **2017**.

CYLview

CYLview, 1.0b; Legault, C. Y., Université de Sherbrooke, **2009** (<http://www.cylview.org>).

NBO7

E. D. Glendening, J. K. Badenhoop, A. E. Reed, J. E. Carpenter, J. A. Bohmann, C. M. Morales, P. Karafiloglou, C. R. Landis, F. Weinhold, NBO 7.0, **2018**, Theoretical Chemistry Institute, University of Wisconsin, Madison.